KINETICS OF ANIONIC SURFACTANT ANOXIC DEGRADATION

A Dissertation

by

JULIANNA GISEL CAMACHO

Submitted to the Office of Graduate Studies of
Texas A&M University
in partial fulfillment of the requirements for the degree of

DOCTOR OF PHILOSOPHY

May 2010

Major Subject: Civil Engineering

KINETICS OF ANIONIC SURFACTANT ANOXIC DEGRADATION

A Dissertation

by

JULIANNA GISEL CAMACHO

Submitted to the Office of Graduate Studies of
Texas A&M University
in partial fulfillment of the requirements for the degree of

DOCTOR OF PHILOSOPHY

Approved by:

Chair of Committee,	Robin Autenrieth
Committee Members,	Bill Batchelor
	Kung-Hui Chu
	Thomas Wood
Head of Department,	John Niedzwecki

May 2010

Major Subject: Civil Engineering

ABSTRACT

Kinetics of Anionic Surfactant Anoxic Degradation. (May 2010)

Julianna Gisel Camacho, B.S., University of Puerto Rico;

M.S., Texas A&M University

Chair of Advisory Committee: Dr. Robin Autenrieth

The biodegradation kinetics of Geropon TC-42® by an acclimated culture was investigated in anoxic batch reactors to determine biokinetic coefficients to be implemented in two biofilm mathematical models. Geropon TC-42® is the surfactant commonly used in space habitation. The two biofilm models differ in that one assumes a constant biofilm density and the other allows biofilm density changes based on space occupancy theory. Extant kinetic analysis of a mixed microbial culture using Geropon TC-42® as sole carbon source was used to determine cell yield, specific growth rate, and the half-saturation constant for S_0/X_0 ratios of 4, 12.5, and 34.5. To estimate cell yield, linear regression analysis was performed on data obtained from three sets of simultaneous batch experiments for three S_0/X_0 ratios. The regressions showed non-zero intercepts, suggesting that cell multiplication is not possible at low substrate concentrations. Non-linear least-squares analysis of the integrated equation was used to estimate the specific growth rate and the half-saturation constant. Net specific growth rate dependence on substrate concentration indicates a self-inhibitory effect of Geropon TC-42®. The flow rate and the ratio of the concentrations of surfactant to nitrate were

the factors that most affected the simulations. Higher flow rates resulted in a shorter hydraulic retention time, shorter startup periods, and faster approach to a steady-state biofilm. At steady-state, higher flow resulted in lower surfactant removal. Higher influent surfactant/nitrate concentration ratios caused a longer startup period, supported more surfactant utilization, and biofilm growth. Both models correlate to the empirical data. A model assuming constant biofilm density is computationally simpler and easier to implement. Therefore, a suitable anoxic packed bed reactor for the removal of the surfactant Geropon TC-42® can be designed by using the estimated kinetic values and a model assuming constant biofilm density.

DEDICATION

To my mom, dad, brother, and Sean.

In memory of Dr. Tim Kramer.

ACKNOWLEDGEMENTS

I thank my committee members: Dr. Robin Autenrieth, my committee chair, for her guidance and advice; and Drs. Bill Batchelor, Kung-Hui Chu and Thomas Wood for their suggestions, availability, and commitment.

I thank the Louis Stokes Alliances for Minority Participation, Shannon Henderson, the Space Engineering and the Department of Civil Engineering for their financial support.

I thank my fellow students and co-workers for their help, support, and friendship. Special thanks go to my friends Adi and Selcuk for their help, support, encouragement, and patience.

Finally, thanks to my mother, father and brother for their encouragement and to Sean for his patience, love and, support.

NOMENCLATURE

ε	Reactor porosity
μ	Specific growth rate (1/time)
μ_{max}	Maximum specific growth rate (1/time)
γ	Stochiometric coefficient for nitrate utilization
A	Reactor cross-sectional area (area)
A_f	Biofilm cross-sectional area
b	Decay coefficient
b_S	Biofilm shear loss coefficient
BSA	Bovine Serum Albumin
$D_{f,N}$	Nitrate diffusion coefficient in the biofilm (area/time)
$D_{f,S}$	Surfactant diffusion coefficient in the biofilm (area/time)
f_e	Portion of e^- used for energy
f_s	Portion of e^- used for synthesis
GMB	Growth Medium Base
ISS	International Space Station
K_S	Half-saturation Constant (mass/volume)
$K_{S,N}$	Monod half-saturation constant of nitrate (mass/volume)
$K_{S,S}$	Monod half-saturation constant of the surfactant (mass/volume)
$K^*_{S,S}$	Dimensionless Monod half-saturation constant of the surfactant
$K_{S,1}$	Half-saturation constant for limiting substrate 1 (mass/volume)

$K_{S,2}$	Half-saturation constant for limiting substrate 2 (mass/volume)
L	Thickness of the liquid-biofilm interface (length)
L_f	Thickness of the biofilm (length)
q	Maximum specific substrate utilization rate (mass/(mass)(time))
Q	Flow rate (volume/time)
r_{growth}	Rate of biomass formation (mass/(volume)(time))
$r_{substrate\ utilizarion}$	Rate of substrate utilization (mass/(volume)(time))
$r_{ut,N}$	Nitrate utilization rate (mass/volume time)
$r_{ut,S}$	Rate of utilization of the surfactant (mass/volume time)
S	Substrate concentration (mass/volume)
S_b	Substrate concentration in the bulk liquid (mass/volume)
$S_{b,N}^{0}$	Influent nitrate concentration (mass/volume)
$S_{b,S}^{0}$	Influent surfactant concentration (mass/volume)
$S_{b,N}^{*}$	Dimensionless nitrate concentration in the bulk liquid
$S_{b,S}^{*}$	Dimensionless surfactant concentration in the bulk liquid
$S_{b,N}$	Nitrate concentration in the bulk liquid (mass/volume)
$S_{b,S}$	Surfactant concentration in the bulk liquid (mass/volume)
S_f	Substrate concentration in the biofilm (mass/volume)
$S_{f,N}$	Nitrate concentration in the biofilm (mass/volume)
$S_{f,S}$	Surfactant concentration in the biofilm (mass/volume)
$S_{f,N}^{*}$	Dimensionless nitrate concentration in the biofilm

$S^*_{f,S}$	Dimensionless surfactant concentration in the biofilm
S_i	Substrate concentration in the liquid-biofilm interface (mass/volume)
$S_{i,N}$	Nitrate concentration in the liquid-biofilm interface (mass/volume)
$S_{i,S}$	Surfactant concentration in the liquid-biofilm interface (mass/volume)
$S^*_{i,N}$	Dimensionless nitrate concentration in the liquid-biofilm interface
$S^*_{i,S}$	Dimensionless surfactant concentration in the liquid-biofilm interface
S_0	Initial surfactant concentration (mass/volume)
S_1	Concentration limiting substrate 1 (mass/volume)
S_2	Concentration limiting substrate 2 (mass/volume)
t	Time
TSS	Total Suspended Solids (mass/volume)
V	Reactor volume (volume)
V_f	Biofilm volume
Y	Cell yield (mass/mass)
X_a	Active cell mass (mass/volume)
X_b	Biomass concentration in the bulk liquid (mass/volume)
X^*_b	Dimensionless biomass concentration in the bulk liquid
X_f	Biofilm density (mass/volume)
X^*_f	Dimensionless biofilm density
X_0	Initial biomass concentrations (mass/volume)

TABLE OF CONTENTS

CHAPTER Page

CHAPTER Page

Page

LIST OF FIGURES

Page

Page

LIST OF TABLES

CHAPTER I

INTRODUCTION

PROBLEM STATEMENT

Humans consume approximately 2.3 L of water and produce approximately 0.2 L per day (Silverthorn et al. 2004). Water is also used for personal hygiene and meal preparation. Under conditions of limited freshwater availability, like during times of drought and in some specialized situations, recycling wastewater becomes an important consideration (Bubenheim et al. 1997). In the case of human space habitation, wastewater reuse is essential since water is the heaviest of the life support elements. The estimated water use for life support per person is 27 L/day (Philistine 2005). An estimated cost of launching water to low-earth orbit is $22,000/kg, which makes re-supply costly (Bubenheim et al. 1997). Furthermore, transporting large amounts of water would displace scientific and other payloads (Bubenheim et al. 1997). Therefore, it is necessary to develop a method of water recovery that will provide potable water suitable for crew consumption and system use.

Research has shown that biological water processors (BWPs) can transform wastewater's organic constituents and urinary nitrogen into biologically stable inorganic compounds prior to downstream separation processes (Muirhead et al. 2003; Vega et al. 2004). Biological treatment processes use microorganisms to break down compounds into simple molecules. This process offers advantages over chemical/physical treatment

---

This dissertation follows the style of *Journal of Environmental Engineering*.

by operating with minimal energy, provide significant mass savings, and are a proven Earth-based technologies (Strayer et al. 1999). Also, biological reactors have an inherent advantage over physical/chemical approaches by efficiently providing elemental recycling (e.g., carbon, nitrogen, etc.) (Vega et al. 2004).

Performance of a biological water reclamation system is dependent on the source and composition of the influent wastewater. There are three primary wastewater sources aboard a manned spacecraft: humidity condensate, urine, and hygiene water. Humidity condensate is the result of condensation of water from the ambient air. It is lightly contaminated with ammonia and with water-soluble organics. Urine contains salts, excreted organic metabolic by-products, and high concentrations of nitrogen compounds (Verstoko et al. 2004). The main sources of hygiene wastewater are hand washing, showering, clothes washing, oral hygiene, eating utensil cleaning, and cookware cleaning. This waste stream contains soap, salts, and organics. Soaps (surfactants) are the major chemical constituents of concern. The hygiene wastewater source constitutes the largest waste stream, representing 75 to 95% of the total liquid and solid wastes (Bubenheim et al. 1997). Geropon TC-42® is the principal surfactant used in space habitation and it has been shown to be phytotoxic to lettuce by Bubenheim et al. (1997) at concentrations of 250 mg/L or higher, which resulted in browning of the roots and root death. Little information is available on the effects of Geropon TC-42® ingestion by humans.

In order to design a biological treatment system for removal of surfactants, the biokinetics of surfactant degradation must be well defined (Sharvelle et al. 2007). Further, a biological treatment process for space applications needs to be designed with consideration for zero or low gravity conditions. Poor mass transfer of oxygen between gas and liquid phases in microgravity is an important consideration in the design of bioreactors for use in space (Strayer et al. 1999). Bacteria that can use soluble nitrate instead of oxygen would eliminate oxygen mass transfer problems. Denitrifying bacteria can use soluble nitrate as a terminal electron acceptor (Rittmann and McCarty 2001). This research focused on the biodegradation of Geropon TC-42® in NASA Whole Body Shower Shampoo by denitrification. The objectives of the research are: (1) to estimate biodegradation rate and microbial growth parameters for Geropon® TC-42 under anoxic conditions using nitrate as terminal electron acceptor; (2) to develop a biofilm mathematical model assuming constant biofilm density applied to a completely mixed packed bed reactor; (3) to develop a biofilm mathematical model using the concept of space occupancy applied to a completely mixed packed bed reactor; and (4) compare the results of the 2 mathematical models to empirical laboratory data of a completely mixed packed bed reactor.

BACKGROUND

Surfactants

Surfactants are characterized by having both hydrophilic and hydrophobic groups and are major ingredients of synthetic detergents used worldwide for both domestic and industrial applications (Dhouib et al. 2003). There are three types of surfactants

commonly present in personal cleansing products and detergents; anionic, nonionic, and amphoteric. The surfactant used in this study is an anionic surfactant. Anionic synthetic detergents may be classified into sulfates and sulfonates (Figure 1).

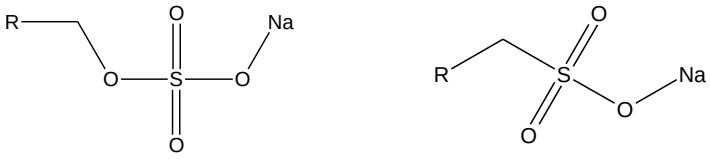

Sulfate Sulfonate

Figure 1. Anionic synthetic detergents classification

Due to their favorable physiochemical properties, surfactants are extensively used in many fields of technology and research (Perales et al. 1999). After use, large quantities of surfactants and their derivatives are released to aquatic and terrestrial environments (Hosseini et al. 2007). The fate of surfactants in biological treatment systems is becoming increasingly important as water reuse systems become more common and regulations for trace contaminant release by wastewater treatment plants are more stringent (Sharvelle et al. 2007).

NASA Whole Body Shower Soap

Geropon TC-42® is an anionic detergent since it is a sodium salt that ionizes to yield Na^+ and a negative ion. NASA Whole Body Shower Soap is manufactured by Rhodia North American Chemicals and is approximately 60% water and 24% Geropon TC-42® (formerly Igepon TC-42®). Geropon TC-42® is a commercially available anionic surfactant that is used as a skin and hair care product. It is a sulfonated amide

with the chemical structure shown in Figure 2. The "R" is a carboxylic chain of eleven to seventeen carbons. The manufacturer reports that it exhibits mild detergency properties without scum formation. The International Nomenclature of Cosmetic Ingredients name for Geropon TC-42® is sodium methyl cocoyl taurate.

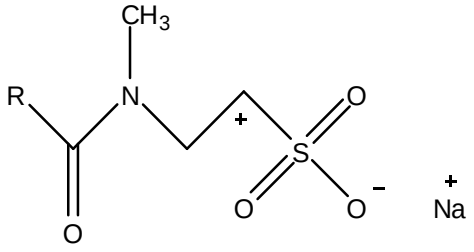

Figure 2. Chemical structure of Geropon® TC-42

Denitrification in Wastewater Treatment

The primary goal of wastewater treatment is the removal and degradation of organic matter via biological oxidation carried out by microorganisms. Bacteria that use organic carbon as their energy source and cellular carbon source are called heterotrophs (Davis and Cornwell 1998; Maier 2000). In environmental engineering, carbon sources are termed the substrate and function as electron donors in the chemical activities performed by cells during metabolism (Davis and Cornwell 1998; Maier 2000). Organic carbon tends to be oxidized preferentially with the electron acceptor that supplies the most energy to the microorganisms, namely free oxygen. With an excess of organic carbon, aerobic bacteria use dissolved oxygen until it is depleted, whereupon reduction of other electron acceptors becomes energetically favorable. Once oxygen is consumed, facultative anaerobes use nitrate as an electron acceptor (Rivett et al. 2008).

The type of electron acceptor used for respiration determines the type of decomposition used by a mixed culture of microorganism. Denitrification involves the reduction of nitrate via a chain of microbial reduction reactions to nitrogen gas (Knowles 1982). The organisms capable of denitrification tend to be ubiquitous in surface water, soil, and groundwater (Beauchamp et al. 1989). The nitrate reduction reaction can be written as a half-reaction to illustrate the role of electron transfer in the process (Tesoriero et al. 2000):

$$2NO_3^- + 12H^+ + 10e^- \rightarrow N_2 + 6H_2O \quad \textbf{(1)}$$

The end products of denitrification are nitrogen gas, carbon dioxide, water, and new cell mass. Although denitrification has a stable endpoint at nitrogen gas, the process can be arrested at any of the intermediate stages. This is important because nitrite is significantly more toxic than nitrate ((WHO) 2004) and nitrogen oxides are environmentally destructive gases. The other product of the denitrification reaction is the oxygen rejected at each step. This is typically released as bicarbonate ions, carbon dioxide, or sulphate ions (Rivett et al. 2008).

Biodegradation Stoichiometry

Effective reactor design requires that stoichiometric estimates of target compounds and limiting nutrients be estimated so that feeds and reactor sizes can be approximated. The biodegradation stoichiometry was based on the assumption that an average 14 carbon chain represents the undefined functional group "R" (Figure 2). It was also assumed that the sodium salt would dissociate in solution. Therefore, the chemical formula used is $C_{14}H_{29}ONCH_3C_2H_4SO_3H$ with formula weight 351 g/mol.

Microorganisms obtain energy for growth and maintenance from oxidation-reduction reactions involving an electron donor and an electron acceptor. In this study, Geropon TC-42® was biodegraded under denitrifying conditions where the electron donor is Geropon TC-42® and the electron acceptor is nitrate (NO_3^-). Bacterial growth can be described by a linear combination of two reactions: an energy reaction and a synthesis reaction. The overall reaction can be obtained by multiplying the energy reaction by the fraction of electron equivalents (f_e) in the energy reaction, multiplying the synthesis reaction by the fraction of electron equivalents (f_s) in the synthesis reaction and summing the results. Cell maintenance and respiration represent net energy losses. The energetics are related to the stoichiometry in the balanced chemical equations.

Using the protocol described by Rittmann and McCarty (2001), the energy reaction for Geropon TC-42® can be expressed as:

$$\tfrac{1}{24}C_{14}H_{29}ONCH_3C_2H_4SO_3^-H^+ + \tfrac{1}{5}NO_3^- + \tfrac{1}{5}H^+ \rightarrow \tfrac{1}{24}N_2 + \tfrac{17}{24}CO_2 + \tfrac{41}{60}H_2O + \tfrac{17}{24}H_2S + \tfrac{17}{24}NH_3 \quad \textbf{(2)}$$

Consistent with the energy reaction assuming complete transformation of Geropon TC-42®, the synthesis reaction for the formation of cells with a chemical formula $C_5H_7O_2N$ is

$$\tfrac{1}{24}C_{14}H_{29}ONCH_3C_2H_4SO_3^-H^+ + \tfrac{1}{28}NO_3^- + \tfrac{1}{28}H^+ \rightarrow \tfrac{1}{28}C_5H_7O_2N + \tfrac{89}{168}CO_2 + \tfrac{10}{21}H_2O + \tfrac{1}{24}NH_3 + \tfrac{1}{24}H_2S \quad \textbf{(3)}$$

To obtain an overall reaction that includes energy generation and synthesis, equation 2 is multiplied by f_e, equation 3 is multiplied by f_s, and they are added. According to Rittmann and McCarty (2001), when NO_3^- is used as an electron acceptor

and nitrogen source it can be assumed that f_s is 0.55 and f_e is 0.45. Therefore the overall reaction is

$$0.0417C_{14}H_{29}ONCH_3C_2H_4SO_3^-H^+ + 0.1096NO_3^- + 0.1096H^+ \rightarrow 0.1N_2 + 0.0357C_5H_7O_2N + 0.6101CO_2 + 0.5694H_2O + 0.0417NH_3 + 0.0417SH_2 \quad \textbf{(4)}$$

Microbial Growth Kinetics

Microbial growth kinetics are represented as a chemical reaction with known stoichiometry and defined kinetic functions (Rhodes and Stanbury 1997). The simplest equation for microbial growth rate applies to cells that grow at a constant rate per unit mass of cells (Bazin 1983). This constant rate is called the specific growth rate (μ) and can be used to mathematically represent the rate of cell generation as a function of the concentration of cell mass termed the concentration of active biomass (X_a) by:

$$r_{growth} = \mu X_a \quad \textbf{(5)}$$

The effect of the concentration of a growth-limiting nutrient (S) on the specific growth rate can be expressed by the Monod equation (Rittmann and McCarty 2001):

$$\mu = \mu_{\max} \frac{S}{K_S + S} \quad \textbf{(6)}$$

where, $\mu_{\max}$ is the maximum specific growth rate (1/time) for the culture, S is the substrate concentration (mass/volume), and K_S is the half-saturation constant (mass/volume). Therefore, the rate of biomass growth is:

$$r_{growth} = \mu_{\max} \frac{S}{K_S + S} X_a \quad \textbf{(7)}$$

The rate of growth of cell mass is related to the rate of substrate utilization by the cell yield (*Y*) (Maier 2000). The cell yield is the total cell mass produced per substrate mass consumed (Rittmann and McCarty 2001):

$$Y = -\frac{r_{growth}}{r_{substrate utilization}} = -\frac{\Delta X_a}{\Delta S} \quad \textbf{(8)}$$

The substrate utilization rate can be expressed in terms of the biomass growth rate as:

$$r_{substrate utilization} = -\frac{1}{Y} r_{growth} \quad \textbf{(9)}$$

when equation 7 and 9 are combined the rate of substrate utilization becomes:

$$r_{substrate utilization} = -\frac{1}{Y} \frac{\mu_{\max} S}{K_S + S} X_a \quad \textbf{(10)}$$

Biofilms

Biofilms are of great interest in biotechnology because they offer advantages over suspended cells reactors by facilitating cell/liquid separation, simplifying downstream treatment, and reducing the number of unit operations and space needed for treatment (Costerton et al. 1994). A biofilm can be defined as a complex coherent structure of cells and cellular products, which either form spontaneously as large, dense granules, or grow attached on a solid surface (Nicolella et al. 2000).

An important characteristic of biofilms, which should be taken into account when developing a biofilm model, is that the substrate has to cross the solid/liquid interface and be transported through the biofilm to reach the microbial cells. Typically, biofilm

models only consider one substrate as the limiting factor for growth and consumption. A single substrate-limiting biofilm for the estimation of substrate utilization in an idealized deep biofilm was developed by Williamson and McCarty (1976a; 1976b) and later modified to describe deep, shallow, and fully penetrated biofilm by Rittmann and McCarty (1978),(1981). The single substrate-limiting biofilm model has since been used and developed into simplified algebraic expression for biofilm kinetics incorporating Monod-type substrate utilization and diffusive mass transfer relating bulk-substrate concentration and biofilm thickness with steady-state substrate utilization (Fouad and Bhargava 2005a; b; Lin and Lee 2006; Suidan and Wang 1985). The limitation of these biofilm models is that they only consider the electron donor as reaction limiting.

Assuming that a single nutrient substrate limits the growth of biomass is a simplistic description of biological growth conditions. Substrates can be grouped according to their physiological function. (Zinn et al. 2004) Homologous nutrients are those that accomplish the same physiological functions during growth (Bader 1978). Heterologous nutrients satisfy different physiological requirements (Egli 1995). Due to the complex interaction between different types of nutrient substrates, multiple substrates should be assumed to limit biomass growth. The situation when two substrates are rate limiting within a biofilm is called dual limitation and the single-substrate limiting biofilm models do not apply (Rittmann and Dovantzis 1983). In aerobic and anaerobic growth conditions dual substrate-limitation biofilms, the electron donor and the electron acceptor substrates together limit the overall cell growth rate. Two theoretical models have been proposed to describe dual limitation of cell growth:

the non-interacting model (Belova et al. 1996; Delhomenie and Heitz 2005; Fraleigh and Bungay 1986; Kissel et al. 1984; Rittmann and Dovantzis 1983; Sykes 1973; Williamson and McCarty 1976b) and the multiplicative (double-Monod) model (Bae and Rittmann 1996; Borden and Bedient 1986; Howell and Atkinson 1976; Kissel et al. 1984; Lau et al. 1984; Molz et al. 1986; Qi and Morgenroth 2005; Sinclair and Ryder 1975). The non-interacting model states that the growth of an organism is limited only by the more severely limiting substrate, while the other substrate has no effect on the kinetics (Bae and Rittmann 1996). The multiplicative model assumes that two substrates directly limit the overall growth rate if the substrates are present at sub-saturating concentrations (Bae and Rittmann 1996). The limitation effects are multiplicative and can be expressed by:

$$\mu = \mu_{\max}\left(\frac{S_1}{K_{S,1}+S_1}\right)\left(\frac{S_2}{K_{S,2}+S_2}\right) \qquad \textbf{(11)}$$

where, μ is the specific cell growth rate, μ_{max} is the Monod maximum specific growth rate, S_1 and S_2 are the two limiting substrate concentrations, and $K_{S,1}$ and $K_{S,2}$ are the two half-saturation constant.

Because biofilms are beneficial methods for wastewater treatment in places where space is at a premium, they are excellent candidates for wastewater treatment in space habitation. Another important consideration in the design of biofilm reactors for space habitation is poor mass transfer of oxygen in microgravity. Bacteria that can use soluble nitrate instead of oxygen would eliminate oxygen mass transfer problems. One important pollutant present in space habitation wastewater is the surfactant Geropon TC-42® found in NASA Whole Body Shower Soap. In this study, a biofilm model was

developed for the utilization of Geropon TC-42® as the electron donor and nitrate as the terminal electron acceptor.

The surfactant utilization rate is defined by the multiplicative double-Monod kinetic model (equation 11). The surfactant serves as the electron donor and nitrate is the electron acceptor. The substrate utilization rate within the biofilm is described by:

$$r_{ut,S} = \frac{\mu_{\max}}{Y} \frac{S_{f,S} S_{f,N}}{\left(K_{S,S} + S_{f,S}\right)\left(K_{S,N} + S_{f,N}\right)} X_f \qquad \textbf{(12)}$$

where, $r_{ut,S}$ is the utilization rate of the surfactant (mass/volume time), $S_{f,S}$ is the surfactant concentration in the biofilm (mass/volume), $S_{f,N}$ is the nitrate concentration in the biofilm (mass/volume), $K_{S,S}$ is the Monod half-saturation constant of the surfactant (mass/volume), $K_{S,N}$ is the Monod half-saturation constant of nitrate (mass/volume), and X_f is the biofilm density (mass/volume). The utilization rate for the nitrate is directly proportional to the rate of surfactant utilization. The relationship can be described by:

$$r_{ut,N} = \gamma \, r_{ut,S} \qquad \textbf{(13)}$$

where, γ is the stoichiometric coefficient for nitrate utilization.

Anoxic Biofilm Reactor

A bioreactor is a reactor that supports a biologically active environment. Organisms growing in bioreactors may be suspended or immobilized. A biofilm reactor is a bioreactor where the biomass exists in an anchored form, either on the surface of an inert media or attached to one another. The media could be stationary as in a packed-bed

or mobile as in a fluidized bed system. A packed bed reactor is a reactor that is filled with a packing material. The purpose of a packed bed is to improve contact between two phases. Typically, in such reactors, the rate of substrate conversion is limited by the rate of transport of substrate into the biofilm (Saravanan and Sreekrishnan 2006).

An anoxic biofilm process is defined in this study as a column filled with inert media and sealed from the atmosphere to maintain a mostly oxygen-free environment. Microorganisms become attached to the inert packing media and trapped in void spaces. As the substrate passes through the packing material, it is utilized by the attached biomass.

OBJECTIVES

Three objectives guided the research to understand the biodegradation of Geropon TC-42® by denitrification using an anoxic mixed-culture biofilm on inert media. First, a mathematical description for the kinetics of a biofilm on inert non-absorbing media was derived. Second, the physical and biokinetic coefficients required for a mathematical model for the simulation of the process were determined. Third, two biofilm models were developed. Fourth, the biofilm models were compared to experimental data using a simple experimental system.

Objective 1. The Monod kinetic parameters describing the biodegradation of Geropon TC-42® by denitrification were measured.

Task 1. Estimate the maximum specific growth rate, half-saturation constant and true growth yield by batch extant kinetic experiments.

Objective 2. Develop a constant density anoxic biofilm on inert media model.

Task 2. Determine basic assumptions, boundary conditions, and initial condition.

Task 3. Develop mathematical model based on substrate and biomass material balances.

Objective 3. Develop an anoxic biofilm on inert media model using the concept of space occupancy.

Task 4. Determine basic assumptions, boundary conditions, and initial condition.

Task 5. Develop mathematical model based on substrate and biomass material balances.

Objective 4. Compare model results with experimental results.

Task 6. Design experimental system

Task7. Conduct continuous flow studies.

DISSERTATION OVERVIEW

This dissertation is composed of five chapters. The content of each chapter is summarized below.

Chapter I introduces the problem description, gives basic background, and states objectives of the research.

Chapter II, "Anionic surfactant biodegradations kinetics by an acclimated mixed culture", provides batch kinetics experiment description and data analysis for the determination of cell yield (Y), specific growth rate (μ_{max}), and the half-saturation

constant (K_S). Monod biodegradation kinetics in anoxic conditions were used in this study.

Chapter III, "Constant density biofilm model on inert media", describes the material balances used to derive a one-dimensional double substrate-limiting constant density biofilm model on inert media using the multiplicative Monod kinetics and a solution strategy for a non-steady state biofilm reactor.

Chapter IV, "Biofilm model on inert media using the concept of space occupancy", describes the concept of space occupancy and the material balances used to derive a one-dimensional double substrate-limiting biofilm model on inert media using multiplicative Monod kinetics and a solution strategy for a non-steady state biofilm reactor.

Chapter V, "Continuous flow study" is a comparative study on the start-up performance of a packed bed reactor. Simulations were performed with the two different biofilm models and compared to experimental data for the biodegradation of Geropon TC-42® under anoxic conditions.

Chapter VI, provides a summary and conclusions of the overall research, discusses the importance of this research, and provides suggestions for recommended future research.

CHAPTER II

ANIONIC SURFACTANT BIODEGRADATION KINETICS BY AN ACCLIMATED MIXED CULTURE

In this chapter, the cell yield (Y), specific growth rate (μ_{max}), and the half-saturation constant (K_S) were estimated for Geropon TC-42® under anoxic conditions. The following sections describe the laboratory techniques used and the analytical methods employed to estimate the kinetic parameters.

OVERVIEW

Surfactants are one of the most common xenobiotics that enter waters systems; therefore biokinetic parameters used to design wastewater treatment systems need to be well characterized. An acclimated culture in anoxic batch reactors was used to investigate the biodegradation kinetics of Geropon TC-42®, the surfactant commonly used in space habitation. Extant kinetic analysis of a mixed microbial culture using Geropon TC-42® as sole carbon source was used to determine cell yield (Y), specific growth rate (μ_{max}), and the half-saturation constant (K_S) for S_0/X_0 ratios of 4, 12.5, and 34.5. To estimate cell yield, linear regression analysis was performed on data obtained from three sets of simultaneous batch experiments for three S_0/X_0 ratios. The surfactant cell yields were 0.28, 052, and 0.49 mg TSS/mg surfactant for S_0/X_0 ratios of 4, 12.5, and 34.5, respectively with non-zero regression intercepts suggesting that cell multiplication is not possible at low substrate concentrations.

Non-linear least-squares analysis of the integrated equation was used to estimate the specific growth rate and the half-saturation constant. Net specific growth rate dependence on substrate concentration was used to gauge inhibitory effects. The surfactant K_S values were estimated to be 10, 126, and 6.9 g/L for S_0/X_0 ratios of 4, 12.5, and 34.5, respectively. The μ_{max} values were estimated to be 260, 833, and 14.5 g/g-d for S_0/X_0 ratios of 4, 12.5, and 34.5, respectively. The nitrate cell yield was 0.10 mg TSS/mg surfactant, the saturation constant was approximately 5 g/L, and the maximum growth rate was approximately 1 g/g-d for all S_0/X_0 ratios. A self-inhibitory effect of Geropon TC-42® was demonstrated in the reduced K_S and μ_{max} values at the highest S_0 treatment. A suitable wastewater treatment system for human space habitation can be designed by using estimated values to determine reactor volume, flow rate, and residence time for an anoxic attached culture plug flow reactor.

INTRODUCTION

Surfactants are among the most widely disseminated xenobiotics that enter waste streams and the aquatic environment (Dhouib et al. 2003). Biodegradation is the most important mechanism for the irreversible removal of chemicals from the aquatic environment (Berna et al. 2007). Most surfactants are reported to be at least partially biodegradable (Sharvelle et al. 2007). Although extensive research exists regarding surfactant biodegradation, biokinetic parameters used to design wastewater treatment systems have not been well characterized for most surfactants (Sharvelle et al. 2007). Geropon TC-42® is the principal surfactant used in space habitation. Eventhough limited information is available on the biodegradation of Geropon TC-42® in aerobic or

anaerobic environments, it has been shown to be bioavailable for aerobic degradation (Levine et al., 2000b). As the National Aeronautics and Space Administration (NASA) prepares for human exploration of the Moon, Mars, and beyond, re-supplying water from Earth will not be economically feasible or practical (Bubenheim et al. 1997). Therefore, it is necessary to design and develop a method to recovering wastewater that will provide safe potable water for crew consumption and system use.

Poor mass transfer of oxygen between gas and liquid phases in microgravity will be a challenge in the design of bioreactors for use in space habitats (Strayer et al. 1999). Bacteria that can use soluble nitrate instead of oxygen, also known as denitrifying bacteria, would eliminate oxygen mass transfer problems. This research focuses on the biodegradation of Geropon TC-42®, the surfactant in NASA Whole Body Shower Shampoo, as an electron donor and nitrate as an electron acceptor. The objective of this research was to estimate the kinetic parameters of Geropon TC-42® by an anoxic mixed-culture in order to design and develop a method to recover potable water from wastewater. In this study, microbial growth kinetics were applied to a material balance in a batch reactor to determine cell yield (Y), specific growth rate (μ_{max}), and the half-saturation constant (K_S).

Intrinsic and Extant Data

Kinetic constants that represent a specific transformation by a stable microbial population can be determined from steady-state chemostat culture or batch cultures evaluated in time. Grady et al. (1996) defined a commonly used nomenclature for the interpretation of kinetic data results. Kinetic constants are divided into intrinsic and

extant. Intrinsic data are defined as kinetic constants that express the maximum capability of the fastest growing members of the microbial community (Molchanov et al. 2007). In a kinetic experiment in which multiple population duplications occur, changes in the composition of the microbial community impact intrinsic kinetic data (Grady et al. 1996). A short batch experiment can be used to determine extant kinetic constants where only limited changes in the protein synthesis and synthesis of new enzymes occur before the substrate is depleted making changes in the physiological state minimal (Grady et al. 1996). Using short batch kinetics tests for the determination of the kinetic data constants is recommended because they represent the response of the culture community at the time of harvest (Chudova et al. 1992; Miyanaga et al. 2007; Molchanov et al. 2007). Steady-state conditions in chemostat or process units at treatment facilities are approximated and therefore extant kinetic data can be determined.

Experimental Techniques for the Estimation of Kinetic Parameters

Three experimental techniques typically used for the estimation of kinetic parameters are initial rate measurements, steady-state chemostat studies, and batch studies. For the initial rate measurement technique, the initial biomass concentration and the duration of the batch experiments are chosen so that the substrate concentration can be considered constant (Jones and Kelly 1983; Nemati et al. 1998; Nemati and Webb 1997; Nyavor et al. 1996). Cell growth rate is measured at various substrate concentrations and used to estimate kinetic parameters. Although this method neglects the lag phase in bacterial growth that often occurs following the introductions of cell

suspension into an oxidation reactor, lag phase is negligible for acclimated suspensions like the ones used in this study (Molchanov et al. 2007).

In steady-state chemostat studies the accumulation of substrate and biomass is zero and the concentration of substrate and biomass in the reactor is constant. Operating the reactor at different dilution rates, the dependency of μ on the steady-state substrate concentration can be obtained, and the kinetic constants are derived from the Monod equation (equation 6) (Gomez et al. 1996; Ioslovich et al. 2004; Nikolov et al. 2001). Besides the typical problems with continuously stirred tank reactors (i.e. voids, non-ideal mixing), bacteria tend to alter their kinetic properties due to cell physiological changes under the different steady-state conditions (Molchanov et al. 2007).

In batch culture growth kinetics, cells harvested during the logarithmic growth phase are introduced to fresh media with known initial substrate and biomass concentrations (Agarry and Solomon 2008; Molchanov et al. 2007; Sahinkaya and Dilek 2007; Sharvelle et al. 2008; Smith et al. 1998; Song et al. 2008). The substrate and biomass concentrations are measured as a function of time and the data are fit to a kinetic model. If the duration of the batch experiment is sufficient to allow for several cell divisions, a change in physiological state is expected to occur (Molchanov et al. 2007). The kinetics measured under such conditions are intrinsic rather than that of the initial culture. This problem can be managed by controlling the duration of the batch experiment so that multiple population replications do not occur and an extant kinetic data set is generated. (Grady et al. 1996).

MATERIALS AND METHODS

Culture Enrichment

The bacteria used in this research were cultivated by enrichment techniques. The inoculum for these cultures was obtained from the activated sludge basin of the Carter Creek Wastewater Treatment Plant, College Station, Texas in April 2008. To survive and compete successfully, most microorganisms are able to meet many of the environmental challenges by adjusting their cellular composition with respect to both structure and metabolic function (Kovarova-Kovar and Egli 1998). Therefore, denitrifying bacteria are expected to be found in the mixed liquor because denitrification is widespread among heterotrophic and autotrophic bacteria, many of which can shift between oxygen and nitrogen respiration (Rittmann and McCarty 2001). All cultures were incubated on a 35º C orbital shaker (Lab-Line® Orbit Environ-Shaker). A batch feed-and-draw method was used to grow bacterial enrichments in sterile 500 mL media bottles. Fresh substrate solution was injected into the bottles every two days by first allowing suspended microorganisms to settle and withdrawing an equal volume of supernatant. Enrichment cultures were used throughout the research to ensure consistency of all batch and model verification tests.

Denitrifying bacteria were enriched with media containing Geropon TC-42® as the sole carbon source (i.e., electron donor) and nitrate at 10% excess as the electron acceptor. The inorganic growth medium base (GMB) contained (per liter of de-ionized water) 0.5 g of $MgSO_4 \cdot 7H_2O$, 0.5 g of NH_4Cl, 0.5 g of KH_2PO_4, 0.1 g of $CaCl_2$, and 0.85 g of $NaNO_3$ (Kniemeyer et al. 1999). After autoclaving, 2 ml of a trace element (1 liter

of distilled water contained 2.1 mg of $FeSO_4 \cdot 7H_2O$, 30 mg of H_3BO_3, 100 mg of $MnCl_2 \cdot 4H_2O$, 190 mg of $CoCl_2 \cdot 6H_2O$, 24 mg of $NiCl_2 \cdot 6H_2O$, 29 mg of $CuSO_4 \cdot 5H_2O$, 144 mg of $ZnSO_4 \cdot 7H_2O$, 36 mg of $NaMoO_4 \cdot 7H_2O$, and 5.2 g of EDTA, pH 6.5), 1 ml of vitamin solution (4 mg of 4-aminobenzoic acid, 2 mg of D-(1)-biotin, 10 mg of nicotinic acid, 5 mg of calcium D-(1)-pantothenate, 15 mg of pyridoxin hydrochloride, 4 mg of folic acid, and 1 mg of lipoic acid in 100 ml of 10 mM NaH_2PO_4, pH 7.1), and 50 ml of $NaHCO_3$ solution (1 M) were added and the solution was sparged with nitrogen gas (Kniemeyer et al. 1999). All chemicals used in the study are reagent grade chemicals.

Batch Biokinetic Experiments

Enriched cell suspension samples were taken for the batch biokinetic experiments. The suspension was centrifuged (RCF = 7500, 10 min) and cells washed with a sterile and filtered 0.1 M sodium phosphate buffer solution at pH 6.9 three times and then re-suspended in GMB. Enough Geropon TC-42® stock solution, nitrate stock solution and GMB were mixed to achieve an initial surfactant concentration (S_0) of 16, 50 mg-L^{-1} or 130 mg-L^{-1} with 10% excess nitrate by mass following the theoretically derived biodegradation reaction.

$$0.0417C_{14}H_{29}ONCH_3C_2H_4SO_3^-H^+ + 0.1096NO_3^- + 0.1096H^+ \rightarrow 0.1N_2 + 0.0357C_5H_7O_2N + 0.6101CO_2 + 0.5694H_2O + 0.0417NH_3 + 0.0417SH_2 \quad \textbf{(14)}$$

Triplicate reactors were prepared by transferring 150 mL of the Geropon TC-42® mixture to each of the sterile 150 mL media bottles with septum caps. In accordance with published surfactant biodegradation kinetic research, to initiate biodegradation, rinsed concentrated biomass was added to each reactor to achieve initial biomass

concentration (X_0) of 4 mg-L^{-1} for all reactors yielding S_0/X_0 ratios of 4, 12.5 or 34.5 with units mg surfactant-L^{-1} and mg TSS-L^{-1}, respectively (Dhouib et al. 2003; Jurado et al. 2007; Laspidou and Rittmann 2004a; Sharvelle et al. 2007; Sharvelle et al. 2008). Control reactors identical to the experimental reactor with no biomass were run simultaneously. Samples were taken from each reactor at designated sampling times and filtered through a 0.2-μm filter. Samples were analyzed for Geropon TC-42®, nitrate, and biomass concentrations. Experiments were conducted at 32 °C in an orbital shaker.

Surfactant Analytical Procedure

Levine (2000a) has shown that Geropon TC-42® concentration can be determined by a direct approach utilizing ion pairing reversed-phase chromatography coupled with suppressed conductivity detection. A Dionex DX-600 ion chromatography system equipped with a conductivity cell (DS3) and self-regenerating suppressor (Dionex ASRS Ultra 4 mm) was used to determine Geropon TC-42® concentration (Levine et al. 2000a). Separation was achieved on a Dionex IonPac NS1 column (10 μm, 250 mm×4mm) using a gradient of acetonitrile and 5 mM ammonium hydroxide using 25 mM sulfuric acid as a regenerant. The gradient program used was: 5% acetonitrile for the first 5 min followed by a linear increase to 45% over the next 15 min and hold at 45% for 10 min. Flow rate of the mobile phase was kept at 1 ml/min. The suppressor is operated in the external chemical mode using 25 mM sulfuric acid as a regenerant at 4 ml-min^{-1}. The dynamic analytical range was from 1 to 25 mg/L.

Biomass Analytical Procedure

Since a direct measurement of biomass concentration is cumbersome, most of the published kinetic studies rely on the measurement of an indirect parameter like measurement of oxygen uptake rate, measurement of substrate concentrations with time, or the change in solution turbidity (Molchanov et al. 2007). In this study, a relationship of total suspended solids (TSS) and protein concentration was developed to determine biomass concentration. TSS was measured according to Standard Method 2540D (Eaton et al. 2007). A bovine serum albumin (BSA) protein assay was used to quantify biomass. The protein assay kit is manufactured by Pierce Biotechnology (Rockford, IL). Biomass measurements were conducted with a UV-Visible spectrophotometer measuring the absorbance of BSA at 750 nm. The Pierce Biotechnology Protein Assay is a procedure for the determination of solubilized protein concentration. It involves a reaction of protein with cupric sulfate and tartrate in an alkaline solution, resulting in the formation of tetradentate copper-protein complexes, and subsequent measurement at 750 nm with a spectrophotometer. The concentration range was 25 to 1500 mg/L of BSA. Comparison to a standard curve provides a relative measurement of protein concentration that is related to total suspended solids.

Nitrate Analytical Procedure

Nitrate concentration was measured using a Dionex-80 system equipped with a conductivity cell and self-regenerating suppressor according to EPA Method 300.1 (Hautman and Munch 1997). Separation was achieved on a Dionex IonPac AS14A column with a dynamic analytical range from 0.1 to 100 mg/L.

RESULTS

Kinetic modeling using the generic Monod equation (equation 6) was applied to batch suspended growth kinetic tests on a range of Geropon TC-42® concentrations (16-138 mg/L).

$$\frac{dS}{dt} = -\frac{\mu_{\max}}{Y}\frac{S}{K_S + S}X \qquad \textbf{(15)}$$

Samples drawn from the reactors at different time intervals were analyzed for Geropon TC-42® and nitrate (Figures 3 and 4). Tests were used to determine biokinetic coefficients: cell yield (Y), specific growth rate (μ_{max}), and the half-saturation constant (K_S). Control reactor results showed that the removal of Geropon TC-42® via any other means than biodegradation was negligible. As expected, no lag phase occurred in the degradation of Geropon TC-42® because cultures had been acclimated (Sahinkaya and Dilek 2007).

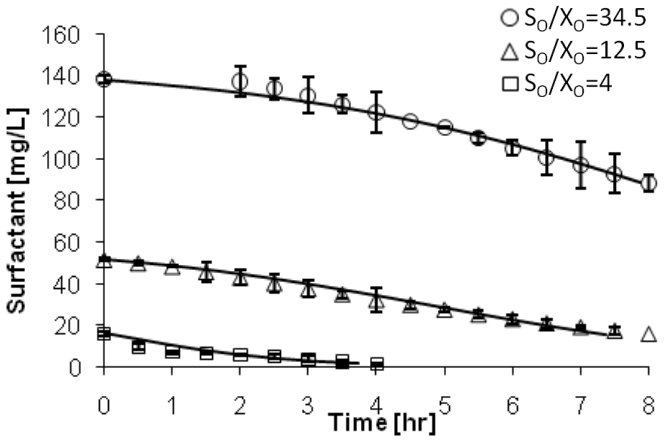

Figure 3. Time course variation of Geropon TC-42®. Data points represent experimental data, while smooth curves are the results of fitting the integrated Monod equation.

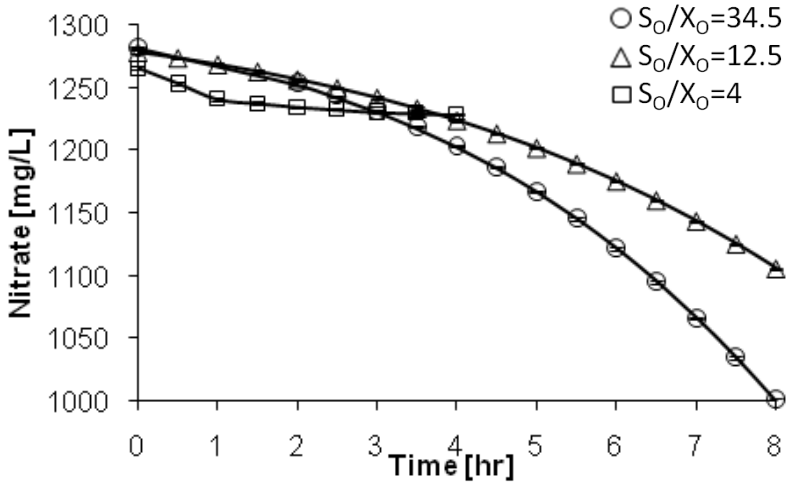

Figure 4. Time course variation of nitrate. Data point represents experimental data, while smooth curves are the results of fitting the integrated Monod equation.

Further, net specific growth rate dependence on substrate concentration was used to gauge any inhibitory effects. The rate of substrate utilization and microbial growth can be slowed by inhibitory compounds. Substrate utilization slows if the inhibitor affects a single enzyme active in that substrate's utilization. If the inhibitor affects a general cell function, biomass generation could decrease, decreasing substrate utilization. Nevertheless, some inhibitors can increase substrate utilization as the cell tries to compensate for the negative effects of the inhibitor. (Rittmann and McCarty 2001).

Evaluation of Cell Yield

To estimate surfactant and nitrate cell yield (*Y*), linear regression analysis was performed on data obtained from three sets of simultaneous batch experiments for each

S_0/X_0 ratio to fit equation 16. Linear curves were obtained with R^2 values ranging from 0.89 to 0.98 using the following expression for *Y*:

$$Y = -\frac{r_{growth}}{r_{substrateutilization}} = -\frac{\Delta X_a}{\Delta S} \quad \textbf{(16)}$$

The surfactant cell yield increased from 0.28 to 0.5 mg TSS/mg surfactant with an increase in S_0/X_0 from 4 to 12.5 and 34.5 (Figure 5). With an increase in surfactant utilization there was a proportional increase in biomass concentration. For Geropon TC-42® utilization by enriched activated sludge under anoxic conditions at 32ºC, the substrate converted into biomass was larger with the same substrate utilization, but with higher initial surfactant concentration *(S_0)*. Further, the regression intercept did not cross at zero suggesting that cell multiplication is not possible at low substrate concentrations. The data is linear for the 12.5 S_0/X_0 ratio. Therefore, slopes were determined for different parts of the graph and used for the evaluation of K_S and μ_{max}.

The nitrate cell yield was 0.10 mgTSS/mgNO_3 for the 3 S_0/X_0 ratios (Figure 6). The initial nitrate concentration was approximately the same for all experiments. The substrate converted into biomass did not vary for the three experiments and the regression intercept of zero suggests that cell multiplication is not affected by low concentrations.

(a) S_0/X_0=4

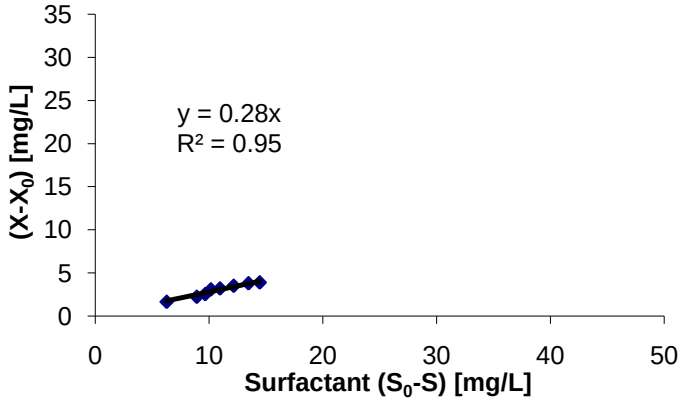

(b) S_0/X_0=12.5

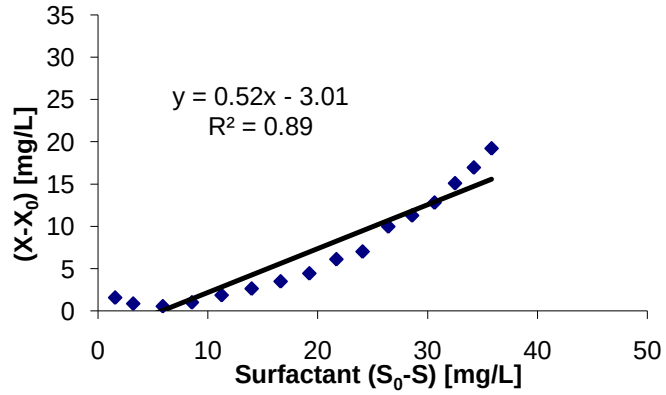

(c) S_0/X_0=34.5

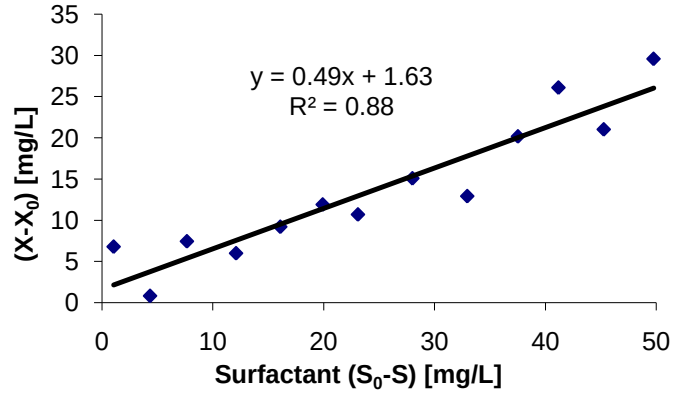

Figure 5. Surfactant Cell Yield (a)S_0/X_0=4 (b) S_0/X_0=12.5 (c) S_0/X_0=34.5

(a) $S_0/X_0=4$

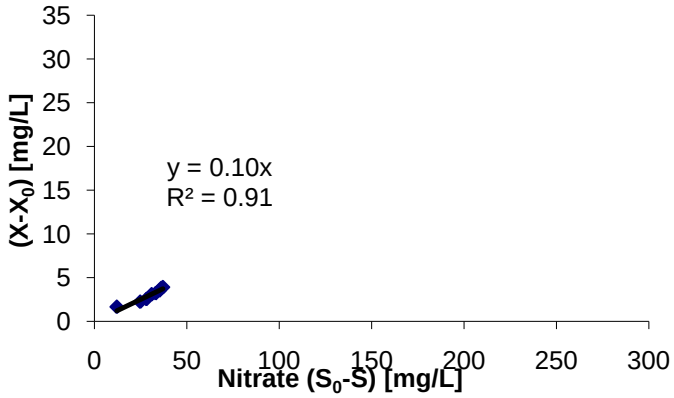

(b) $S_0/X_0=12.5$

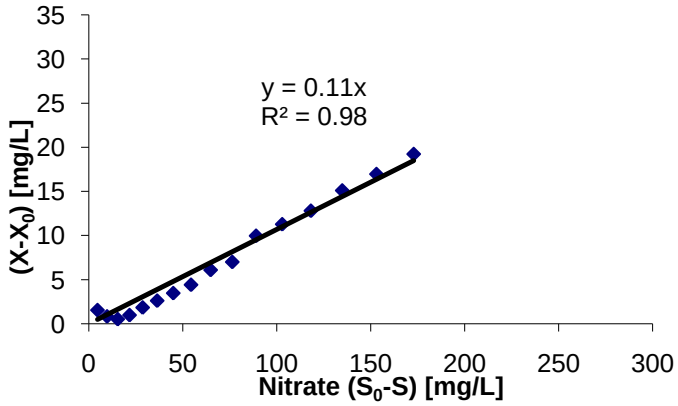

(c) $S_0/X_0=34.5$

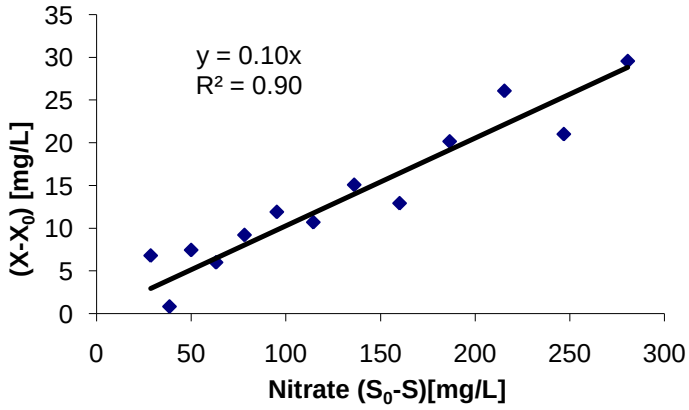

Figure 6. Nitrate Cell Yield for a. $S_0/X_0=4$ b. $S_0/X_0=12.5$ c. $S_0/X_0=34.5$

Evaluation of Specific Growth Rate and Half-Saturation Constant

A linearized form of the Monod equation can be used to evaluate bacterial reaction rates by plotting the inverse rate and substrate concentration. However, application of linear regression to linearized data is not appropriate because the resulting transformations of the measurement errors are unknown. Nonlinear curve-fitting methods are more adaptable and can be used to directly compare experimental data to an equation or model proposed to describe the process occurring in the experiment. (Kumar et al. 2005; Robinson 1985; Smith et al. 1997; Smith et al. 1998).

Non-linear least-squares analysis of nonlinear equations can provide accurate estimates of rate coefficients (Smith et al. 1998). The integrated Monod equation is useful in many applications for evaluating bacterial transformation rate coefficients. According to Smith et. al. (1998), the active cell concentration with growth substrate utilization can be described by

$$X_a = X_{a,0} + Y(S_0 - S) \quad \textbf{(17)}$$

Equations 15 and 17 can be combined to obtain the integrated Monod equation for growth substrate:

$$t = \frac{Y}{\mu_{\max}}\left\{\left(\frac{K_S}{X_{a,0}+YS_0}+\frac{1}{Y}\right)\ln\left[X_{a,0}+Y(S_0-S)\right]+\left(\frac{K_S}{X_{a,0}+YS_0}\right)\ln\left(\frac{S_0}{X_{a,0}S}\right)-\frac{1}{Y}\ln\left(X_{a,0}\right)\right\} \quad \textbf{(18)}$$

where $\frac{\mu_{\max}}{Y}$ is the maximum specific rate of substrate utilization (q_{max}). Estimates of the parameters and the 95% confidence standard error were determined by trial and error using the solver function in a spreadsheet program following the procedure described by

Smith et al. (1998). To define a curve for nonlinear parameter estimation, 8 to 10 data points have been shown to be sufficient by Robinson (1985). A minimum of 9 data points were used for the nonlinear analysis in this study to determine the kinetic constants.

The surfactant saturation constant (K_S) increased from 10 to 126 g/L with an increase in S_0/X_0 from 4 to 12.5, but decreased to 6.9 g/L for a S_0/X_0 ratio of 34.5 (Figure 7 and Table 1). The maximum growth rate (μ_{max}) increased from 260 to 833 g/g-d with an increase from 4 to 12.5, in S_0/X_0 but decreased from 833 to 14.5 g/g-d with an increase in S_0/X_0 from 12.5 to 34.5 (Figure 7 and Table 1). Since the data for change in biomass concentration and change in substrate concentration form the experiment with S_0/X_0 ratio of 12.5 was not linear, the estimates were also calculated using Y within the slope range of the data and were found to be within the reported error range. The nitrate saturation constant was approximately 5 g/L for all S_0/X_0 ratios (Figure 8 and Table 2). The maximum growth rate was approximately 1 g/g-d for all S_0/X_0 ratios (Figure 8 and Table 2).

Table 1. Surfactant maximum growth rate, half-saturation, and maximum specific rate of substrate utilization estimates and confidence standard error (S.E.)

S_0/X_0 (mg/mg TSS)	**4**		**12.5**		**34.5**	
Kinetic Parameters	Estimate	S.E.	Estimate	S.E.	Estimate	S.E.
K_S (g/L)	10.5	7.2	126	82	6.9	1.1
μ_{max} (d^{-1})	261	17	834	54	14.5	2.0
q_{max} (g/g-d)	966	66	1603	104	29.6	5.0

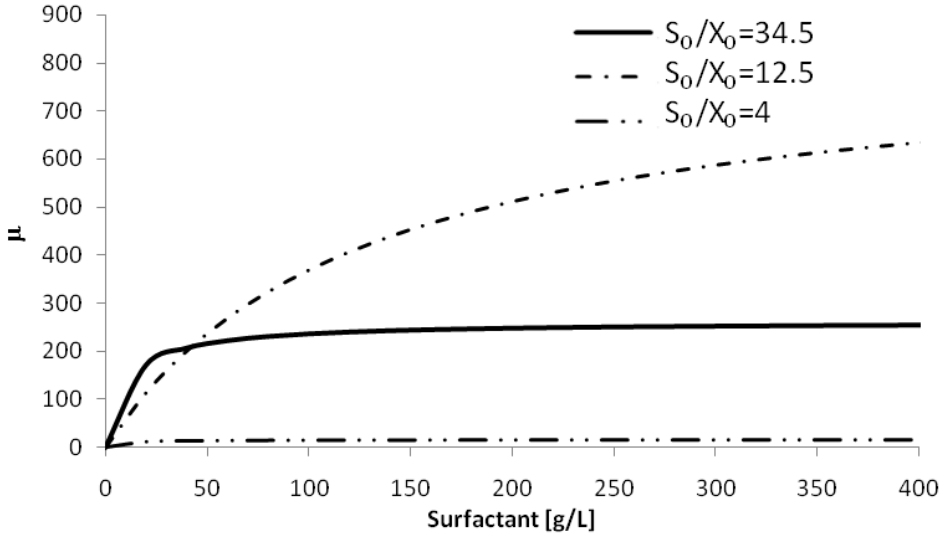

Figure 7. Net specific growth rate dependence on surfactant concentration

Table 2. Nitrate maximum growth rate, half-saturation, and maximum specific rate of substrate utilization estimates and confidence standard error (S.E.)

S_0/X_0 (mg/mg TSS)	**4**		**12.5**		**34.5**	
Kinetic Parameters	Estimate	S.E.	Estimate	S.E.	Estimate	S.E.
K_S (g/L)	5.4	2.5	5.9	0.5	4.7	1.5
μ_{max} (d^{-1})	1.1	0.4	1.2	0.1	1.3	0.3
q_{max} (g/g-d)	11	4.0	12.3	0.9	13	3.2

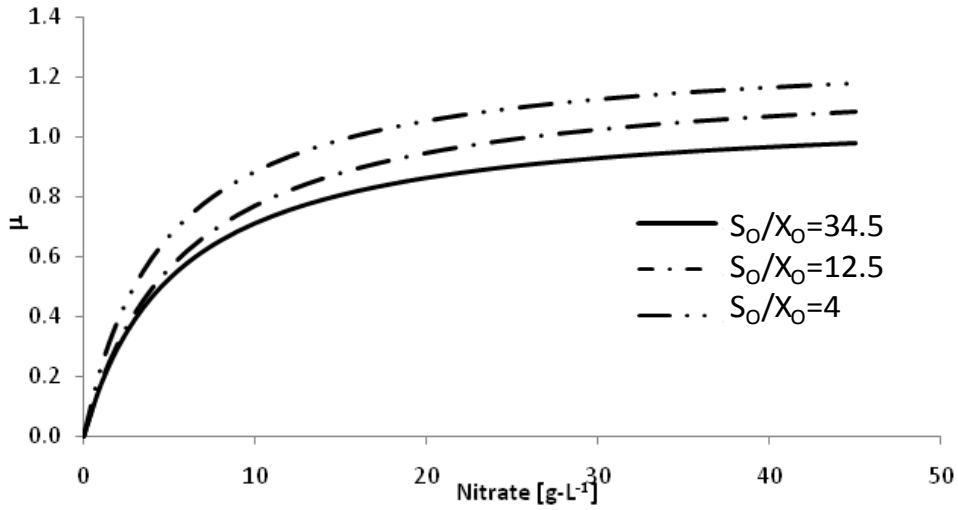

Figure 8. Net specific growth rate dependence on nitrate concentration

Comparison of Experimental Nitrate Utilization and Theoretical Nitrate Demand

Nitrate utilization was calculated as the amount of nitrate utilized form time zero to the end of each time interval. The theoretical nitrogen demand (ThND) was calculated as the stoichiometric amount of nitrate required to completely oxidize the surfactant carbon to CO_2. Comparison of the ThND to the observed nitrogen utilization reveals the relationship between the degradation mechanism of the surfactant and inhibition effects. At low concentrations (Figure 9) the ThND closely follows the observed nitrate demand. This suggests that at low surfactant to biomass ratios, there is little inhibition. At higher surfactant to biomass ratios (Figures 10 and 11) the ThND is higher than the observed nitrate demand. This suggests that when there is more surfactant present, inhibition behavior is indicated or there is a step in the degradation pathway of the surfactant that does not utilize nitrate for conversion to CO_2. The

average difference between the ThND and observed nitrate demand at a S_0/X_0 of 12.5 was approximately 0.2. The average difference between the ThND and observed nitrate demand at a S_0/X_0 of 34.5 was approximately 0.4. Therefore, 2.8 fold increase in S_0/X_0 ratio yielded in a 2 fold increase in the average difference between the ThND and observed nitrate demand indicating that surfactant self inhibition may be occurring. At the highest surfactant to biomass ratio (S_0/X_0=34.5), the nitrate demand increases then decreases and then increases again (Figure 11). The discontinuous upward trend indicates that nitrate utilization is slowed and then overcome. Possible factors controlling this slowed nitrate use could be mass transport limitations or a limiting step in the degradation pathway of the surfactant that does not utilize nitrate for conversion to CO_2.

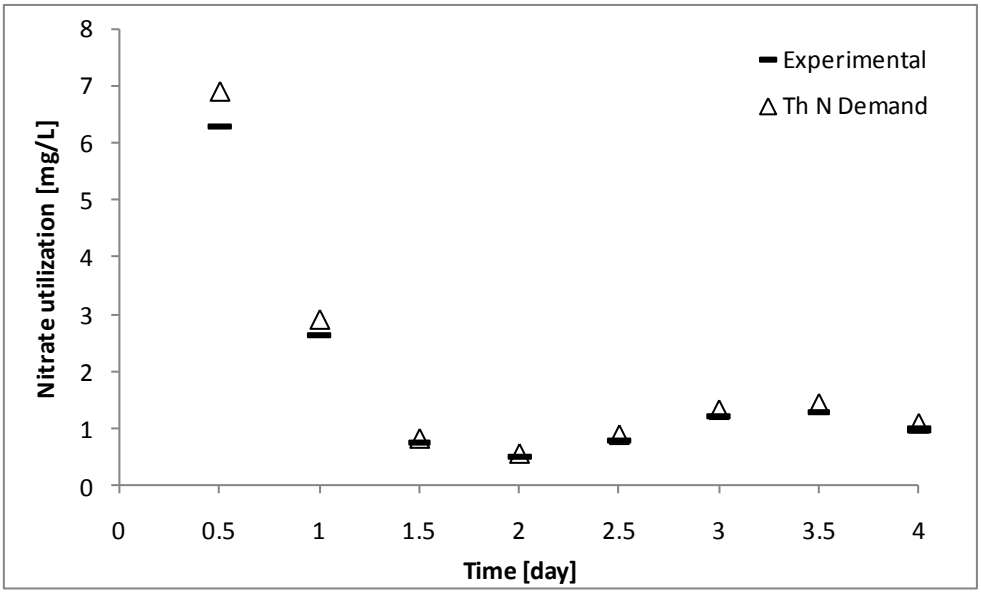

Figure 9. Comparison of experimental nitrate utilization and theoretical nitrate demand (Th N Demand) for S_0/X_0=4

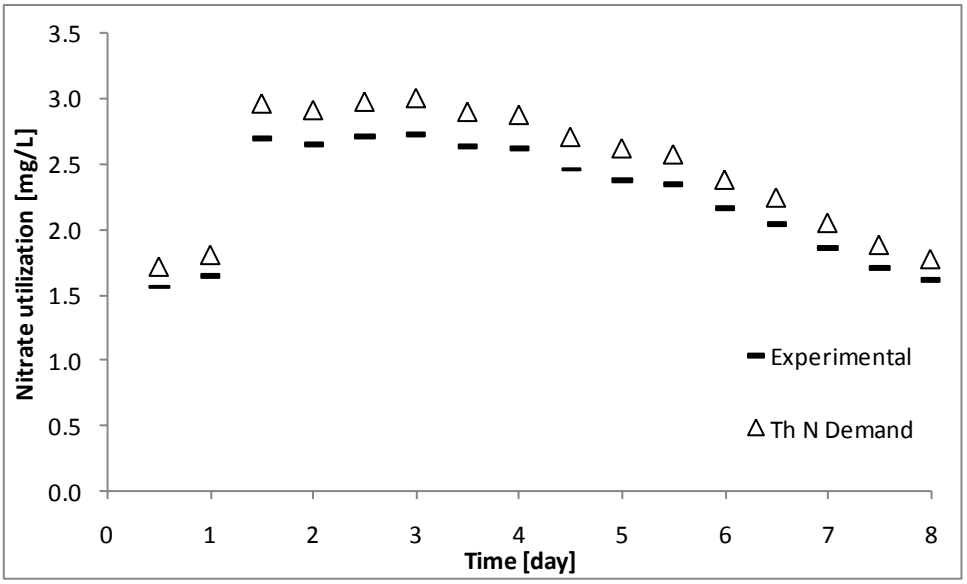

Figure 10. Comparison of experimental nitrate utilization and theoretical nitrate demand (Th N Demand) for S_0/X_0=12.5

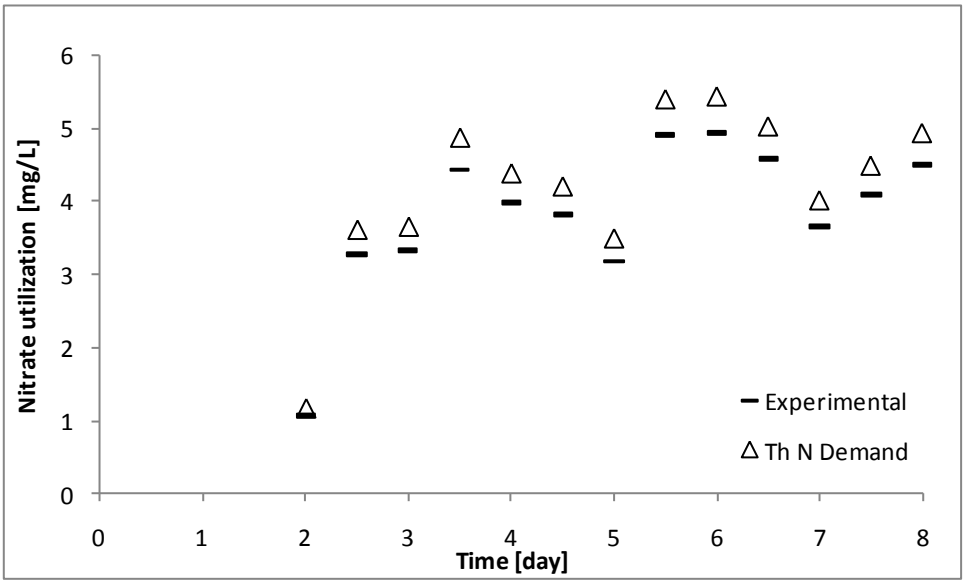

Figure 11. Comparison of experimental nitrate utilization and theoretical nitrate demand (Th N Demand) for S_0/X_0=34.5

DISCUSSION

Repeatability of Kinetic Results

Changes in culture history are largely responsible for the variations observed in values of reported Monod kinetic parameters (Grady et al. 1996; Kovarova-Kovar and Egli 1998; Molchanov et al. 2007). Culture conditions will affect the expressed enzymatic systems and the cell physiological state. The specific cell macromolecular composition will determine enzyme synthesis rates and functions. The three kinetic experiments were initiated with different initial substrate concentrations and the results shown in (Figure 3) reveal standard deviations that are proportional to the concentration values. This indicates that the variance is proportional to the real value which could be described as an analytical error. Considering that it is almost impossible to prepare two solutions with an identical biomass concentration, it can be concluded that the kinetic experiments can be reproduced.

Inhibition

As a simplifying assumption, the degradation of Geropon TC-42® was assumed to depend on only one enzyme and therefore any inhibitor would affect the single enzyme that is active in substrate utilization. While this may be an oversimplification, it provides an approximation of the case in which degradation kinetics are controlled by the slowest enzyme reaction. How an inhibitor affects growth and substrate utilization kinetics can be reflected in the value of the kinetic parameters. The most common types of inhibition were reviewed by Rittman and McCarty (2001) and are: self-inhibition, competitive inhibition, and non-competitive inhibition. In self-inhibition, high

concentrations of the substrate slow the enzyme-catalyzed degradation and affect both q_{max} and K_S. In competitive inhibition, a separate inhibitor binds the catalytic site of the degradative enzyme excluding substrate binding and the only parameter affected is K_S. In non-competitive inhibition, a separate inhibitor binds with the degradative enzyme at a site different from the reaction site slowing substrate utilization; only affecting the parameter q_{max}. Self-inhibition characteristics were observed for surfactant kinetics because both q_{max} and K_S changed for different S_0/X_0 (Table 1). Because Geropon TC-42® is not a common substrate, its degradation is most probably dependent on only one specialized enzyme, and therefore, high surfactant concentrations will slow the enzyme-catalyzed degradation affecting both q_{max} and K_S. No inhibition characteristics were observed for nitrate kinetics as the parameters did not vary significantly with changes in S_0/X_0 ratios. Inhibitory effects were observed for surfactant utilization but not for nitrate utilization because the degradation of Geropon TC-42® most probably depends on only one specialized enzyme and nitrate degradation does not.

CONCLUSION

The biodegradation kinetics of Geropon TC-42® by a mixed microbial culture was investigated using batch experiments. The mixed culture produced data which can be used in real-scale biodegradation applications. Estimated kinetic values can be used in plug flow, batch or continuously stirred tank reactor mass balances to determine design parameters like reactor volume, flow rate, biomass retention time, and residence time for anoxic suspended or attached culture. Surfactant degradation data indicates that biomass to surfactant mass ratios should be around 12.5. Lower ratios will not sustain

biomass metabolism and higher ratios will inhibit substrate utilization. At reactor start-up, a small initial substrate removal lag phase should be expected due to the steep slope observed at low surfactant concentrations in the curver of initial net specific growth rate.

Special considerations need to be taken into account when designing a wastewater treatment system for human space habitation due to low gravity and space availability. The system should address poor oxygen mass transfer, footprint restrictions, ease of maintenance for astronauts, transport from Earth to final location, and system start-up. A suitable wastewater treatment system can be designed by using estimated values to determine reactor volume, flow rate, and residence time for an anoxic attached culture plug flow reactor.

CHAPTER III

CONSTANT MICROBIAL DENSITY BIOFILM MODEL ON INERT MEDIA

In this chapter, a mathematical description of the kinetics of an anoxic biofilm on inert media that accounts for the dynamic nature of the biofilm is derived using diffusive mass transport assumed to follow Fick's law, and double substrate-limiting biodegradation. The model was constructed from component-models using appropriate boundary and initial conditions to define the system. The anoxic biofilm model was developed based on the principles of substrate biodegradation under anoxic conditions. The derived system represents a mathematical description for the kinetics of an anoxic double substrate-limited biofilm on inert media.

INTRODUCTION

Biofilms are dynamic systems where mass transport in and out is coupled with microbial growth and death. Mathematical models have been developed to describe biofilms in processes or reactors for a wide range of applications (Rittmann and McCarty 2001). Therfore, biofilm reactors for wastewater treatment have become technically as well as economically feasible options. Advances in models to optimize reactor design and enhance operational efficiency have been studied by Saravanan and Sreekrishnan (2006). Rittmann et al. (2002) also reported a one-dimensional transient-state, multiplespecies biofilm model focusing on the kinetics of growth-related microbial products. Multidimensional modeling approaches to investigate the structural

heterogeneity of the biofilm have been studied by Alpkvist et al. (2006), Laspidou and Rittmann (Laspidou and Rittmann 2004a; b) , and Laspidou et al. (2005).

For the design and operation of biofilm systems in wastewater treatment processes, models typically assume a constant biofilm thickness where the biofilm growth changes are not considered significant (Wanner and Reichert 1996). However, these models do not account for the dynamic nature of the biofilm. Defining the biofilm as a layer of microorganisms formed by their attachment on an inert surface, the biofilm/liquid interface can be considered as a moving boundary accounting for biofilm growth. Biofilm growth is closely related to microbial growth, which has an auto-catalytic effect on the substrate dynamics (Lee and Park 2007). In this study, a mathematical description for the kinetics of a biofilm on an inert medium that accounts for the dynamic nature of the biofilm is developed. The model incorporates diffusive mass transport, double substrate-limiting biodegradation, and biofilm growth. The diffusive mass transport is assumed to follow Fick's law and to only occur in the perpendicular direction to the inert media due to the small dimension of the biofilm. Further, even though the density of the biofilm most likely changes as a function of the perpendicular distance to the inert media, it is assumed constant on average across the depth of the biofilm.

An anoxic biofilm process is defined in this study as a column filled with inert media and sealed from the atmosphere to maintain a mostly oxygen-free environment. Microorganisms become attached to the inert packing media and trapped in void spaces. As the substrate passes through the packing material, it is utilized by the attached

biomass. The one-dimensional double substrate-limiting constant microbial density biofilm model on inert media was applied to the microbial anoxic degradation of Geropon TC-42® as the electron donor and nitrate as the terminal electron acceptor.

MODEL DESCRIPTION

Assumptions for Biofilm Kinetic Model

The derivation of the mathematical expressions describing the dual-substrate limiting utilizations in the anoxic biofilm is based on the same assumptions made by Chang and Rittmann (1987):

1. The biofilm is homogeneous.
2. The biofilm density is constant.
3. Attachment of bacteria from fsuspended biomass is negligible; therefore, an increase in biofilm thickness is due to the growth of biofilm.
4. The biofilm growth does not affect the flow pattern of liquid in the reactor because the biofilm volume is negligible with respect to the volume of the inert material.
5. The suspended biomass is kinetically negligible in the liquid phase.
6. Two substrates are both diffusion and reaction limiting within the biofilm.
7. Fick's law governs diffusion in the biofilm.
8. Biofilm is fully penetrated because growth depends on the concentration of surfactant inside the biofilm with boundary condition stating that the concentration of surfactant is zero at the wall.

Two implications of these assumptions are that a homogeneous biofilm implies diffusion is only in the perpendicular direction to the inert media and a constant biofilm density requires a dynamic biofilm/liquid phase boundary.

Time-variant Spatial Distribution of Soluble Components within the Biofilm

The biofilm model is based on a material balance across the biofilm volume where concentration gradients are governed by diffusion following Fick's second law and biologically mediated reactions governed by double Monod kinetics (equation 11). The conceptual basis of the biofilm on inert media used in this study is illustrated in Figure 12. Mass transport by diffusion is assumed to be one-dimensional because the biofilm is assumed to be thin in the *z* direction relative to the *x* and *y* directions (Grady 1982).

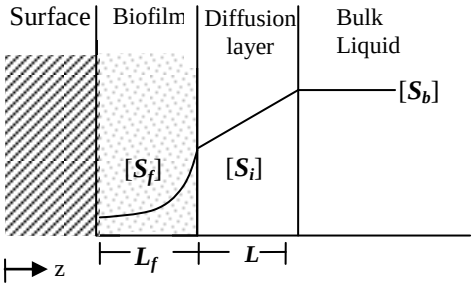

Figure 12. Concentration profile for one substrate in biofilm (adapted from Rittmann and McCarty (2001))

The biofilm characteristics depicted (Figure 12) are defined as: S_b is the substrate concentration in the bulk liquid, S_i is the substrate concentration in the liquid-biofilm interface S_f is the substrate concentration in the biofilm, L is the thickness of the liquid-biofilm interface, and L_f is the thickness of the biofilm.

The governing non-steady-state partial differential equation for surfactant utilization in the biofilm is:

$$\frac{\partial S_{f,S}}{\partial t} = D_{f,S}\frac{\partial^2 S_{f,S}}{\partial z_f^2} - r_{ut,S} \qquad 0 \le z \le L_f \qquad \textbf{(19)}$$

where $S_{f,S}$ is the surfactant concentration in the biofilm (mass/volume), $D_{f,S}$ is the surfactant diffusion coefficient in the biofilm (area/time), and $r_{ut,S}$ is the utilization rate of the surfactant described in equation 12 (mass/volume time) with the initial condition,

$$S_{f,S} = 0 \qquad \text{at } t = 0 \text{ and } 0 \le z \le L_f \qquad \textbf{(20)}$$

The boundary condition at the biofilm/attachment-media interface eliminates diffusion through the inert attachment-media.

$$\frac{\partial S_{f,S}}{\partial z_f} = 0 \qquad \text{at } z_f = L_f \text{ and } t \ge 0 \qquad \textbf{(21)}$$

A relationship between the mass flux at the biofilm/liquid and the difference between the concentrations at the interface and that in the bulk liquid is in accord with Fick's first law as specified in the boundary condition.

$$\frac{\partial S_{f,S}}{\partial z_f} = \frac{D_{b,S}}{D_{f,S}L}\left(S_{b,S} - S_{f,S}\right) \quad \text{at } z_f = 0 \qquad \textbf{(22)}$$

where, $D_{b,S}$ is the bulk phase surfactant diffusivity (area/time), L is the boundary layer thickness (distance) and $S_{b,S}$ is the surfactant concentration in the bulk liquid (mass/volume).

Within the anoxic biofilm, denitrifying bacterial growth requires nitrate as the electron acceptor. The governing non-steady-state partial differential equation and boundary conditions for nitrate utilization in the anoxic biofilm is:

$$\frac{\partial S_{f,N}}{\partial t} = D_{f,N}\frac{\partial^2 S_{f,N}}{\partial z_f^2} - r_{ut,N} \qquad 0 \le z \le L_f \qquad \textbf{(23)}$$

where, $S_{f,N}$ is the surfactant concentration in the biofilm (mass/volume), $D_{f,N}$ is the nitrate diffusion coefficient in the biofilm (area/time), and $r_{ut,N}$ is the nitrate utilization rate described in equation 13 (mass/volume time). The boundary and initial conditions are similar to those for surfactant utilization (equation 19):

$$S_{f,N} = 0 \qquad \text{at } t = 0 \text{ and } 0 \le z \le L_f \qquad \textbf{(24)}$$

$$\frac{\partial S_{f,N}}{\partial z_f} = 0 \qquad \text{at } z_f = L_f \text{ and } t \ge 0 \qquad \textbf{(25)}$$

$$\frac{\partial S_{f,N}}{\partial z_f} = \frac{D_{b,N}}{D_{f,N}L}\left(S_{b,N} - S_{f,N}\right) \text{ at } z_f = 0 \qquad \textbf{(26)}$$

where, $D_{b,N}$ is the bulk phase surfactant diffusivity (area/time), and $S_{b,N}$ is the surfactant concentration in the bulk liquid (mass/volume).

Time-variant Spatial Distribution of Particulates within the Biofilm

The biomass in the biofilm is dynamic with the potential to increase or decrease with time. However, to satisfy the assumption of constant biofilm density, the biofilm volume must increase as the biofilm grows. Therefore, the thickness of the biofilm increases as the volume increases, and the substrate diffuses through a boundary that is moving with time. The moving boundary is the biofilm-liquid interface. Since the

biofilm grows proportional to surfactant and nitrate uptake, at any position inside the biofilm, a material balance on biofilm is

$$\frac{d\left(X_f\,dz\right)}{dt} = \mu_{\max}\frac{S_{f,S}S_{f,N}}{\left(K_{S,S}+S_{f,S}\right)\left(K_{S,N}+S_{f,N}\right)}\left(X_f\,dz\right) - b\left(X_f\,dz\right) - b_S\left(X_f\,dz\right) \qquad \textbf{(27)}$$

where, *dz* is the thickens of a differential section of biofilm, *b* is the decay coefficient, and b_S is the biofilm shear stress loss coefficient. The biofilm volume can only grow in the *z* direction because the biofilm can only grow attached to the available inert media. Integrating equation 27 over the entire biofilm thickness,

$$\int_0^{L_f}\frac{d\left(X_f\,dz\right)}{dt} = \int_0^{L_f}\mu_{\max}\frac{S_{f,S}S_{f,N}}{\left(K_{S,S}+S_{f,S}\right)\left(K_{S,N}+S_{f,N}\right)}\left(X_f\,dz\right) - \int_0^{L_f} b\left(X_f\,dz\right) - \int_0^{L_f} b_S\left(X_f\,dz\right) \qquad \textbf{(28)}$$

yields

$$\frac{d\left(X_f L_f\right)}{dt} = \mu_{\max}\int_0^{L_f}\frac{S_{f,S}S_{f,N}}{\left(K_{S,S}+S_{f,S}\right)\left(K_{S,N}+S_{f,N}\right)}\left(X_f\,dz\right) - bX_f L_f - b_S X_f L_f \qquad \textbf{(29)}$$

The initial condition used to solve equation 29 is

$$L_f = L_{f,0} \text{ at } t = 0 \qquad \textbf{(30)}$$

Time-variant Distribution of Soluble Components in the Bulk Phase

The anoxic biofilm simulation used to develop the bulk phase concentration profiles was a completely mixed packed bed column reactor having a sufficiently high recycle flow rate to achieve the same bulk concentration throughout the length reactor. It was also assumed that utilization by suspended biomass was negligible.

Material balances for both the surfactant and nitrate included influent concentrations and diffusion from bulk to biofilm through the biofilm interphase. The

differential expressions for both surfactant ($S_{b,S}$) and nitrate ($S_{b,N}$) changes with time are expressed in the following equations:

$$\frac{dS_{b,S}}{dt} = \frac{Q}{V\varepsilon}\left(S^0_{b,S} - S_{b,S}\right) - \frac{D_{b,s}}{L}\left(S_{b,S} - S_{i,S}\right)\frac{A}{V\varepsilon} \quad \textbf{(31)}$$

$$\frac{dS_{b,N}}{dt} = \frac{Q}{V\varepsilon}\left(S^0_{b,N} - S_{b,N}\right) - \frac{D_{b,N}}{L}\left(S_{b,N} - S_{i,N}\right)\frac{A}{V\varepsilon} \quad \textbf{(32)}$$

with the following initial conditions,

$$S^0_{b,S} = 0 \text{ at } t = 0 \quad \textbf{(33)}$$

$$S^0_{b,N} = 0 \text{ at } t = 0 \quad \textbf{(34)}$$

where, Q is the flow rate (volume/time), V is the reactor volume (volume), ε is the porosity, $S^0_{b,S}$ is influent surfactant concentration (mass/volume), A is the reactor cross-sectional area (area) , X_b is the biomass concentration in the bulk liquid (mass/volume), and $S^0_{b,N}$ is influent nitrate concentration (mass/volume).

SOLUTION METHODS

Numerical Methods

The one-dimensional double substrate-limiting constant microbial density biofilm model on inert media consists of two non-linear partial differential equations (PDE), one integral differential equation, and two non-linear ordinary differential equations (ODE). The model was solved by first approximating the integral as a summation with differential volumes equal to the space grid used to solve the partial differential equations. The system of equations was solved using the "pdepe solver" provided in MATLAB software (The MathWorks Inc., Natick, MA). The "pdepe

solver" converts partial differential equations into ordinary differential equations using second order accurate spatial discretization based on a fixed set of user-specified nodes. After discretization, elliptic equations give rise to algebraic equations. The time integration is done with "ode15s" which solves the differential-algebraic equations. A summary of the model can be found in appendix A.

Determination and Selection of Model Parameters

Some values of the model parameters were adopted directly from the literature, some were calculated from reported relationships, and some were determined by laboratory measurements. Solute diffusivities in water were obtained from tabulations; film diffusivities were assumed to be 80% of diffusivities in water (Williamson and McCarty 1976a; 1976b). The shear stress loss coefficient was calculated according to Rittman and McCarty (2001) by

$$b_s = 0.0842 \times [\sigma]^{0.58} \quad \textbf{(35)}$$

where σ is the shear stress and is defined by White (1999) as

$$\sigma = \frac{F_D}{A} \quad \textbf{(36)}$$

where F_D is the drag force for a non spherical particle and A is the biofilm surface area. F_D is defined by Clark (1996) as

$$F_D = 3X\pi\mu U d_e \quad \textbf{(37)}$$

where X is the shape factor, μ is the absolute viscosity of water, d_e is the equivalent volume diameter, and U is the free-stream velocity defined as

$$U = \frac{\varepsilon Q}{A_c} \quad \textbf{(38)}$$

where Q is the flow rate, ε is the reactor porosity and A_c is the reactor cross-sectional area. A summary of the model parameters and the values used in this model simulation are shown in Table 3.

Table 3. Double substrate-limiting constant microbial density biofilm model parameters.

Symbol	Description	Value	References
Kinetic			
q_{max}	Maximum specific utilization	29.6 mg/mg-d	Chapter 2
b	Decay rate coefficient	0.079 day^{-1}	Alpkvist et al. (2006)
b_s	Shear stress loss coefficient	$0.0842 \times [\sigma]^{0.58}$	(Rittmann et al. 2001)
K_S	Substrate saturation coefficient	6.9 mg/cm^3	Chapter 2
K_{NO3}	Nitrate saturation coefficient	4.7 mg/cm^3	Chapter 2
Stoichiometric			
Y	Yield of biomass on substrate	0.5 mg/mg	Chapter 2
Mass transfer			
$D_{b,S}$	Substrate bulk-phase diffusivity	0.8 cm^2/day	Velev et al. (2000)
$D_{b,N}$	Nitrate bulk-phase diffusivity	1 cm^2/day	Alpkvist et al. (2006)
$D_{f,S}$	Substrate diffusivity in biofilm	0.64 cm^2/day	Velev et al. (2000)
$D_{f,N}$	Nitrate diffusivity in biofilm	0.8 cm^2/day	Alpkvist et al. (2006)
L	Boundary layer thickness	60 micro m	Alpkvist et al. (2006)
Miscellaneous			
X	Particle shape factor	1.08	Clark (1996)
V_R	Reactor volume	430 cm^3	Laboratory data
ε	Reactor porosity	0.8	Laboratory data
Q	Influent flow rate	Variable	
A_c	Reactor cross-sectional area	20.27 cm^3	Laboratory data
A_f	Biofilm surface area	40 cm^3	Laboratory data
$S_{b,S}^0$	Substrate influent concentration	Variable	
$S_{b,N}^0$	Influent concentration of nitrate	Variable	

MODEL PERFORMANCE EVALUATION

To understand the performances of the model as conditions change, several numerical simulations were performed. The parameters that have an effect on reactor performance can be classified into: biological parameters, mass transport parameters, reactor geometry parameters, and operational parameters. The effects of changes in the operational and surfactant mass transport parameters were evaluated because they are the easiest to control in laboratory, pilot-scale, and system application situations. The effect of changes on the mass transport parameters were also evaluated due to the proprietary nature of the surfactant (Geropon TC-42®). The parameters that where changed in the different simulations were: influent surfactant concentration, influent nitrate concentration, flow rate, and surfactant diffusion coefficient. In all simulation studies, the following initial conditions were used: the particulates concentration in the biofilm (X_f) was 40mg/cm^3, the initial concentrations of the soluble components (S_b, N_b) in the bulk phase were all zero, and the initial biofilm thickness was 10 μm.

Effects of Flow Rate

The effect of changes in the influent flow rate on the surfactant effluent concentration and biofilm depth propagation were determined by changing the influent flow rate between 0.12 and 118 mL/min and maintaining the influent surfactant and nitrate concentrations both at 1.5 mg/cm^3 (Figure 13). As expected, higher flow rates made the dilute-in curve (Figure 13) steeper and caused it to reach a higher peak. The higher flow rate caused higher loadings, which resulted in the lower surfactant removal efficiencies and an increase in the time necessary to reduce the effluent substrate

concentration to the minimal level except for the highest flow rate (118 mL/min). At 0.12, 1.18, and 11.8 mL/min the effluent concentration are predicted to reduce to 0.0167, 0.168, and 0.022 g/L; but at 118 mL/min the effluent concentration is predicted to reduce to 0.015 g/L. The lower effluent substrate and time necessary to reduce the effluent substrate concentration to the minimal level at the higher flow rate could be due to the higher mixing effect making substrate more uniformly distributed and readily available throughout the reactor volume and therefore the surface of the biofilm.

Higher flow rates resulted in a shorter hydraulic retention time and shorter startup periods (Figure 13). A shorter hydraulic retention time is expected at high flow rates because retention time is inversely proportional to flow rate. A shorter startup period is due to the increased movement of bacteria and substrate caused by higher flow rates. Since the substrate is more uniformly distributed, the bacteria can encounter substrate faster and therefore the biofilm depth can propagate faster. Propagation of the biofilm for different influent flow rates (Figure 14) resulted in the biofilm reaching steady state faster at higher flow rates. Even though biofilm propagated faster at higher flow rates, it is not a determining factor in the biofilm steady-state depth since it was approximately 0.015 cm for all flow rates (Figure 14).

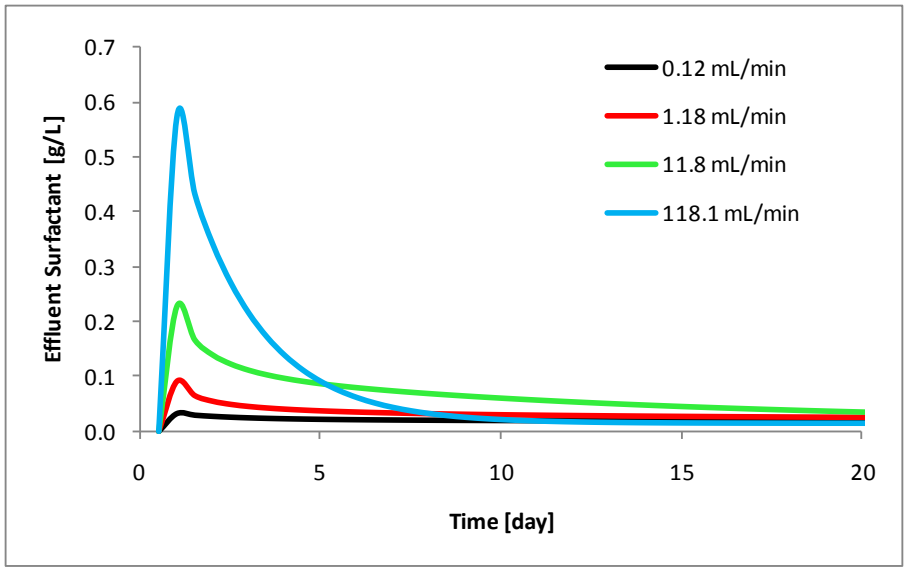

Figure 13. Effect of the influent flow rate (Q) on the surfactant effluent concentration

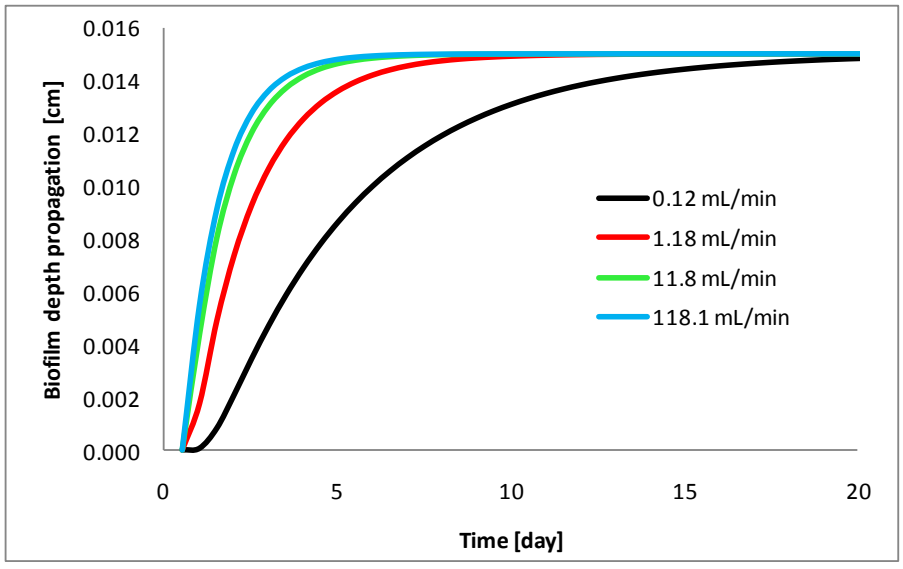

Figure 14. Effect of the influent flow rate (Q) on the biofilm depth propagation

Effects of Influent Surfactant/Nitrate Concentration Ratio

The influent substrate is one of the operational parameters that affect the substrate loading rate. The effects of influent surfactant/nitrate concentration ratio on

the effluent surfactant concentration, effluent nitrate concentration, and biofilm depth propagation was studied by changing the influent surfactant and nitrate concentrations to achieve a ratio between 0.001 and 1.0 while keeping the influent flow rate at the operational flow rate of the laboratory test apparatus (11.8 mL/min). The effects on the surfactant effluent concentration are shown in Figure 15 for all influent surfactant/nitrate concentration ratios. A clearer view of the lowest two influent surfactant/nitrate concentration ratios is shown in Figure 16. Higher influent surfactant/nitrate concentration ratios resulted in longer startup periods because the biofilm would require more time to acclimate to the higher concentrations. The effluent substrate concentration minimal level increased proportionally with increases in influent surfactant/nitrate concentration ratios. A tenfold increase in influent surfactant/nitrate concentration ratio resulted in a tenfold increase in effluent substrate concentration minimal level.

Higher influent surfactant/nitrate concentration ratio supported more surfactant utilization and biofilm growth as shown by the propagation the biofilm for different influent concentration ratios. The effects on the biofilm depth propagation are shown in Figure 17 for all influent surfactant/nitrate concentration ratios. A clearer view of the lowest two influent surfactant/nitrate concentration ratios is shown in Figure 18. At the lowest surfactant influent concentration, the biofilm initially reduced in size (Figure 18) suggesting that the assumed initial biofilm depth was larger than that supported by the available substrate surfactant concentration.

Influent surfactant/nitrate concentration ratio did not significantly affect the nitrate effluent curve as shown in Figure 19. However, the higher influent surfactant/nitrate concentration ratio supported more nitrate utilization. Since the effluent concentration of this operational unit is higher than the nitrate maximum contaminant level (MCL) in drinking water (45 mg/L) by more an order of ten, further water treatment would be needed to achieve drinking water standards.

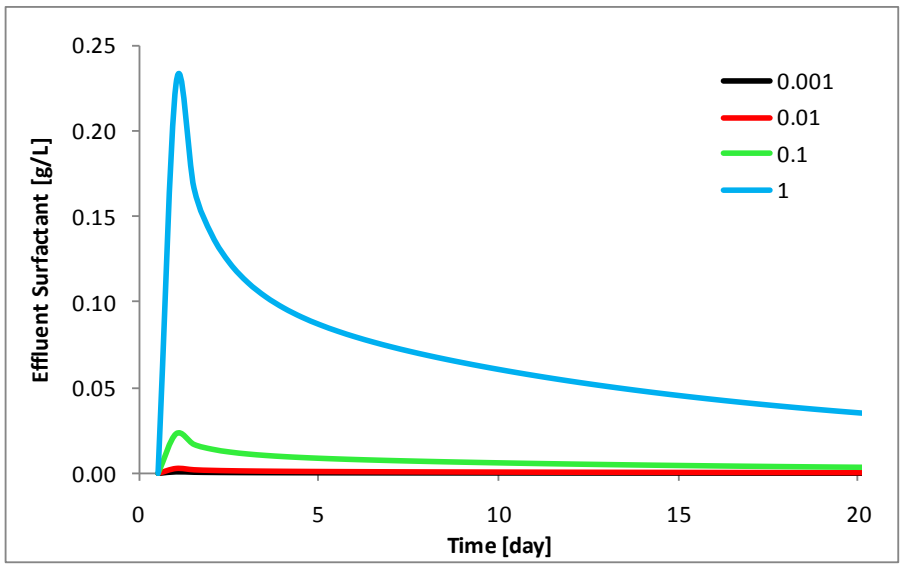

Figure 15. Effect of all influent surfactant/nitrate concentration ratios ($g \cdot L^{-1}$/ $g \cdot L^{-1}$) on the surfactant effluent concentration

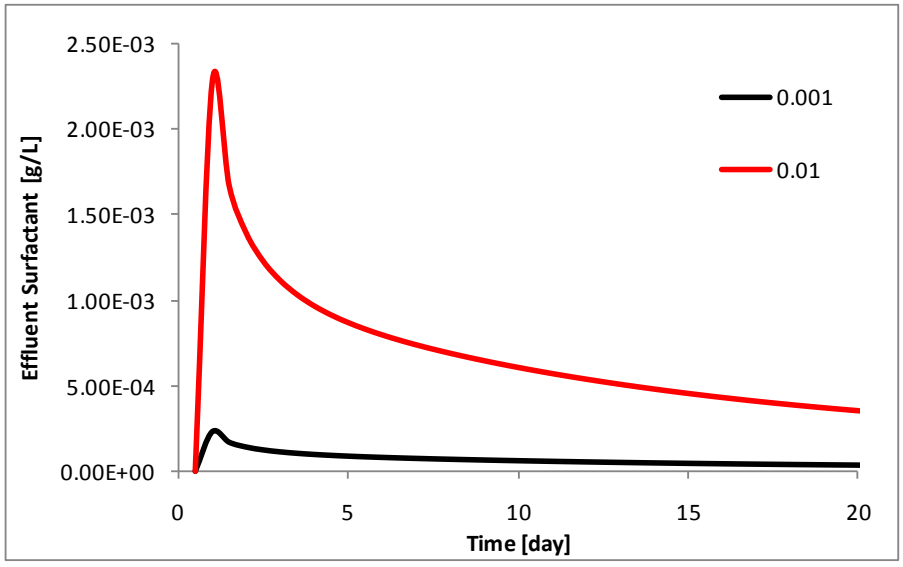

Figure 16. Effect of the lowest influent substrate/nitrate concentration ratio ($g \cdot L^{-1}$/ $g \cdot L^{-1}$) on the surfactant effluent concentration

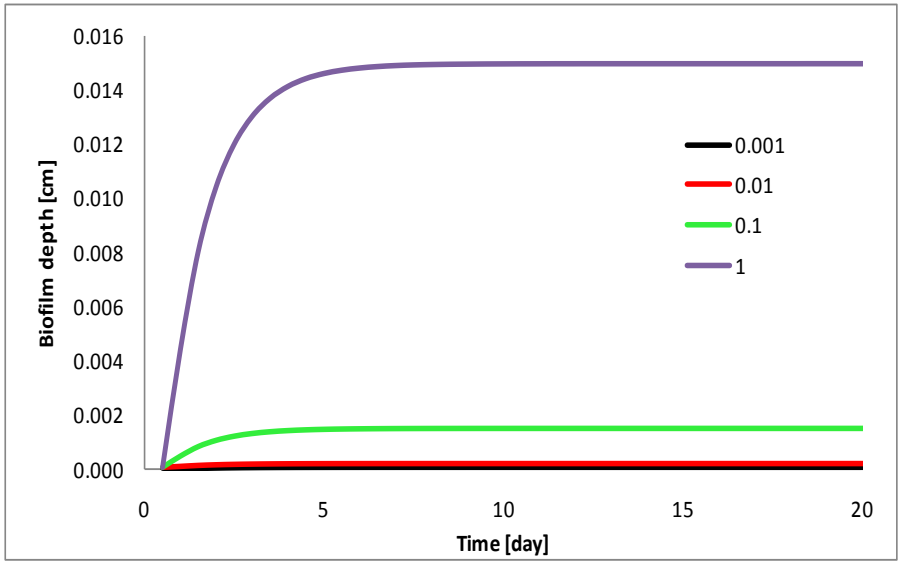

Figure 17. Effect of all influent substrate/nitrate concentration ratios ($g \cdot L^{-1}$/ $g \cdot L^{-1}$) on the biofilm depth propagation

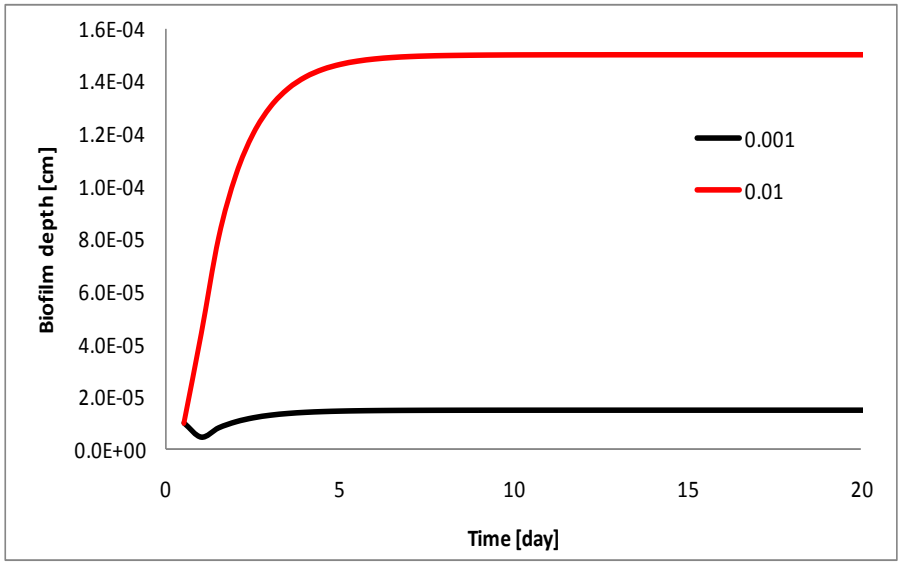

Figure 18. Effect of the lowest influent substrate/nitrate concentrations ratio ($g \cdot L^{-1}/ g \cdot L^{-1}$) on the biofilm depth propagation

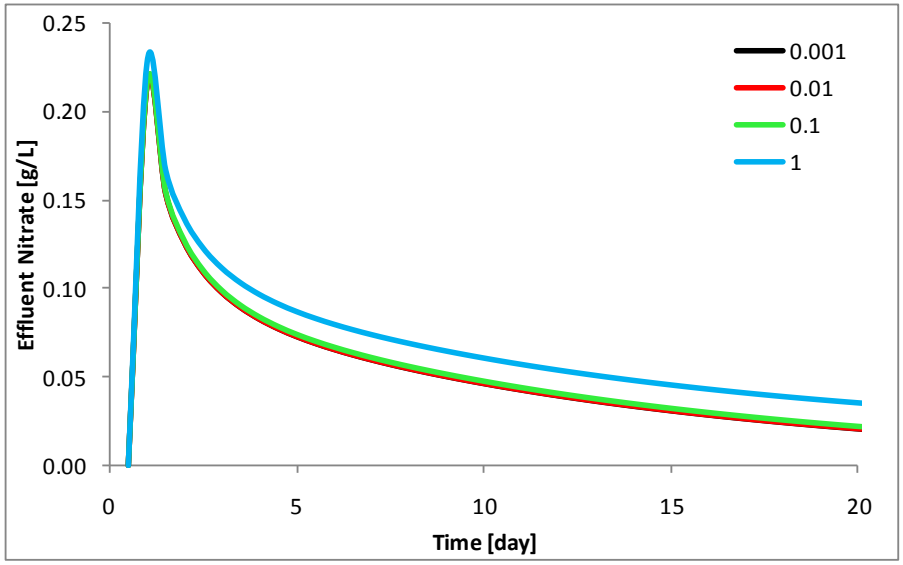

Figure 19. Effect of the influent substrate/nitrate concentration ratio ($g \cdot L^{-1}/ g \cdot L^{-1}$) on the nitrate effluent concentration

Effects of Surfactant Diffusion Coefficient

The effect of the surfactant diffusion coefficient on the surfactant effluent concentration, nitrate effluent concentration, and biofilm depth propagation were determined by changing the surfactant diffusion coefficient (0.2, 0.4, 0.6, 0.8 and 1 cm^2/day) and keeping the influent flow rate, the influent surfactant concentration, and the nitrate surfactant concentration at the laboratory reactor operational values of 11.8 mL/min, 1.5 g/L, and 1.5 g/L respectively. The surfactant diffusion coefficient did not affect the surfactant or nitrate effluent curve since all the diffusion coefficients predicted the same effluent curves. The surfactant and nitrate effluent curve are shown in Figure 20 and Figure 21. Only one curve is visible in each figure because all curves overlap. The diffusion coefficient and the liquid film inter-phase layer are so small as compared to the biofilm depth, that changes in the coefficient did not affect the value of the effluent concentration which has a magnitude much larger than the diffusion coefficient. The diffusion coefficient was more important in the biofilm depth propagation since mass transfer dictates the available substrate in the biofilm and the magnitude of the biofilm is closer to the magnitude of the diffusion coefficient than the effluent concentrations (Figure 22). The propagation of the biofilm for two surfactant diffusion coefficients (0.6 and 0.8 cm^2/day) is shown in Figure 22. Only two surfactant diffusion coefficients are shown in the figure because the curve for 0.2, 0.4, and 0.6 cm^2/day overlapped and the curve for 0.8 and 1 cm^2/day overlapped. The propagation of the biofilm shows that the biofilm reached steady state faster at lower surfactant diffusion coefficients. Even though biofilm propagated faster at lower surfactant diffusion

coefficients, it is not a determining factor in the biofilm steady-state depth since it was approximately 0.015 cm for all surfactant diffusion coefficients (Figure 22).

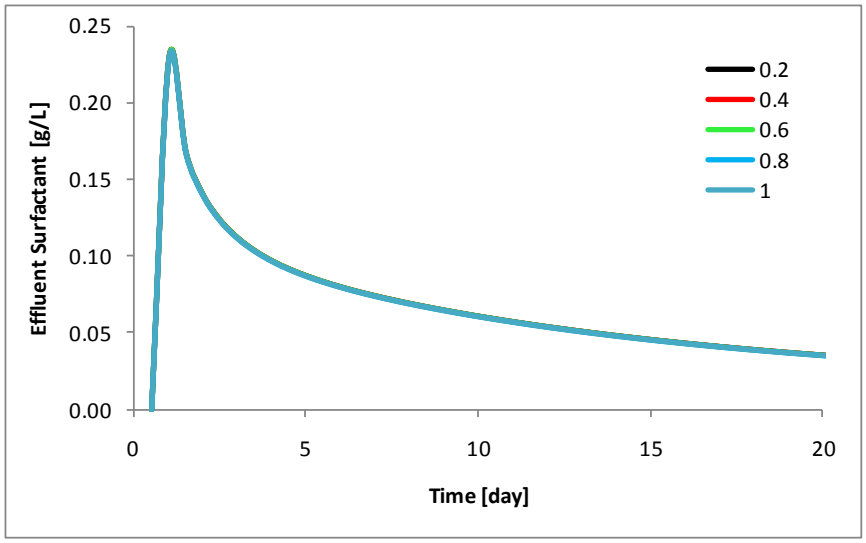

Figure 20. Effect of the surfactant diffusion coefficient on the surfactant effluent concentration

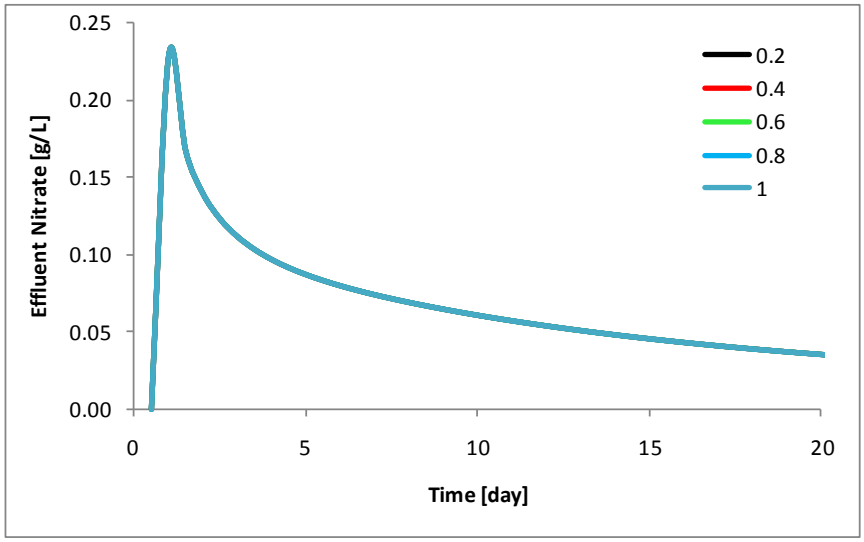

Figure 21. Effect of the surfactant diffusion coefficient on the nitrate effluent concentration

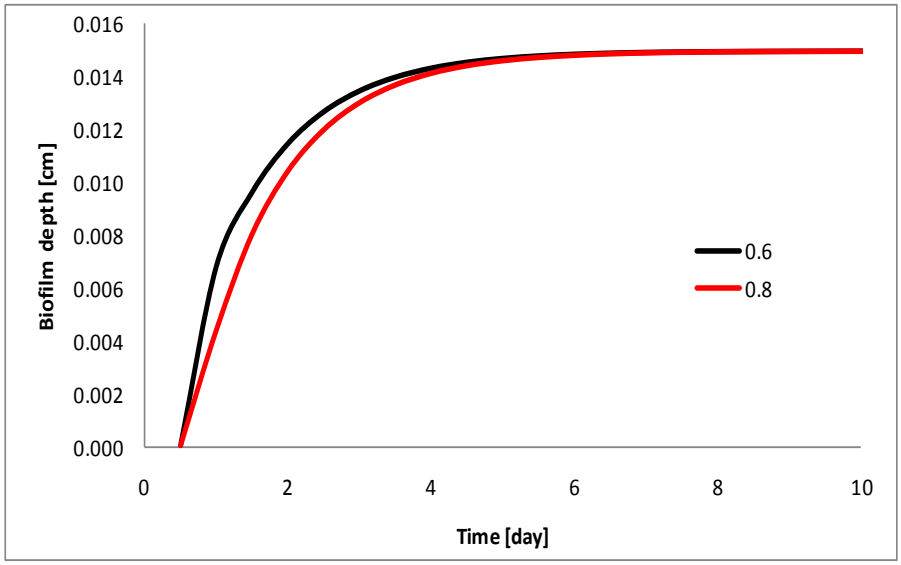

Figure 22. Effect of the influent surfactant diffusion coefficient on the biofilm depth propagation

CONCLUSIONS

Three features were used in the development of the model used in this study: simultaneous utilization and molecular diffusion, dual substrate-limiting biofilm, and a varying biofilm thickness. The sensitivity analysis showed that the surfactant diffusion coefficient does not affect the performance of the system. The influent flow rate, surfactant concentration, and nitrate concentration were most affected by the performance of the system. Higher flow rates resulted in a shorter hydraulic retention time, shorter startup periods, and faster biofilm steady-state. At steady-state, the higher flow resulted in lower surfactant removal. Higher influent surfactant/nitrate concentration ratios generated a longer startup period, sustained more surfactant utilization, and supported more biofilm growth. Influent surfactant/nitrate concentration ratios did not significantly affect the nitrate effluent curve. The model presented in this

study could be employed for the design of an anoxic biofilm treatment process for the removal of the surfactant Geropon TC-42®.

CHAPTER IV

BIOFILM MODEL ON INERT MEDIA USING THE CONCEPT OF SPACE OCCUPANCY

In the previous chapter, biofilm modeling was described by mass transport of substrates and microbial conversions assuming a homogeneous microbial density in the biofilm. In this chapter, a mathematical description of the kinetics of an anoxic biofilm on inert media is derived from component-models using the concept of space occupancy to allow changes in the microbial biofilm density. Appropriate boundary conditions and initial conditions were imposed to define the mathematical model system. The anoxic biofilm model was developed based on the principles of substrate biodegradation under anoxic conditions. The derived system represents a mathematical description for the kinetics of an anoxic double substrate-limited biofilm on inert media.

INTRODUCTION

Biofilm processes are used for potable water and wastewater treatment processes. Mathematical models have been developed to facilitate design biofilm treatment technologies. A weakness in the early biofilm models developed was how to describe substrate dynamics within biofilms, including substrate mass transport and utilization. Models like that developed by Williamson and McCarty (1976b) assumed predefined biofilm thickness and homogeneous microbial density in the biofilm. Biofilm growth is closely related to microbial growth, which has an auto-catalytic effect on the substrate dynamics (Lee and Park 2007). Assuming constant density may cause inaccurate model

predictions. In a biofilm, microorganisms are subject to variable conditions depending on time and distance from the film surface. Because the environmental differences present in a biofilm create non-homogeneous biofilm growth, particulate movement, such as inert residues, should be considered. Moreover, relocation of the biomass including all particulate components such as active microorganisms, inert residues, and extracellular polymeric substances (EPS) should be considered as the biomass exceeds a certain limit of space availability (Lee and Park 2007).

In this study, a model was developed that takes into account the non-homogenous nature of the biofilm, particulate movement within the biofilm, and biomass attachment and detachment. The model was based on those developed by Wanner and Reichert (1996) and Lee and Park (2007). The model consists of a set of one-dimensional material balance equations where the biofilm thickness and the temporal and spatial distribution of dissolved (nutrients, electron donors, and electron acceptors) and particulate (microbial cells) components in a biofilm are modeled as a function of mass transport and bacterial reaction processes. The primary difference between the present model and constant microbial density biofilm model on inert media is that in this study dissolved components in the biofilm are not exclusively transported by molecular diffusion and that displacement of particulate components is not exclusively a result of biofilm volume changes (Costerton et al. 1994; Wanner and Reichert 1996). The biofilm liquid phase volume fraction (porosity) was assumed to vary with time and space (Wanner and Reichert 1996; Zhang and Bishop 1994a).

An anoxic biofilm process is defined in this study as a column filled with inert media and sealed from the atmosphere to maintain a mostly oxygen-free environment. Microorganisms become attached to the inert packing media and trapped in void spaces. As the substrate passes through the packing material, it is utilized by the attached biomass. The one-dimensional double substrate-limiting biofilm model on inert media using the concept of space occupancy was applied to the microbial anoxic degradation of Geropon TC-42® as the electron donor and nitrate as the terminal electron acceptor.

MODEL DESCRIPTION

The transport processes and the mathematical expressions considered to describe the biofilm model are described in this section.

Concept of Space Occupancy

Lee and Park (2007) presented a biofilm model using the concept of space occupancy (ν) which is defined as the change of local biofilm volume induced by the change in unit mass of that component and is considered constant for each component in this study:

$$\nu_i = \frac{\partial V_{fl}}{\partial m_i} \tag{39}$$

where ν_i is the space occupancy of component *i*, m_i is the mass of component *i*, and V_{fl} is the local biofilm volume. A condition that must be met with the definition of space occupancy is that none of the concentrations of the components in a mixed-culture biofilm system can be varied independent from each other during the biofilm growth expressed as

$$V_{fl} = \sum_{i=1}^{n_x} m_i \nu_i \qquad \textbf{(40)}$$

where n_x is the number of the components considered in the model.

Time-variant Spatial Distribution of Soluble Components within the Biofilm

The method to derive soluble and particulate material balance equations for a one-dimensional model was adopted from Wanner and Reichert (1996). The model was simplified by considering only a flat biofilm geometry defined with constant biofilm surface area (*A*). The time-variant spatial distribution of surfactant and nitrate within the biofilm can be expressed by the following material balance equation taking into account component diffusion and bacterial utilization

$$\frac{\partial S_{f,i}}{\partial t} = \frac{\partial}{\partial z}\left(D_{eff,S,i} \frac{\partial S_{f,i}}{\partial z} \right) - r_{ut,S,i} \qquad 0 \le z \le L_f \qquad \textbf{(41)}$$

where $S_{f,i}$ is the concentration of a soluble component in the biofilm (mass/volume), $D_{eff,S,i}$ is the effective diffusivity of the soluble component (area/time), and $r_{ut,S,i}$ is the utilization rate of the surfactant (mass/volume time) (Table 4 on p. 67). The effective diffusivity was considered a function of biofilm internal porosity (ε^3) using the random porous cluster described by Zhang and Bishop (1994b)

$$\frac{D_{eff,S,i}}{D_{B,S,i}} = \varepsilon^3 \qquad \textbf{(42)}$$

where $D_{B,S,i}$ is the bulk liquid-phase diffusivity of the soluble component (area/time). The initial (eq. 38) and boundary (eqns. 39 and 40) conditions used to solve equation 36 are

$$S_{f,i} = 0 \qquad \text{at } t = 0 \text{ and } 0 \le z \le L_f \tag{43}$$

The boundary condition at the biofilm/attachment-media interface expresses that there is no diffusion through the inert attachment-media.

$$\frac{\partial S_{f,i}}{\partial z} = 0 \qquad \text{at } z = L_f \text{ and } t \ge 0 \tag{44}$$

The boundary condition at the biofilm/liquid interface expresses that the mass flux from the bulk liquid to the biofilm/liquid boundary layer must be the same as the flux from the biofilm/liquid boundary layer to the biofilm surface.

$$\frac{\partial S_{f,i}}{\partial z} = \left(\frac{D_{B,S,i}}{D_{eff,S,i} L_{BL}} + u_L \right) \left(S_{B,i} - S_{f,i} \right) \qquad \text{at } z = 0 \tag{45}$$

where L_{BL} is the boundary layer thickness (distance), u_L is the velocity of the biofilm surface movement, and $S_{B,i}$ is the bulk concentration of a soluble component (mass/volume). The velocity of the biofilm surface movement is included in equation 40 because it is necessary for the dynamic modeling of biofilm due to the movement of the biofilm surface.

Time-variant Spatial Distribution of Particulates within the Biofilm

The active biomass in the biofilm is described as the particulate components within the biofilm to distinguish them from soluble compounds within the biofilm. The time-variant spatial distribution of heterotrophic biomass, extracellular polymeric substances (EPS), and inert components within the biofilm can be expressed by the following material balance equation accounting diffusion, advective flux and bacterial growth as described by Wanner and Reichert (1996) and Lee and Park (2007).

$$\frac{\partial X_{f,i}}{\partial t} = \frac{\partial}{\partial z}\left(D_{eff,X,i} \frac{\partial X_{f,i}}{\partial z} \right) - u_f \frac{\partial X_{f,i}}{\partial z} - \frac{\partial u_f}{\partial z} X_{f,i} + r_{gr,X,i} \quad \textbf{(46)}$$

where $X_{f,i}$ is the concentration of a soluble component in the biofilm (mass/volume), $D_{eff,X,i}$ is the effective diffusivity of the soluble component (area/time), u_f is the advective velocity of the biofilm solid matrix (distance/time) and $r_{gr,X,i}$ is the growth rate of particulate matter in the biofilm (mass/volume time) (Table 4). The first term describes the diffusion of particulates within the biofilm and is included because according to Lee and Park (2007) it enhances the stability of the numerical solution. The fourth term describes the net biomass growth. The second and third terms describe the change in particulate concentration within the biofilm due to advective flux. The concept of space occupancy is used to describe the advective flux by assuming that any change in local biofilm volume due to bacterial growth is dissipated by the advection in the *z* direction at a rate of u_f and is mathematically expressed by

$$\frac{\partial u_f}{\partial z} = \sum_{k=1}^{n_x} \upsilon_k r_{gr,X,k} \quad \textbf{(47)}$$

The initial (eq. 43) and boundary (eqns. 44 and 45) conditions used to solve equation 41 are

$$X_{f,i} = 0 \qquad \text{at } t = 0 \text{ and } 0 \le z \le L_f \quad \textbf{(48)}$$

The boundary condition at the biofilm/attachment-media interface expresses that there is no diffusion through the inert attachment-media.

$$\frac{\partial X_{f,i}}{\partial z} = 0 \qquad \text{at } z = L_f \text{ and } t \ge 0 \quad \textbf{(49)}$$

The boundary condition at the biofilm/liquid interface expresses that the mass flux from the bulk liquid to the biofilm/liquid boundary layer must be the same as the flux from the biofilm/liquid boundary layer to the biofilm surface.

$$\frac{\partial X_{f,i}}{\partial z} = D_{eff,X,i}\left(\left(u_{de} - u_{at}\right)X_{f,i} - \left(k_{de,i}X_{f,i} - k_{at,i}X_{B,i}\right)\right) \qquad \text{at } z = 0 \qquad \textbf{(50)}$$

where u_{de} and u_{at} are the attachment and detachment velocities at the biofilm surface (distance/time), $k_{at,i}$ is the constant attachment rate coefficient for each particulate components (time^{-1}); and $k_{de,i}$ is the biofilm thickness dependent detachment rate coefficient for each particulate components (time^{-1}). In this study we use the following expression for u_{de} and u_{at} as defined by Lee and Park (2007) and defined by Morgenroth and Wilderer (2000) and Wanner and Reichert (1996).

$$u_{at} = \sum_{k=1}^{n_x} \upsilon_k k_{at,k} X_{B,k} \qquad \textbf{(51)}$$

$$u_{de} = \sum_{k=1}^{n_x} \upsilon_k k_{de,k} X_{f,k} \qquad \textbf{(52)}$$

The equation that describes the relationship between the detachment rate coefficient and the biofilm thickness is

$$k_{de,i} = c_{de,i} L_f^2 \qquad \textbf{(53)}$$

where $c_{de,i}$ is the detachment constant.

Table 4. Growth rate microbial kinetics for SO model (Lee and Park 2007)

Component	Process rate
Surfactant (S_S)	$-\frac{\mathbf{1}}{\boldsymbol{Y_H}}\left(\boldsymbol{\mu_{H,max}}\frac{\boldsymbol{S_{f,S}S_{f,N}}}{\boldsymbol{(K_S+S_{f,S})(K_N+S_{f,N})}}\boldsymbol{X_{f,H}}\right)+\boldsymbol{(1-Y_I)(b_HX_{f,H})}+\boldsymbol{(b_HX_{f,H})}$
Nitrate (S_N)	$-\frac{\boldsymbol{(1-Y_H-Y_E)}}{\boldsymbol{Y_H}}\left(\boldsymbol{\mu_{H,max}}\frac{\boldsymbol{S_{f,S}S_{f,N}}}{\boldsymbol{(K_S+S_{f,S})(K_N+S_{f,N})}}\boldsymbol{X_{f,H}}\right)$
Heterotroph (X_H)	$\left(\boldsymbol{\mu_{H,max}}\frac{\boldsymbol{S_{f,S}S_{f,N}}}{\boldsymbol{(K_S+S_{f,S})(K_N+S_{f,N})}}\boldsymbol{X_{f,H}}\right)-\boldsymbol{(b_HX_{f,H})}$
Inerts (X_I)	$\boldsymbol{Y_I(b_HX_{f,H})}$
EPS (X_E)	$\frac{\boldsymbol{Y_E}}{\boldsymbol{Y_H}}\left(\boldsymbol{\mu_{H,max}}\frac{\boldsymbol{S_{f,S}S_{f,N}}}{\boldsymbol{(K_S+S_{f,S})(K_N+S_{f,N})}}\boldsymbol{X_{f,H}}\right)+\frac{\boldsymbol{Y_E}}{\boldsymbol{Y_H}}\boldsymbol{(b_HX_{f,H})}-\boldsymbol{(b_HX_{f,H})}$

Time-variant Distribution of Biofilm Depth

The depth of the biofilm is dependent on the movement of the surface at the biofilm/liquid interface. The surface movement depends on particulate advection, detachment, and attachment

$$\frac{dL_f}{dt}=u_L=u_f\left(L_f\right)-u_{de}+u_{at} \quad \textbf{(54)}$$

where L_f is the biofilm thickens, and u_L is the velocity of the biofilm surface,

Time-variant Soluble and Particulate Components in the Bulk Phase

A completely mixed biofilm reactor with constant volume was used to simulate the dynamic process. Assuming that surfactant and nitrate utilization in the bulk solution is negligible, the following material balance describes the time-variant soluble components in the bulk phase

$$\frac{dS_{b,i}}{dt} = \frac{Q\left(S_{B,i}^{0} - S_{B,i}\right) + \frac{D_{B,S,i}}{L_{BL}} A\left(S_{f,i} - S_{B,i}\right)}{\left(V_r - AL_f\right)} \quad \textbf{(55)}$$

where Q is the influent flow rate, $S_{B,i}^{0}$ is the influent concentration of soluble component, A is the biofilm surface area, and V_r is the reactor volume.

Assuming that heterotrophic biomass, EPS, and inert components growth in the bulk solution is negligible and that particulate component influent concentration is zero the following material balance describes the time-variant particulate components in the bulk phase.

$$\frac{dX_{b,i}}{dt} = \frac{A\left(k_{de}X_{f,i} - k_{at}X_{B,i}\right) + \left(Au_L - Q\right)X_{B,i}}{\left(V_r - AL_f\right)} \quad \textbf{(56)}$$

SOLUTION METHODS

Numerical Methods

The one-dimensional double substrate-limiting constant microbial density biofilm model on inert media consists of five non-linear partial differential equations (PDE), and six non-linear ordinary differential equations (ODE). The system of equations was solved using the "pdepe solver" provided in MATLAB software (The MathWorks Inc., Natick, MA). The "pdepe solver" converts partial differential equations into ordinary differential equations using second order accurate spatial discretization based on a fixed set of user-specified nodes. After discretization, elliptic equations give rise to algebraic equations. The time integration is done with "ode15s" which solves the differential-algebraic equations. A summary of the model can be found in appendix B.

Determination and Selection of Model Parameters

Some values of the model parameters were adopted directly from the literature, and some were determined by laboratory measurements. A summary of the model parameter values (and their sources) used in this study are listed in Table 5.

Table 5. Biofilm model on inert media using the concept of space occupancy model parameters

Symbol	Description	Value	References
Kinetic			
μ_{max}	Maximum specific growth rate	4..5 day^{-1}	Chapter 2
b_H	Heterotroph decay rate coefficient	0.079 day^{-1}	Alpkvist et al. (2006)
b_E	EPS decay rate coefficient	0.336 day^{-1}	Alpkvist et al. (2006)
K_S	Substrate saturation coefficient	6.9 mg/cm^3	Chapter 2
K_{NO3}	Nitrate saturation coefficient	4.7 mg/cm^3	Chapter 2
Stoichiometric			
Y_H	Yield of biomass on substrate	0.5 mg/mg	Chapter 2
Y_E	Yield of EPS on substrate	0.289 mg/mg	Alpkvist et al. (2006)
Y_I	Yield of inert biomass	0.4 mg/mg	Alpkvist et al. (2006)
Mass transfer			
$D_{b,S}$	Substrate bulk-phase diffusivity	0.8 cm^2/day	Velev et al. (2000)
$D_{b,N}$	Nitrate bulk-phase diffusivity	1 cm^2/day	Alpkvist et al. (2006)
$D_{f,S}$	Substrate diffusivity in biofilm	0.64 cm^2/day	Velev et al. (2000)
$D_{f,N}$	Nitrate diffusivity in biofilm	0.8 cm^2/day	Alpkvist et al. (2006)
L_{BL}	Boundary layer thickness	60 micro m	Alpkvist et al. (2006)
$D_{eff,X}$	Effective diffusivity for particulate	5×10^{-5} cm^2/day	Wanner and Reichert (1996)
Miscellaneous			
V_R	Reactor volume	430 cm^3	Laboratory data
ε	Reactor porosity	0.8	Laboratory data
Q	Influent flow rate	Variable	
A_c	Reactor cross-sectional area	20.27 cm^3	Laboratory data

Table 5. continued

Symbol	Description	Value	References
$S_{b,S}^{0}$	Substrate influent concentration	Variable	$S_{b,S}^{0}$
$S_{b,N}^{0}$	Influent concentration of nitrate	Variable	
c_{de}	Detachment rate constant	10 $cm^{-1}day^{-1}$	Lee and Park (2007)
$k_{at,X}$	Attachment rate coefficient	0.2 cm/day	Wanner and Reichert (1996)
$v_{SO,H}$	SO of heterotrophs	0.033 cm^3/mg	Lee and Park (2007)
$v_{SO,I}$	SO of inert biomass	0.0044 cm^3/mg	Lee and Park (2007)
$v_{SO,E}$	SO of EPS	0.0044 cm^3/mg	Lee and Park (2007)

MODEL PERFORMANCE EVALUATION

To gain insight into the performance of the system as conditions are changed, several numerical simulations were performed. The parameters that have an effect on reactor performance can be classified accordingly: biological parameters, mass transport parameters, reactor geometry parameters, and operational parameters. Effects on changes on the operational parameters were evaluated because they are the easiest to control in laboratory, pilot-scale, and system application situations. The effect of changes on the mass transport parameters were also evaluated due to the proprietary nature of the surfactant (Geropon TC-42®). The parameters that where changed in the different simulations were: influent surfactant concentration, influent nitrate concentration, flow rate, and surfactant diffusion coefficient. In all simulation studies, the following initial conditions were imposed: the initial concentrations of the soluble components ($S_{b,i}$) in the bulk phase were all zero, and the initial biofilm thickness was 10 μm.

Effects of Flow Rate

The effect of changes in the influent flow rate on the surfactant effluent concentration and biofilm depth propagation were determined by changing the influent flow rate between 0.12 and 118 mL/min and maintaining the influent surfactant and nitrate concentrations at 1.5 g/L (Figure 23). As expected, higher flow rates resulted in the dilute-in curve (Figure 23) being steeper and caused it to reach a higher effluent concentration. The higher flow rate caused higher loadings, which resulted in lower surfactant removal efficiencies. An increase in the flow rate also increased the time necessary to reduce the effluent substrate concentration to the minimal level. At 0.12, 1.18, 11.8, and 118 mL/min the effluent concentration are predicted to reduce to 0.015, 0.016, 0.020 and 0.024 g/L, respectively.

Higher flow rates resulted in a shorter hydraulic retention time and shorter startup periods (Figure 23). A shorter hydraulic retention time is expected at high flow rates since retention time is inversely proportional to flow rate. A shorter startup period is due to the increased movement of bacteria and substrate caused by higher flow rates. Since the substrate is more uniformly distributed, the bacteria can encounter substrate faster and therefore the biofilm depth can propagate faster. Propagation of the biofilm for different influent flow rates (Figure 24) show that the biofilm reached steady state faster at higher flow rates. Even though biofilm propagated faster at higher flow rates, it is not a determining factor in the biofilm steady-state depth since it was approximately 0.015 cm for all flow rates (Figure 24).

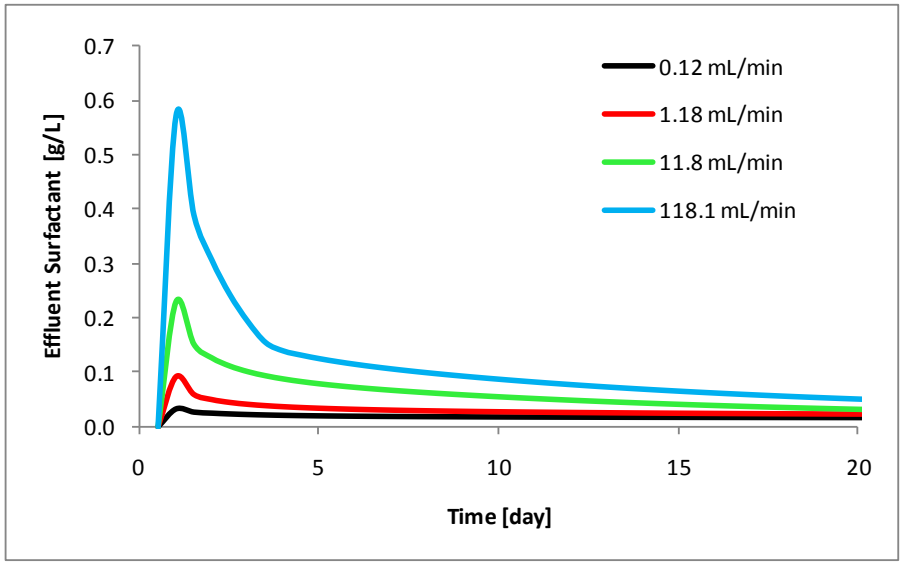

Figure 23. Effect of the influent flow rate (Q) on the surfactant effluent concentration (SO model)

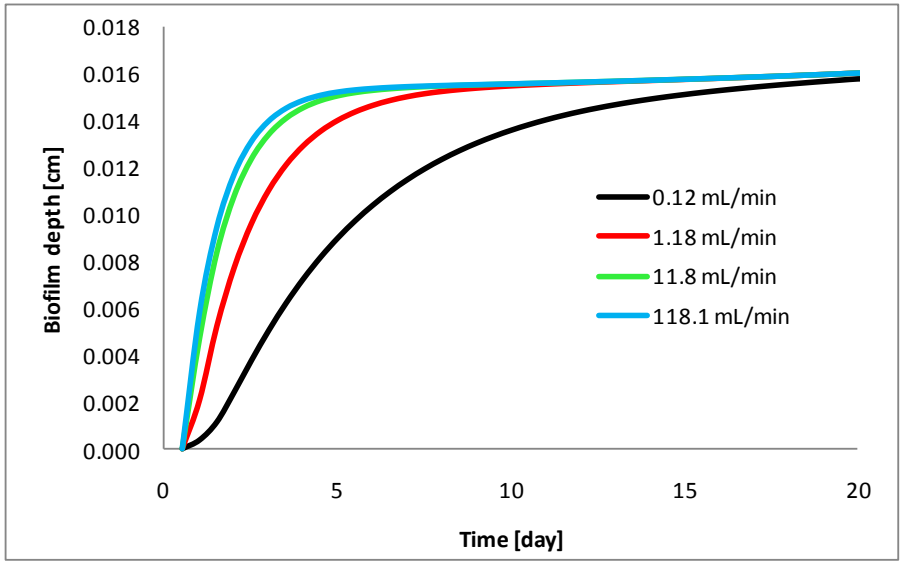

Figure 24. Effect of the influent flow rate (Q) on the biofilm depth propagation (SO model)

Effects of Influent Surfactant/Nitrate Concentration Ratio

The influent substrate is one of the operational parameters that affect the substrate loading rate. The effects of influent surfactant/nitrate concentration ratio on the effluent surfactant concentration, effluent nitrate concentration and biofilm depth propagation was studied by changing the influent surfactant and nitrate concentrations to achieve a ratio between 0.001 and 1.0 while keeping the influent flow rate at the operational flow rate of the laboratory test apparatus (11.8 mL/min). The effects on the surfactant effluent concentration are shown in Figure 25 for all influent surfactant/nitrate concentration ratios. A clearer view of the lowest two influent surfactant/nitrate concentration ratios is shown in Figure 26. Higher influent surfactant/nitrate concentration ratios resulted in longer startup periods because the biofilm would require more time to acclimate to the higher concentrations. The effluent substrate concentration minimal level increased proportionally with increases in influent surfactant/nitrate concentration ratios. A tenfold increase in influent surfactant/nitrate concentration ratio resulted in a tenfold increase in effluent substrate concentration minimal level.

Higher influent surfactant/nitrate concentration ratio supported more surfactant utilization and biofilm growth as shown by the propagation the biofilm for different influent concentration ratios. The effects on the biofilm depth propagation are shown in Figure 27 for all influent surfactant/nitrate concentration ratios. A clearer view of the lowest two influent surfactant/nitrate concentration ratios is shown in Figure 28. At the lowest surfactant influent concentration, the biofilm initially decreased (Figure 28)

suggesting that the assumed initial biofilm depth was larger than that supported by the available substrate surfactant concentration.

Influent surfactant/nitrate concentration ratio did not significantly affect the nitrate effluent curve in Figure 29. However, the higher influent surfactant/nitrate concentration ratio supported more nitrate utilization. Since the effluent concentration of this operational unit is higher than the nitrate maximum contaminant level (MCL) in drinking water (45 mg/L) by more an order of ten, further water treatment would be needed to achieve drinking water standards.

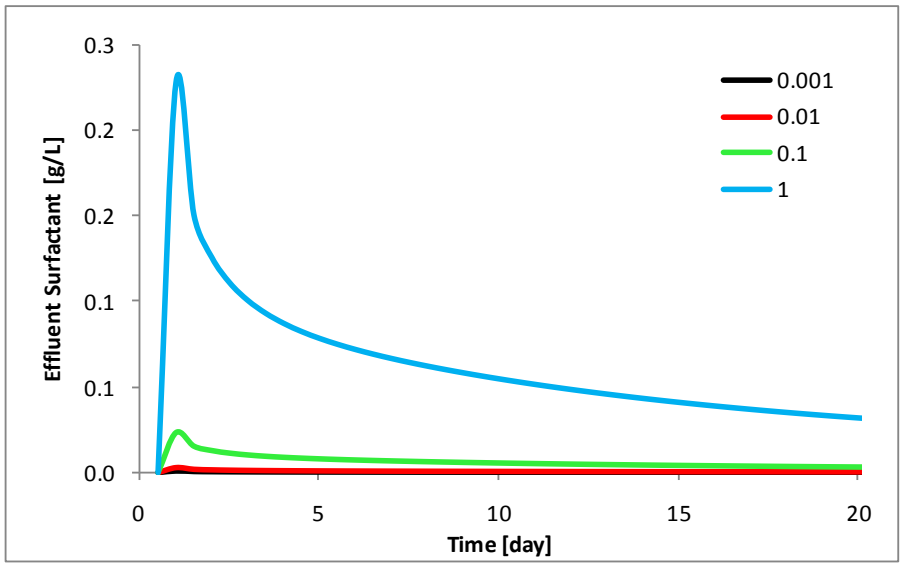

Figure 25. Effect of all influent substrate/nitrate concentration ratios on the surfactant effluent concentration (SO model)

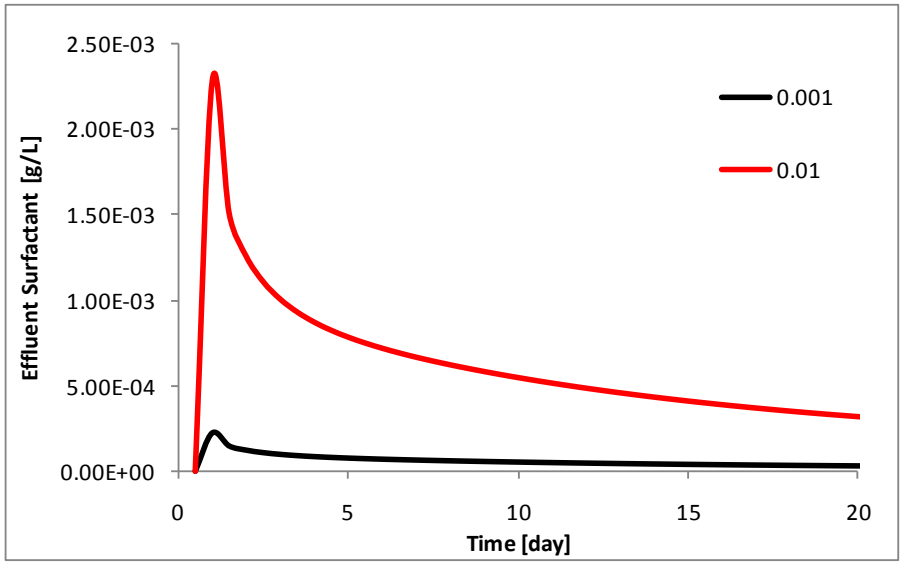

Figure 26. Effect of the lowest influent substrate/nitrate concentration ratio on the surfactant effluent concentration (SO model)

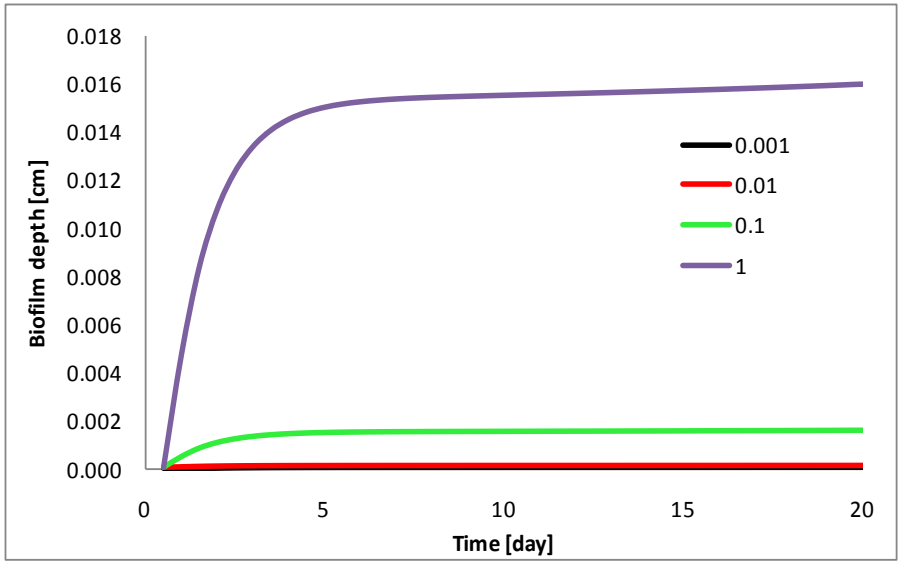

Figure 27. Effect of all influent substrate/nitrate concentrations ratio on the biofilm depth propagation (SO model)

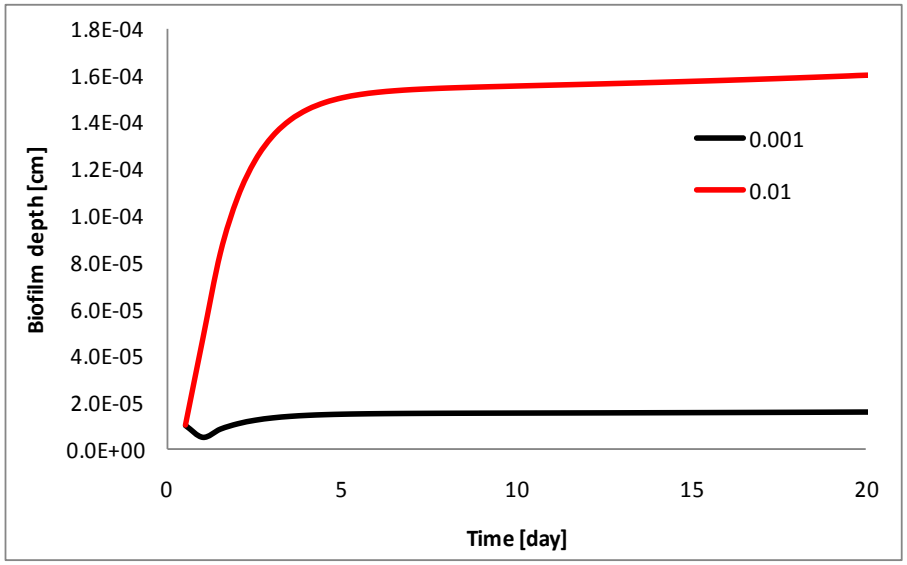

Figure 28. Effect of the lowest influent substrate/nitrate concentrations ratio on the biofilm depth propagation (SO model)

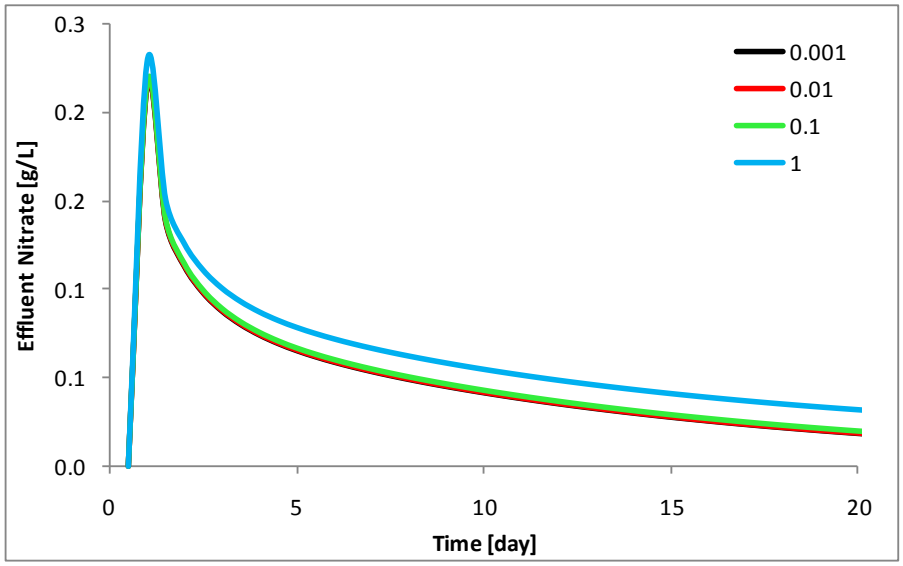

Figure 29. Effect of the influent substrate/nitrate concentration ratio on the nitrate effluent concentration (SO model)

Effects of Surfactant Diffusion Coefficient

The effect of the surfactant diffusion coefficient on the surfactant effluent concentration, nitrate effluent concentration, and biofilm depth propagation were determined by changing the surfactant diffusion coefficient (0.2, 0.4, 0.6, 0.8 and 1 cm2/day) and keeping the influent flow rate, the influent surfactant concentration, and the nitrate surfactant concentration at the laboratory reactor operational values of 11.8 mL/min, 1.5 g/L, and 1.5 g/L respectively. The surfactant diffusion coefficient did not affect the surfactant or nitrate effluent curve since all the diffusion coefficients predicted the same effluent curves (Figure 30 and Figure 31). Only one curve is visible in each figure because all curves overlap. The diffusion coefficient and the liquid film inter-phase layer are so small as compared to the biofilm depth, that changes in the coefficient did not affect the value of the effluent concentration which has a magnitude much larger than the diffusion coefficient. The diffusion coefficient was more important in the biofilm depth propagation since mass transfer dictates the available substrate in the biofilm. Further, the magnitude of the biofilm is closer to the magnitude of the diffusion coefficient than to the effluent concentrations (Figure 32). The propagation of the biofilm for two surfactant diffusion coefficients (0.6 and 0.8 cm2/day) is shown in Figure 32. Only two surfactant diffusion coefficients are shown in the figure because the curve for 0.2, 0.4, and 0.6 cm2/day overlapped and the curve for 0.8 and 1 cm2/day overlapped. The propagation of the biofilm shows that the biofilm reached steady state faster at lower surfactant diffusion coefficients. Even though biofilm propagated faster at lower surfactant diffusion coefficients, it is not a determining factor in the biofilm

steady-state depth since it was approximately 0.015 cm for both surfactant diffusion coefficients (Figure 32).

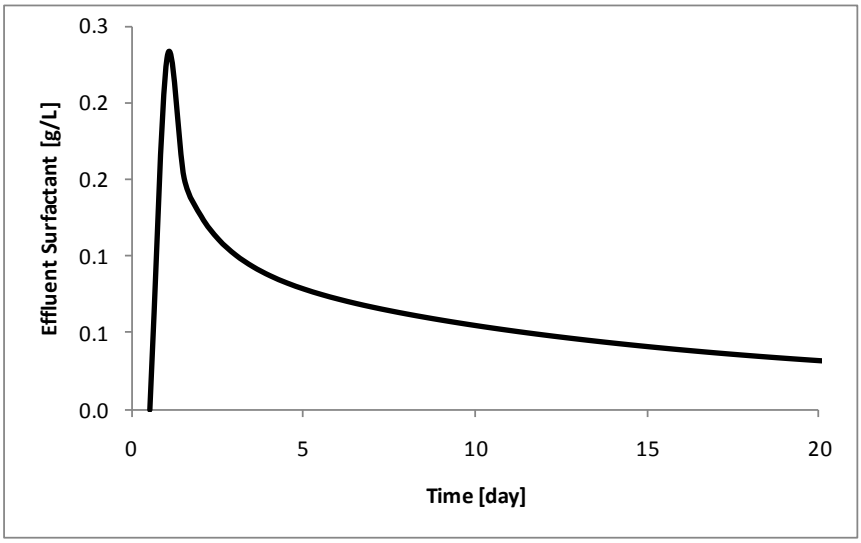

Figure 30. Effect of the surfactant diffusion coefficient on the surfactant effluent concentration (SO model)

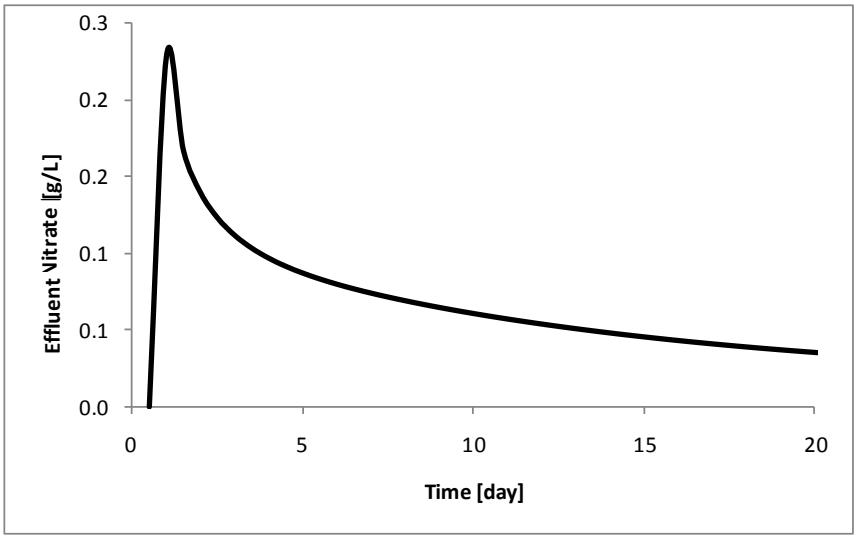

Figure 31. Effect of the surfactant diffusion coefficient on the nitrate effluent concentration (SO model)

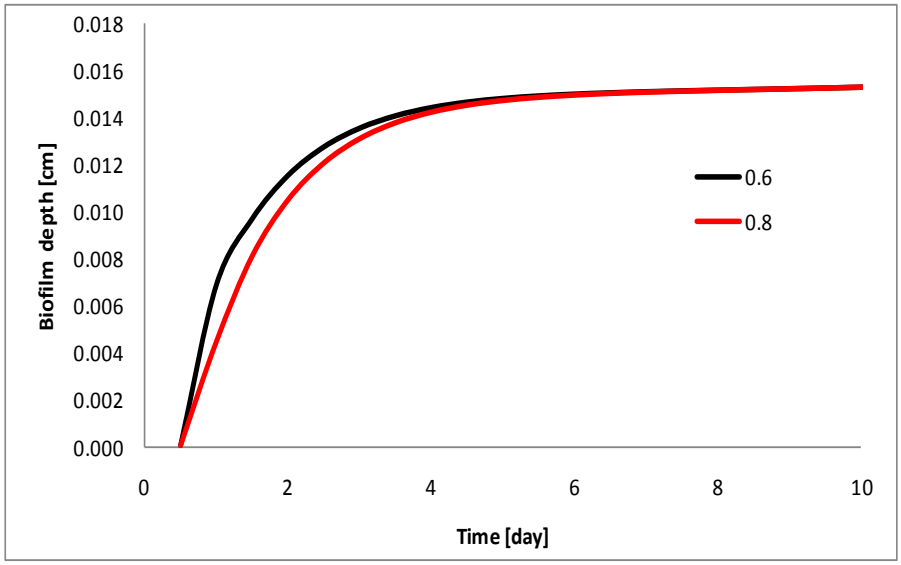

Figure 32. Effect of the surfactant diffusion coefficient on the biofilm depth propagation (SO model)

CONCLUSIONS

A one-dimensional biofilm model was developed based on the assumption that each component has different space occupancy within the biofilm. The special feature used in the development of the model was the concept of space occupancy which allowed for a varying biofilm thickness with changes in the biofilm microbial density. The sensitivity analysis showed that the surfactant diffusion coefficient do not significantly affect the performance of the system. The influent flow rate, surfactant concentration, and nitrate concentration were the factors that most affected the performance of the system. Higher flow rates resulted in a shorter hydraulic retention time, shorter startup periods, and faster biofilm steady-state. Higher flow resulted in the lower steady-state surfactant removal. Higher influent surfactant/nitrate concentration ratios gave longer startup period, supported more surfactant utilization, and biofilm

growth. Influent surfactant/nitrate concentration ratio did not affect the nitrate effluent curve. The model presented in this study could be employed for the design of an anoxic biofilm treatment process for the removal of the surfactant Geropon TC-42®.

CHAPTER V

CONTINUOUS FLOW STUDY

In this chapter, a comparative study was conducted on the start-up performance of a packed bed reactor and biofilm model simulation. Simulations were performed with two different biofilm models and compared to experimental data for the biodegradation of Geropon TC-42® under anoxic conditions. The following sections describe the laboratory techniques used, the analytical methods employed to estimate the kinetic parameters, and the simulations parameters used.

INTRODUCTION

Personal care products have become the center of current environmental research (Onesios et al. 2009). These contaminants are present in the environment from sources such as wastewater treatment plant effluent and confined animal feeding operation run-off (Daughton and Ternes 1999). Because the effects of these compounds on the environment have not been fully characterized, questions have been raised regarding chemical persistence, microbial resistance, and adverse effects on aquatic life (Choong et al. 2006; Crane et al. 2006).

Wastewater reuse and recycling addresses the lack of potable water availability caused by increased demand on natural resources due to population increase. Recycling of wastewater is also important in enclosed space environments where water resources are limited (Levine et al. 2000b). The largest wastewater stream anticipated for long duration space missions is human hygiene water. Whole body shampoo and hand

cleaner from Ecolabs (840 Highway 13, St. Paul, MN 55118) is currently a primary candidate for use in the International Space Station (Garland et al. 2004). It contains 24% sodium N-methyl-N- "Coconut oil acid" taurate (Geropon TC-42®), a sulfonated amide surfactant.

One simple method for recycling human hygiene water is a treatment based on the use of biodegradation. Microbial degradation of the surfactant is a key process in this proposed wastewater treatment approach. Researchers have examined personal care products removal by biodegradation in wastewater treatment plants, membrane bioreactors, sequencing batch reactors, sand columns, and constructed wetlands (Onesios et al. 2009). Several studies have demonstrated that Geropon TC-42® is rapidly degraded by aerobic biological process (Levine et al. 2000b). Not much research has been published on the degradation of Geropon TC-42® under oxygen deprived conditions.

A comparative study was conducted on the start-up performance of a packed bed reactor using Geropon TC-42® and nitrate as electron donor and acceptor, respectively. Geropon TC-42® was chosen as the substrate because it is the main component of the primary candidate soap to be used in space habitats. Nitrate was chosen as the terminal electron acceptor instead of oxygen due to the poor mass transfer of oxygen between gas and liquid phases in microgravity. Simulations were performed with two different biofilm models and compared to experimental data for the biodegradation of Geropon TC-42® under anoxic conditions.

MATERIALS AND METHODS

Test Apparatus and Reactor Configuration

A reactor with a working volume of 0.43 L and packing material was supplied by Johnson Space Center (JSC). A schematic diagram of the configuration of the systems is illustrated in Figure 33. The reactor was packed with Bio-Bale^{TM}, a flexible packing material made of thin strips of polyvinyl chloride (PVC) (Figure 34). Bio-Bale^{TM} was suggested by engineers at JSC because it has a high surface area per unit volume, which maximizes the area on which the microbes can attach and form a biofilm. The Bio-Bale^{TM} was packed to attain a porosity of 0.80 with 62.4 grams of dry Bio-Bale^{TM}.

The system was maintained completely mixed via liquid recirculation. The average recirculation flow rate was approx 2.8mL/min and the influent flow rate of 0.6 mL/min. The recycle stream is an important computational and operational factor. Assuming that the concentration inside the reactor is homogenous simplifies the material balance and the computational procedure. Operationally, a homogenous concentration within the reactor will prevent substrate and biofilm stratification, clogging, and flock formation.

The feed tank was thoroughly cleaned, assembled, and autoclaved before substrate and nutrients were added. The substrate and nutrients were also autoclaved before they were transferred into the feed tank. All the openings were covered with aluminum foil before and after autoclaving. The feed reservoir was designed in such a way that the feed solution stayed bacteria-free and in the absence of molecular oxygen.

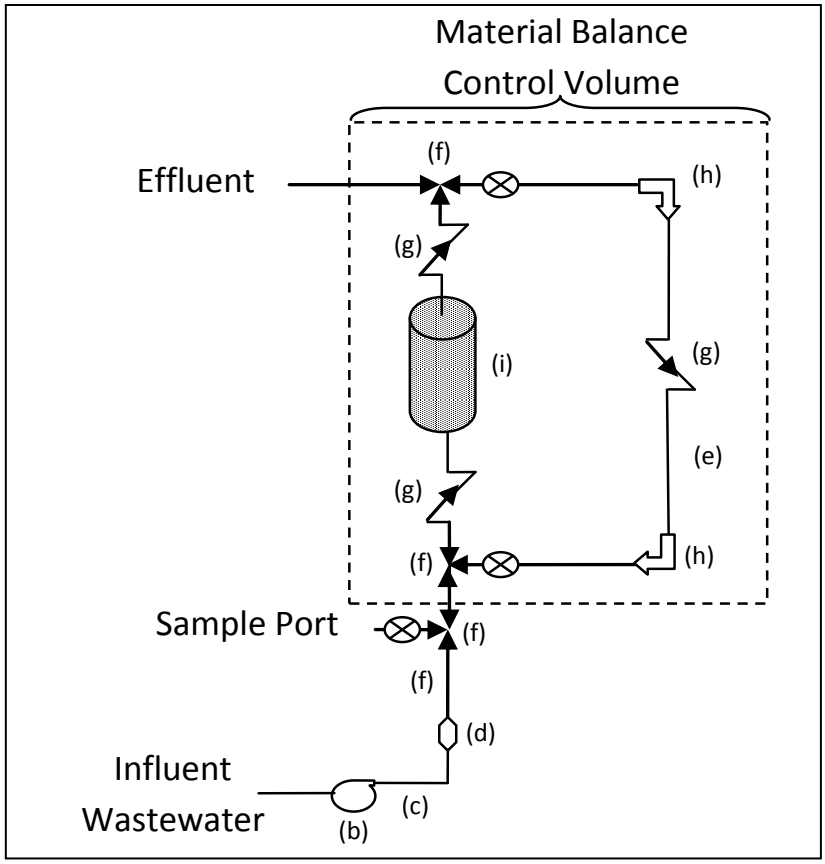

Figure 33. Schematic diagram of the configuration of the systems used for the continuous flow study. (a) Wastewater and effluent collection tanks, (b) Pump and pump head, (c) Tygon® Food L/S 14, (d) Piping adaptor, (e) 1/4" Clear Rigid PVC Pipe, (f) 1/4" Tube O.D. Union Tee and Shut-Off Valve, (g) Check valve, (h) Elbow, and (i) Bio-Bale.

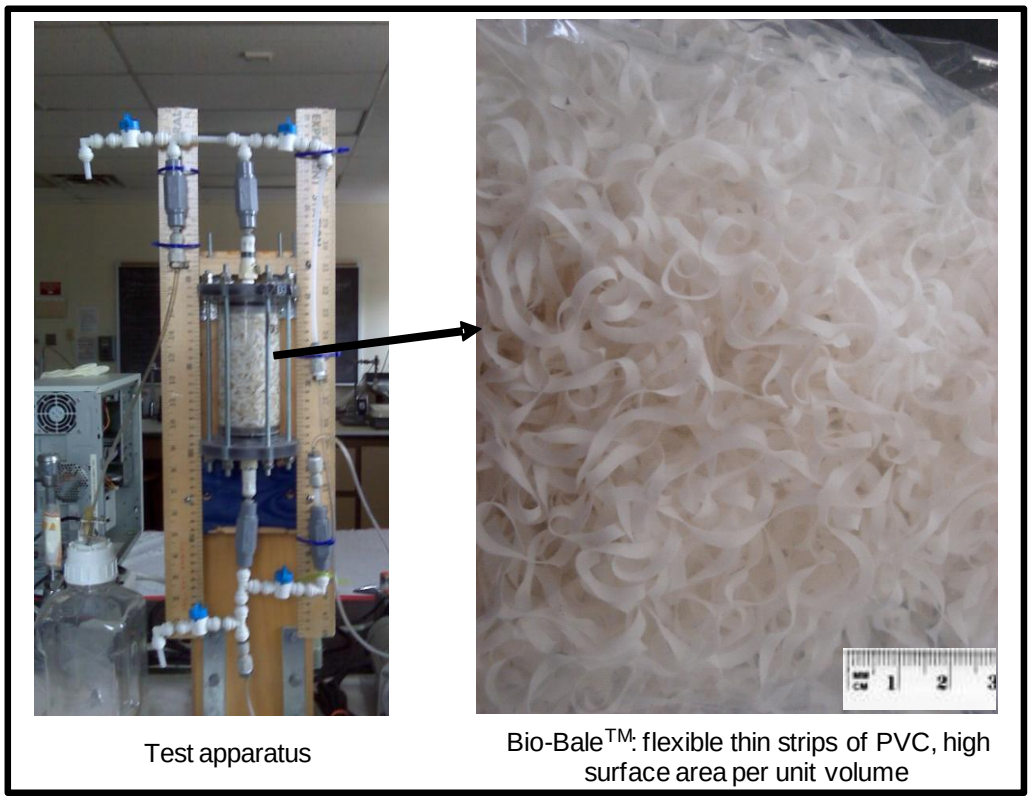

Figure 34. Test apparatus and packing material used for the continuous flow study.

Culture Enrichment

The bacteria used in this research were cultivated by enrichment techniques. The inoculum for these cultures was obtained from the activated sludge basin of the Carter Creek Wastewater Treatment Plant, College Station, Texas in April 2008. To survive and compete successfully, most microorganisms are able to meet many of the environmental challenges by adjusting their cellular composition with respect to both structure and metabolic function (Kovarova-Kovar and Egli 1998). Therefore, denitrifying bacteria are expected to be found in the mixed liquor because denitrification is widespread among heterotrophic and autotrophic bacteria, many of which can shift

between oxygen and nitrogen respiration (Rittmann and McCarty 2001). All cultures were incubated on a 35º C orbital shaker (Lab-Line® Orbit Environ-Shaker). A batch feed-and-draw method was used to grow bacterial enrichments in sterile 500 mL media bottles. Fresh substrate solution was injected into the bottles every two days by first allowing suspended microorganisms to settle and withdrawing an equal volume of supernatant. Enrichment cultures were used throughout the research to ensure consistency of all batch and model verification tests.

Denitrifying bacteria were enriched with media containing Geropon TC-42® as the sole carbon source (i.e., electron donor) and nitrate at 10% excess as the electron acceptor. The inorganic growth medium base (GMB) contained (per liter of de-ionized water) 0.5 g of $MgSO_4 \cdot 7H_2O$, 0.5 g of NH_4Cl, 0.5 g of KH_2PO_4, 0.1 g of $CaCl_2$, and 0.85 g of $NaNO_3$ (Kniemeyer et al. 1999). After autoclaving, 2 ml of a trace element (1 liter of distilled water contained 2.1 mg of $FeSO_4 \cdot 7H_2O$, 30 mg of H_3BO_3, 100 mg of $MnCl_2 \cdot 4H_2O$, 190 mg of $CoCl_2 \cdot 6H_2O$, 24 mg of $NiCl_2 \cdot 6H_2O$, 29 mg of $CuSO_4 \cdot 5H_2O$, 144 mg of $ZnSO_4 \cdot 7H_2O$, 36 mg of $NaMoO_4 \cdot 7H_2O$, and 5.2 g of EDTA, pH 6.5), 1 ml of vitamin solution (4 mg of 4-aminobenzoic acid, 2 mg of D-(1)-biotin, 10 mg of nicotinic acid, 5 mg of calcium D-(1)-pantothenate, 15 mg of pyridoxin hydrochloride, 4 mg of folic acid, and 1 mg of lipoic acid in 100 ml of 10 mM NaH_2PO_4, pH 7.1), and 50 ml of $NaHCO_3$ solution (1 M) were added and the solution was sparged with nitrogen gas (Kniemeyer et al. 1999). All chemicals used in the study are reagent grade chemicals.

Seeding and Attachment

To eliminate substrate degradation by bacteria in the growth media and feed tanks, a rigorous sterilization method was used to prepare bacteria-free growth media and feed solution. Autoclave and filter sterilization were basic techniques employed to prepare the sterile growth media. The feed reservoir and tygon tubing for the column study were autoclaved before use. All the inlets on the reservoir were wrapped with heavy-duty aluminum foil. All the glassware, feed containers, sampling syringe, and vials were autoclaved for 30 minutes. Biofilm attachment in packed bed bioreactor supplied by NASA was accomplished by adding new sterilized medium every 3 days for 9 days to the seeded packed bed bioreactor.

Surfactant Analytical Procedure

Levine (2000a) has shown that Geropon TC-42® concentration can be determined by a direct approach utilizing ion pairing reversed-phase chromatography coupled with suppressed conductivity detection. A Dionex DX-600 ion chromatography system equipped with a conductivity cell (DS3) and self-regenerating suppressor (Dionex ASRS Ultra 4 mm) was used to determine Geropon TC-42® concentration (Levine et al. 2000a). Separation was achieved on a Dionex IonPac NS1 column (10 µm, 250 mm×4mm) using a gradient of acetonitrile and 5mM ammonium hydroxide using 25mM sulfuric acid as a regenerant. The gradient program used was: 5% acetonitrile for the first 5 min followed by a linear increase to 45% over the next 15 min and hold at 45% for 10 min. Flow rate of the mobile phase was kept at 1 ml/min. The

suppressor is operated in the external chemical mode using 25mM sulfuric acid as a regenerant at 4 ml-min^{-1}. The dynamic analytical range was from 1 to 25 mg/L.

Nitrate Analytical Procedure

Nitrate concentration was measured using a Dionex-80 system equipped with a conductivity cell and self-regenerating suppressor according to EPA Method 300.1 (Hautman and Munch 1997). Separation was achieved on a Dionex IonPac AS14A column with dynamic analytical range was from 0.1 to 100 mg/L.

RESULTS AND DISCUSSION

Simulation Study

The goal of the simulation study was to compare the results of the double substrate-limiting constant microbial density biofilm model (model 1) and the one-dimensional double substrate-limiting biofilm model on inert media using the concept of space occupancy model (model 2). The parameters used during the simulation are those in Table 3 and Table 5. The influent flow rate, surfactant concentration, and nitrate concentration at the laboratory reactor operational values of 0.6 mL/min, 1.5 g/L, and 2 g/L respectively.

Comparison of the simulation results shows similar behavior for both models with an approximate surfactant removal efficiency of 98% and an approximate effluent concentration of 20 mg/L (Figure 35). The initial dynamic part of the graph shows that both models behave very similar. The main behavioral difference occurs after the initial effluent peak and is more evident as the reactors reach steady state. Simulations also show that the rector reaches steady-state at approximately 10 days (Figure 35), before

the biofilm which reaches steady-state at approximately 20 days (Figure 36). Model 2 predicts a larger biofilm depth (Figure 36) which is the reason why the model 2 predicts higher surfactant removal. This is consistent with the results of surfactant and nitrate effluent concentrations (Figure 35 and Figure 37) where model 2 predicts a higher removal of both surfactant and nitrate. Both models predict similar effluents and behave similarly because the same material transport and microbial kinetics were used. Further, the same material transport and kinetic parameters are used.

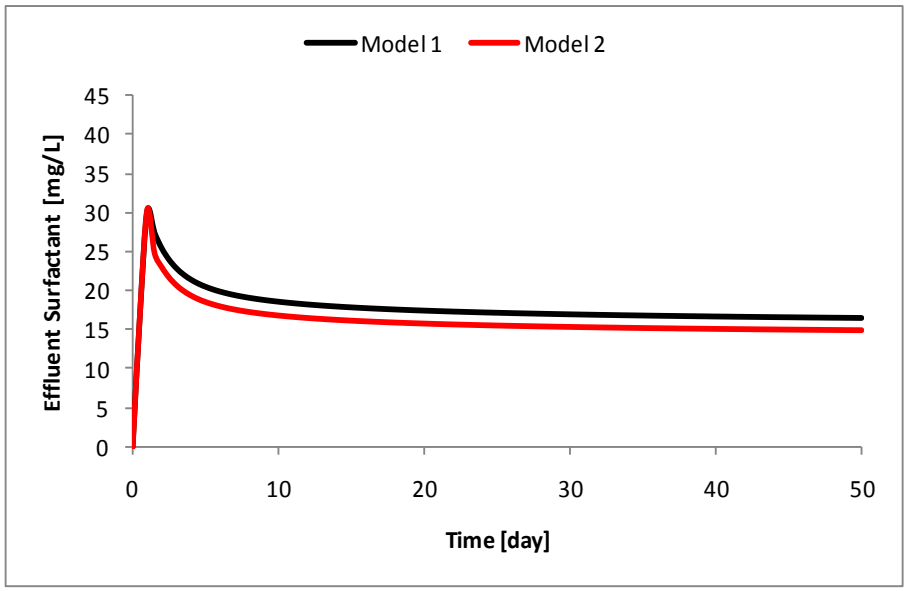

Figure 35. Effluent surfactant concentration for comparable simulations using Model 1 and Model 2

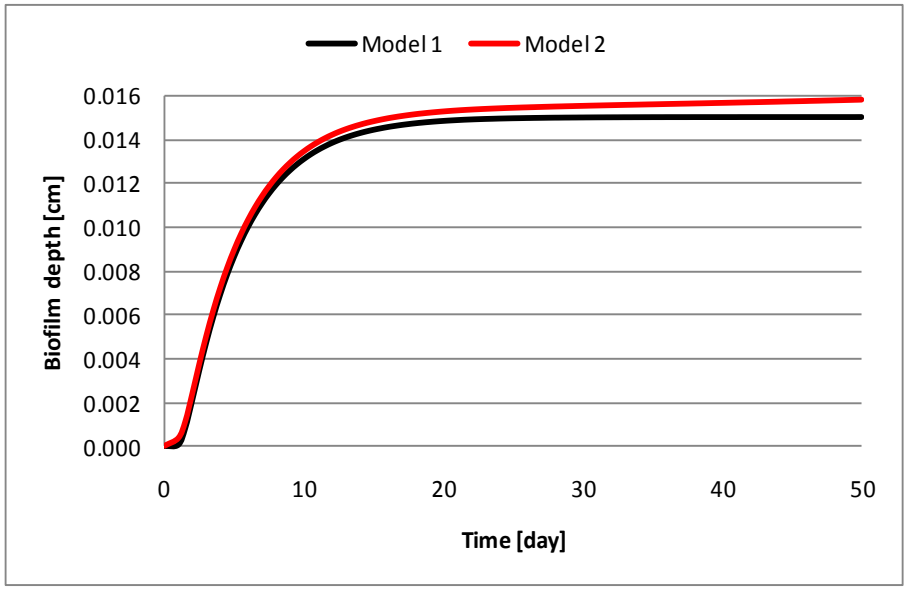

Figure 36. Biofilm depth propagation for comparable simulations using Model 1 and Model 2

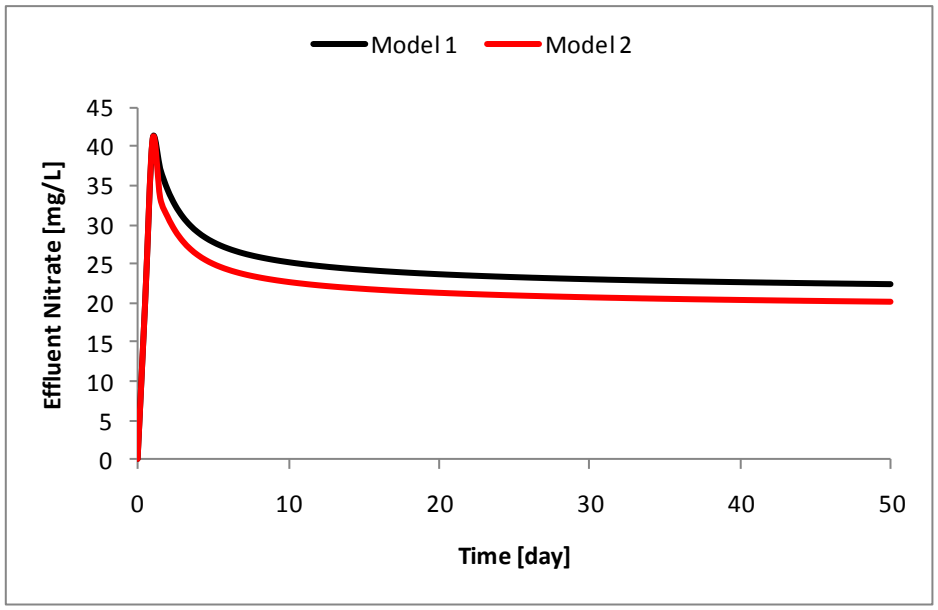

Figure 37. Effluent nitrate concentration for comparable simulations using Model 1 and Model 2

Continuous Flow Study

The goal of the continuous flow study was to evaluate the non-steady-state performance of the anoxic biofilm on inert media. The system was operated with a high influent flow rate to recycle flow rate ratio to maintain mixed conditions inside the reactor for ten days. The influent flow rate was 0.6 mL/min with a retention time of 0.5 days and the recycle rate was 2.8 mL/min. The substrate and nitrate influent concentrations were selected to be 1.5 g/L and 2 g/L respectively, which fall within the range from the early planetary base wastewater ersatz used as a prediction of expected wastewater streams in space human settlements (Verstoko et al. 2004).

Comparison of the simulation results and the experimental data show that both models predict within the experimental error but model one predicts closer to the data points (Figure 38 and Figure 39). Effluent surfactant data is more closely predicted by model 1 before 4 days, but predicted by both models after day 4. Effluent nitrate concentration was most closely predicted by model 1. The shape of the effluent concentration profile correlates to the predicted biofilm depth propagation (Figure 40). The effluent concentration begins to drop after one day, which coincides with the growth of the biofilm at one day.

These results suggest that allowing the biofilm microbial density to change does not enhance the prediction of the model. Comparison of model 1 and 2 suggest that presuming constant biofilm density is a reasonable assumption. Model 2 accounts for the environmental differences present in a biofilm which create non-homogeneous biofilm growth and particulate movement but do not significantly affect the performance

of a biofilm from the perspective of wastewater treatment system design. The main parameters that affect the performance of the system are influent flow rate and influent substrate concentration.

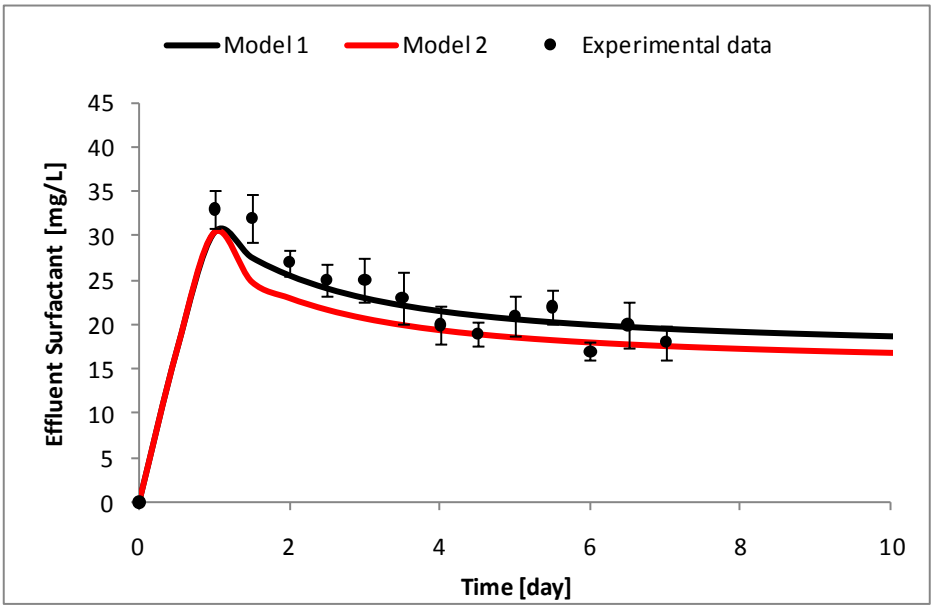

Figure 38. Effluent surfactant concentrations comparison of experimental data and model simulations

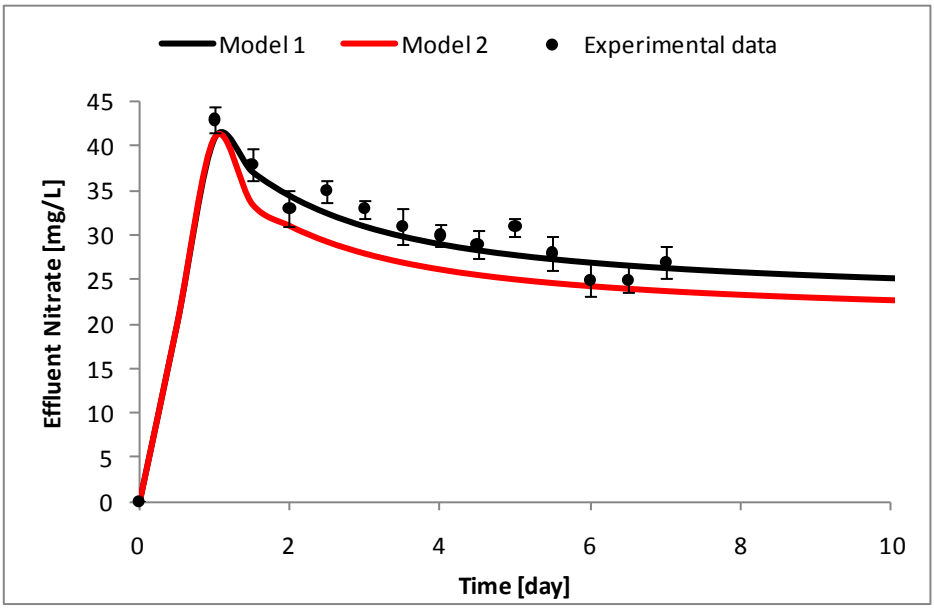

Figure 39. Effluent nitrate concentrations comparison of experimental data and model simulations

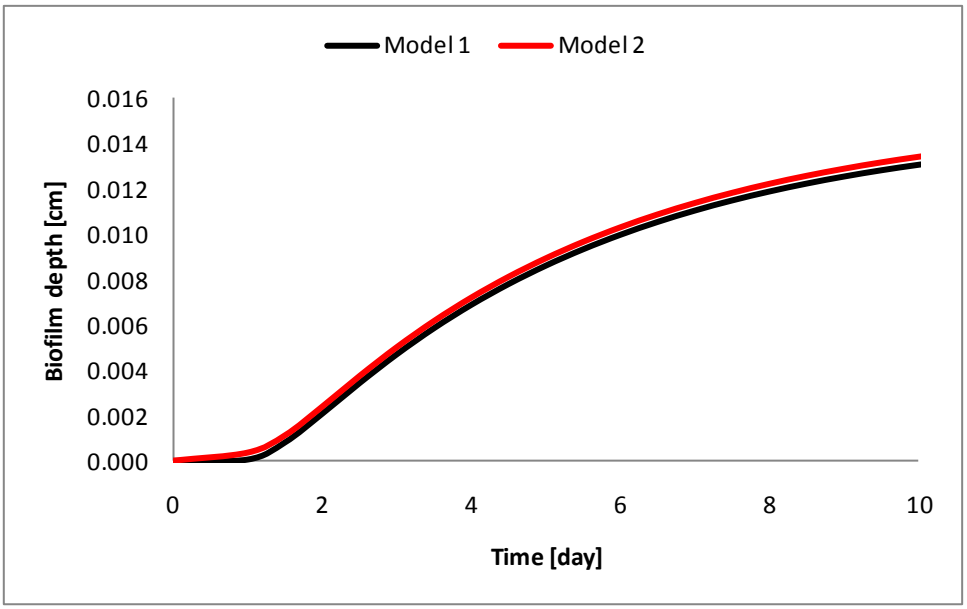

Figure 40. Predicted biofilm depth propagation during experimental period

CONCLUSION

Comparison of the simulation results shows similar behavior for both models with an approximate surfactant removal efficiency of 98% and an approximate effluent concentration of 20 mg/L. Simulations also show that the reactor reaches steady-state within 10 days, before the biofilm which reaches steady-state at approximately 20 days. Model 2 predicts a larger biofilm depth and higher surfactant removal.

Comparison of the simulation results and the experimental data show that both models predict within the experimental error, but model 1 most closely predicts the empirical data. Effluent surfactant and nitrate concentrations were captured by model 1. The shape of the effluent concentration profile correlates to the predicted biofilm depth propagation.

These results suggest that the variables that were included in model 2 but not in model 1 (microbial density change, inters, and extracellular polymeric substances) do not enhance the prediction of the model. Comparison of model 1 and 2 suggest that presuming constant biofilm density is a reasonable assumption. Model 2 accounts for the environmental differences present in a biofilm which create non-homogeneous biofilm growth and particulate movement but do not significantly affect the performance of a biofilm from the perspective of wastewater treatment system design. The main parameters that affect the performance of the system are the influent flow rate and influent substrate concentrations. Since using a model assuming constant biofilm density is computationally simpler and easier to apply, a suitable anoxic packed bed

reactor for the removal of the surfactant Geropon TC-42® can be designed by using the estimated kinetic values and a model assuming constant biofilm density (model 1).

CHAPTER VI

CONCLUSIONS AND FUTURE WORK

CONCLUSIONS

There are three major steps in the experimental approach towards a better understanding of the mixed-culture biofilm on inert media. The first step is the determination of biokinetic coefficients. The biodegradation kinetics of Geropon TC-42® by a mixed microbial culture was investigated using batch experiments. The mixed culture produced data which can be used in real-scale biodegradation applications. Estimated kinetic values can be used in plug flow, batch or continuously stirred tank reactor mass balances to determine design parameter like reactor volume, flow rate, biomass retention time, and residence time for anoxic suspended or attached culture. Surfactant degradation data indicates that biomass to surfactant mass ratios should be around 12.5. Lower ratios will not sustain biomass metabolism and higher ratios will inhibit substrate utilization. At reactor start-up, a small initial substrate removal lag phase should be expected due to the steep initial net specific growth rate slope observed at low surfactant concentrations.

Special considerations need to be taken into account when designing a wastewater treatment system for human space habitation due to low gravity and space availability. The system should address poor oxygen mass transfer, footprint restrictions, ease of maintenance for astronauts, transport form Earth to final location, and system start-up. A suitable wastewater treatment system can be designed by using estimated

values to determine reactor volume, flow rate, and residence time for an anoxic attached culture plug flow reactor.

The second step is to develop a model to describe the concentration profiles and evaluate the effect of key parameters using sensitivity analysis. Two biofilm models were developed. The first model used three features: simultaneous utilization and molecular diffusion, dual substrate-limiting biofilm, and a varying biofilm thickness. The second model was developed based on the assumption that each component has different space occupancy within the biofilm. The sensitivity analysis showed that the surfactant diffusion coefficient does not significantly affect the performance of the system regardless of the model used. The influent flow rate, surfactant concentration, and nitrate concentration were the factors that most affected the performance of the system. Higher flow rates resulted in a shorter hydraulic retention time, shorter startup periods, and faster biofilm steady-state. Higher flow resulted in the lower steady-state surfactant removal. Higher influent surfactant/nitrate concentration ratios gave longer startup period, sustained more surfactant utilization, and supported biofilm growth. Influent surfactant/nitrate concentration ratio did not significantly affect the nitrate effluent curve. The model presented in this study could be employed for the design of an anoxic biofilm treatment process for the removal of the surfactant Geropon TC-42®.

The third step is to compare the model simulations to experimental data. Comparison of the simulation results shows similar behavior for both models with an approximate surfactant removal efficiency of 98% and an approximate effluent concentration of 20 mg/L. Simulations also show that the rector reaches steady-state at

approximately 10 days before the biofilm, which reaches steady-state at approximately 20 days. Model 2 predicts a larger biofilm depth and higher surfactant removal. Comparison of the simulation results and the experimental data show that both models predict within the experimental error, but model one most closely predicts the empirical data. Effluent surfactant and nitrate concentrations were capture by model 1. The shape of the effluent concentration profile correlates to the predicted biofilm depth propagation.

These results suggest that the variables that were included in model 2 but not in model 1 (microbial density change, inters, and extracellular polymeric substances) do not enhance the prediction of the model. Comparison of model 1 and 2 suggest that presuming constant biofilm density is a reasonable assumption. The main parameters that affect the performance of the system are influent flow rate and influent substrate concentration. Since using a model assuming constant biofilm density is computationally simpler and easier, a suitable anoxic packed bed reactor for the removal of the surfactant Geropon TC-42® can be designed by using the estimated kinetic values and a model assuming constant biofilm density.

FUTURE WORK

In order to successfully utilize a biological treatment process to recover water in a manned space habitat, reactor transportation and start-up needs to be addressed. Microorganisms require special preservation methods in order to ensure optimal long-term viability and genetic stability. Microbial preservation method can be classified as metabolically inactive or metabolically active methods. Metabolically inactive

preservation techniques include cryopreservation and drying. Metabolically active methods include periodic transfer on medium or keeping agar cultures under mineral oil. Metabolically inactive preservation techniques are better suited for long term storage and transport. In order to transport a viable wastewater treatment system, microbial preservation techniques and their effect on bacterial performance should be studied. The effect of cryopreservation and warming rate on surfactant removal efficiencies should also be studied.

Because the effects of surfactants and endocrine disruptors on the environment and human health have not been fully characterized, questions have been raised regarding chemical persistence and microbial resistance. Chemical persistence of these compounds is a major concern that needs to be furthered considered when studying wastewater reuse and recycling.

REFERENCES

(WHO), W. H. O. (2004). "Guidelines for drinking water quality." http://www.who.int/water_sanitation_health/dwq/gdwq3rev/en/.

Agarry, S. E., and Solomon, B. O. (2008). "Kinetics of batch microbial degradation of phenols by indigenous Pseudomonas fluorescence." *International Journal of Environmental Science and Technology*, 5(2), 223-232.

Alpkvist, E., Picioreanu, C., van Loosdrecht, M. C. M., and Heyden, A. (2006). "Three-dimensional biofilm model with individual cells and continuum EPS matrix." *Biotechnology and Bioengineering*, 94(5), 961-979.

Bader, F. G. (1978). "Analysis of double-substrate limited growth." *Biotechnology and Bioengineering*, 20(2), 183-202.

Bae, W., and Rittmann, B. E. (1996). "A structured model of dual-limitation kinetics." *Biotechnology and Bioengineering*, 49(6), 683-689.

Bazin, M., ed. (1983). *Mathematics in microbiology*, Academic Press, New York.

Beauchamp, E. G., Trevors, J. T., and Paul, J. W. (1989). "Carbon sources for bacterial denitrification." *Advances in Soil Science*, 10, 113-142.

Belova, S. E., Dorofeev, A. G., and Panikov, N. S. (1996). "Growth and substrate utilization by bacterial lawn on the agar surface: Experiment and one-dimensional distributed model." *Microbiology*, 65(6), 690-694.

Berna, J. L., Cossani, G., Hager, C. D., Rehman, N., Lopez, L., Schowonek, D., Steber, J., Taeger, K., and Wind, T. (2007). "Anaerobic biodegradation of surfactants - Scientific review." *Tenside Surfactants Detergents*, 44(6), 312-318.

Borden, R. C., and Bedient, P. B. (1986). "Transport of dissolved hydrocarbons influenced by oxygen-limited biodegradation .1. Theoretical development." *Water Resources Research*, 22(13), 1973-1982.

Bubenheim, D., Wignarajah, K., Berry, W., and Wydeven, T. (1997). "Phytotoxic effects of gray water due to surfactants." *Journal of the American Society for Horticultural Science*, 122(6), 792-796.

Chang, H. T., and Rittmann, B. E. (1987). "Mathematical-modeling of biofilm on activated carbon." *Environmental Science & Technology*, 21(3), 273-280.

Choong, A. M. F., Teo, S. L. M., Leow, J. L., Koh, H. L., and Ho, P. C. L. (2006). "A preliminary ecotoxicity study of pharmaceuticals in the marine environment." *Journal of Toxicology and Environmental Health*, 69(21), 1959-1970.

Chudova, P., Capdeveille, B., and Chudova, J. (1992). "Explanation of biological meaning of the S0/X0 ratio in batch cultivation." *Water Science and Technology*, 26, 743-751.

Clark, M. (1996). *Transport modeling for environmental engineers and scientists*, John Wiley & Sons, New York.

Costerton, J. W., Lewandowski, Z., Debeer, D., Caldwell, D., Korber, D., and James, G. (1994). "Biofilms, the customized microniche." *J. Bacteriol.*, 176(8), 2137-2142.

Crane, M., Watts, C., and Boucard, T. (2006). "Chronic aquatic environmental risks from exposure to human pharmaceuticals." *Sci. Total Environ.*, 367(1), 23-41.

Daughton, C., and Ternes, T. (1999). "Pharmaceuticals and personal care products in the environment: agents of subtle change?" *Environmental Health Perspectives*, 107, 907-938.

Davis, M. L., and Cornwell, D. A. (1998). *Introduction to environmental engineering*, Third Ed., McGraw Hill, Boston.

Delhomenie, M. C., and Heitz, M. (2005). "Biofiltration of air: A review." *Critical Reviews in Biotechnology*, 25(1-2), 53-72.

Dhouib, A., Hamad, N., Hassairi, I., and Sayadi, S. (2003). "Degradation of anionic surfactants by Citrobacter braakii." *Process Biochemistry*, 38(8), 1245-1250.

Eaton, A. D., Clesceri, L. S., and Greenberg, A. E. (2007). *Standard methods for the examination of water and wastewater*, 19th Ed., American Public Health Association, Washington DC.

Egli, T. (1995). "The ecological and physiological significance of the growth of heterotrophic microorganisms with mixtures of substrates." *Advances in Microbial Ecology*, 14, 305-386.

Fouad, M., and Bhargava, R. (2005a). "Mathematical model for the biofilm-activated sludge reactor." *Journal of Environmental Engineering-Asce*, 131(4), 557-562.

Fouad, M., and Bhargava, R. (2005b). "Modified expressions for substrate flux into biofilm." *Journal of Environmental Engineering and Science*, 4(6), 441-449.

Fraleigh, S. P., and Bungay, H. R. (1986). "Modeling of nutrient gradients in a bacterial colony." *Journal of General Microbiology*, 132, 2057-2060.

Garland, J. L., Levine, L. H., Yorio, N. C., and Hummerick, M. E. (2004). "Response of graywater recycling systems based on hydroponic plant growth to three classes of surfactants." *Water Research*, 38(8), 1952-1962.

Gomez, J. M., Caro, I., and Cantero, D. (1996). "Kinetic equation for growth of Thiobacillus ferrooxidans in submerged culture over aqueous ferrous sulphate solutions." *Journal of Biotechnology*, 48(1-2), 147-152.

Grady, C. P. L. (1982). "Modeling of biological fixed films- A state of the art review." *First Internationals Conference on Fixed-Film Biological Processes*, King's Island, Ohio 61-78.

Grady, C. P. L., Smets, B. F., and Barbeau, D. S. (1996). "Variability in kinetic parameter estimates: A review of possible causes and a proposed terminology." *Water Research*, 30(3), 742-748.

Hautman, D. P., and Munch, D. J. (1997). "Determination of inorganic anions in drinking water by ion chromatography." United States Environmental Protection Agency, Cincinnati OH, Method 300.1.

Hosseini, F., Malekzadeh, F., Amirniiozafari, N., and Ghaemi, N. (2007). "Biodegradation of anionic surfactants by isolated bacteria from activated sludge." *International Journal of Environmental Science and Technology*, 4(1), 127-132.

Howell, J. A., and Atkinson, B. (1976). "Influence of oxygen and substrate concentrations on ideal film thickness and maximum overall substrate uptake rate in microbial film fermenters." *Biotechnology and Bioengineering*, 18(1), 15-35.

Ioslovich, I., Gutman, P. O., and Seginer, I. (2004). "Dominant parameter selection in the marginally identifiable case." *Math. Comput. Simul.*, 65(1-2), 127-136.

Jones, C. A., and Kelly, D. P. (1983). "Growth of Thiobacillus-ferrooxidans on ferrous iron in chemostat culture - influence of product and substrate-inhibition." *Journal of Chemical Technology and Biotechnology B-Biotechnology*, 33(4), 241-261.

Jurado, E., Fernandez-Serrano, M., Nunez-Olea, J., and Lechuga, M. (2007). "Primary biodegradation of commercial fatty-alcohol ethoxylate surfactants: Characteristic parameters." *Journal of Surfactants and Detergents*, 10(3), 145-153.

Kissel, J. C., McCarty, P. L., and Street, R. L. (1984). "Numerical-simulation of mixed-culture biofilm." *Journal of Environmental Engineering-Asce*, 110(2), 393-411.

Kniemeyer, O., Probian, C., Rossello-Mora, R., and Harder, J. (1999). "Anaerobic mineralization of quaternary carbon atoms: Isolation of denitrifying bacteria on dimethylmalonate." *Applied and Environmental Microbiology*, 65(8), 3319-3324.

Knowles, R. (1982). "Denitrification." *Microbiol. Rev.*, 46(1), 43-70.

Kovarova-Kovar, K., and Egli, T. (1998). "Growth kinetics of suspended microbial cells: From single-substrate-controlled growth to mixed-substrate kinetics." *Microbiology and Molecular Biology Reviews*, 62(3), 646-652.

Kumar, A., Kumar, S., and Kumar, S. (2005). "Biodegradation kinetics of phenol and catechol using Pseudomonas putida MTCC 1194." *Biochemical Engineering Journal*, 22(2), 151-159.

Laspidou, C. S., and Rittmann, B. E. (2004a). "Evaluating trends in biofilm density using the UMCCA model." *Water Research*, 38(14-15), 3362-3372.

Laspidou, C. S., and Rittmann, B. E. (2004b). "Modeling the development of biofilm density including active bacteria, inert biomass, and extracellular polymeric substances." *Water Research*, 38(14-15), 3349-3361.

Laspidou, C. S., Rittmann, B. E., and Karamanos, S. A. (2005). "Finite element modelling to expand the UMCCA model to describe biofilm mechanical behavior." *Water Science and Technology*, 52(7), 161-166.

Lau, A. O., Strom, P. F., and Jenkins, D. (1984). "Growth-kinetics of Sphaerotilus-natans and a floc former in pure and dual continuous culture." *Journal Water Pollution Control Federation*, 56(1), 41-51.

Lee, M. W., and Park, J. M. (2007). "One-dimensional mixed-culture biofilm model considering different space occupancies of particulate components." *Water Research*, 41(19), 4317-4328.

Levine, L. H., Judkins, J. E., and Garland, J. L. (2000a). "Determination of anionic surfactants during wastewater recycling process by ion pair chromatography with suppressed conductivity detection." *Journal of Chromatography A*, 874(2), 207-215.

Levine, L. H., Kagie, H. R., and Garland, J. L. (2000b). "Biodegradation pathway of an anionic surfactant (IGEPON TC-42) during recycling waste water through plant hydroponics for advanced life support during long-duration space missions."

Space life sciences: Missions to Mars, radiation biology, and plants as a foundation for long-term life support systems in space, 33rd COSPAR Scientific Assembly, Warsaw, Poland, 16-23July, 249-253.

Lin, Y. H., and Lee, K. K. (2006). "Kinetics of phenol degradation in an anaerobic fixed-biofilm process." *Water Environment Research*, 78(6), 598-606.

Maier, R. M. (2000). "Bacterial Growth." In: *Environmental microbiology*, R. M. Maier, I. L. Pepper, and C. P. Gerba, eds., Academic Press, San Diego, 43-59.

Miyanaga, K., Takano, S., Morono, Y., Hori, K., Unno, H., and Tanji, Y. (2007). "Optimization of distinction between viable and dead cells by fluorescent staining method and its application to bacterial consortia." *Biochemical Engineering Journal*, 37(1), 56-61.

Molchanov, S., Gendel, Y., Ioslvich, I., and Lahav, O. (2007). "Improved experimental and computational methodology for determining the kinetic equation and the extant kinetic constants of Fe(II) oxidation by Acidithiobacillus ferrooxidans." *Applied and Environmental Microbiology*, 73(6), 1742-1752.

Molz, F. J., Widdowson, M. A., and Benefield, L. D. (1986). "Simulation of microbial-growth dynamics coupled to nutrient and oxygen-transport in porous-media." *Water Resources Research*, 22(8), 1207-1216.

Morgenroth, E., and Wilderer, P. A. (2000). "Influence of detachment mechanisms on competition in biofilms." *Water Research*, 34(2), 417-426.

Muirhead, D., Jackson, W. A., Keister, H., Morse, A., Rainwater, K., and Pickering, K. D. (2003). "Performance of a small-scale biological water recovery system." In: *Proceedings of the 33th International Conference on Environmental Systems*, Society of Automotive Engineers, Inc.Warrendale, Pennsylvania, USA, San Francisco, CA, USA, 2003-01-2557.

Nemati, M., Harrison, S. T. L., Hansford, G. S., and Webb, C. (1998). "Biological oxidation of ferrous sulphate by Thiobacillus ferrooxidans: A review on the kinetic aspects." *Biochemical Engineering Journal*, 1(3), 171-190.

Nemati, M., and Webb, C. (1997). "A kinetic model for biological oxidation of ferrous iron by Thiobacillus ferrooxidans." *Biotechnology and Bioengineering*, 53(5), 478-486.

Nicolella, C., van Loosdrecht, M. C. M., and Heijnen, J. J. (2000). "Wastewater treatment with particulate biofilm reactors." *Journal of Biotechnology*, 80(1), 1-33.

Nikolov, L., Karamanev, D., Dakov, L., and Popova, V. (2001). "Oxidation of ferrous iron by Thiobacillus ferrooxidans in a full-scale rotating biological contactor." *Environ. Prog.*, 20(4), 247-250.

Nyavor, K., Egiebor, N. O., and Fedorak, P. M. (1996). "The effect of ferric ion on the rate of ferrous oxidation by Thiobacillus ferrooxidans." *Appl. Microbiol. Biotechnol.*, 45(5), 688-691.

Onesios, K. M., Yu, J. T., and Bouwer, E. J. (2009). "Biodegradation and removal of pharmaceuticals and personal care products in treatment systems: A review." *Biodegradation*, 20(4), 441-466.

Perales, J. A., Manzano, M. A., Sales, D., and Quiroga, J. A. (1999). "Biodegradation kinetics of LAS in river water." *Int. Biodeterior. Biodegrad.*, 43(4), 155-160.

Philistine, C. L. (2005). "International space station water usage analysis." In: *Proceedings of the 35th International Conference on Environmental Systems*, S. of and A. Engineers, eds., Society of Automotive Engineers, Inc.Warrendale, Pennsylvania, USA, Colorado Springs, CO, USA, 2008-01-2009.

Qi, S. Y., and Morgenroth, E. (2005). "Modeling steady-state biofilms with dual-substrate limitations." *Journal of Environmental Engineering-Asce*, 131(2), 320-326.

Rhodes, P. M., and Stanbury, P. F., eds. (1997). *Applied microbial physiology*, Oxford University Press, Oxford.

Rittmann, B. E., and Dovantzis, K. (1983). "Dual limitation of biofilm kinetics." *Water Research*, 17(12), 1727-1734.

Rittmann, B. E., and McCarty, P. L. (1978). "Variable-order model of bacterial-film kinetics." *Journal of the Environmental Engineering Division-Asce*, 104(5), 889-900.

Rittmann, B. E., and McCarty, P. L. (1981). "Substrate flux into biofilms of any thickness." *Journal of the Environmental Engineering Division-Asce*, 107(4), 831-849.

Rittmann, B. E., and McCarty, P. L. (2001). *Environmental biotechnology: Principles and applications*, McGraw Hill, New York.

Rittmann, B. E., Stilwell, D., and Ohashi, A. (2002). "The transient-state, multiple-species biofilm model for biofiltration processes." *Water Research*, 36(9), 2342-2356.

Rivett, M. O., Buss, S. R., Morgan, P., Smith, J. W. N., and Bemment, C. D. (2008). "Nitrate attenuation in groundwater: A review of biogeochemical controlling processes." *Water Research*, 42(16), 4215-4232.

Robinson, J. A. (1985). "Determining microbial kinetic-parameters using nonlinear-regression analysis: Advantages and limitations in microbial ecology." *Advances in Microbial Ecology*, 8, 61-114.

Sahinkaya, E., and Dilek, F. B. (2007). "Biodegradation kinetics of 2,4-dichlorophenol by acclimated mixed cultures." *Journal of Biotechnology*, 127(4), 716-726.

Saravanan, V., and Sreekrishnan, T. R. (2006). "Modelling anaerobic biofilm reactors - A review." *J. Environ. Manage.*, 81(1), 1-18.

Sharvelle, S., Lattyak, R., and Banks, M. K. (2007). "Evaluation of biodegradability and biodegradation kinetics for anionic, nonionic, and amphoteric surfactants." *Water Air and Soil Pollution*, 183(1-4), 177-186.

Sharvelle, S., Skvarenina, E., and Banks, M. K. (2008). "Biodegradation of disodium cocoamphodiacetate by a wastewater microbial consortium." *Water Environment Research*, 80(3), 276-281.

Silverthorn, D. U., Ober, W. C., Garrison, C. W., and Silverthorn, A. C. (2004). *Human physiology: An integrated approach*, Pearson Education, Inc. , San Francisco, CA.

Sinclair, C. G., and Ryder, D. N. (1975). "Models for continuous culture of microorganisms under both oxygen and carbon limiting conditions." *Biotechnology and Bioengineering*, 17(3), 375-398.

Smith, L. H., Kitanidis, P. K., and McCarty, P. L. (1997). "Numerical modeling and uncertainties in rate coefficients for methane utilization and TCE cometabolism by a methane-oxidizing mixed culture." *Biotechnology and Bioengineering*, 53(3), 320-331.

Smith, L. H., McCarty, P. L., and Kitanidis, P. K. (1998). "Spreadsheet method for evaluation of biochemical reaction rate coefficients and their uncertainties by weighted nonlinear least-squares analysis of the integrated monod equation." *Applied and Environmental Microbiology*, 64(6), 2044-2050.

Song, H., Jang, S. H., Park, J. M., and Lee, S. Y. (2008). "Modeling of batch fermentation kinetics for succinic acid production by Mannheimia succiniciproducens." *Biochemical Engineering Journal*, 40(1), 107-115.

Strayer, R. F., Alazraki, M. P., Judkins, J., Adams, J., Garland, J. L., and Hsu, V. (1999). "Development and testing of inocula for biodegradation of Igepon under denitrifying conditions." In: *Proceedings of the 29th International Conference on Environmental Systems*, Society of Automotive Engineers, Inc. Warrendale, Pennsylvania, USA, Denver, CO, USA, 1999-01-1949.

Suidan, M. T., and Wang, Y. T. (1985). "Unified analysis of biofilm kinetics." *Journal of Environmental Engineering-Asce*, 111(5), 634-646.

Sykes, R. M. (1973). "Identification of limiting nutrient and specific growth-rate." *Journal Water Pollution Control Federation*, 45(5), 888-895.

Tesoriero, A. J., Liebscher, H., and Cox, S. E. (2000). "Mechanism and rate of denitrification in an agricultural watershed: Electron and mass balance along groundwater flow paths." *Water Resources Research*, 36(6), 1545-1559.

Vega, L. M., Kerkhof, L., McGuinness, L., and Pickering, K. D. (2004). "Evaluation of performance of five parallel biological water processors." In: *Proceedings of the 34th International Conference on Environmental Systems*, Society of Automotive Engineers, ed., Society of Automotive Engineers, Inc.Warrendale, Pennsylvania, USA, Colorado Springs, CO, USA, 2004-01-2515.

Velev, O. D., Kaler, E. W., and Lenhoff, A. M. (2000). "Surfactant diffusion into lysozyme crystal matrices investigated by quantitative fluorescence microscopy." *J. Phys. Chem. B*, 104(39), 9267-9275.

Verstoko, C. E., Carrier, C., and Finger, B. W. (2004). "Ersatz wastewater formulations for testing water recovery systems." In: *Proceedings of the 34th International Conference on Environmental Systems*, Society of Automotive Engineers, Inc.Warrendale, Pennsylvania, USA, Colorado Springs, CO, USA, 2004-01-2448.

Wanner, O., and Reichert, P. (1996). "Mathematical modeling of mixed-culture biofilms." *Biotechnology and Bioengineering*, 49(2), 172-184.

White, F. (1999). *Fluid mechanics*, McGraw Hill, Boston.

Williamson, K., and McCarty, P. L. (1976a). "Verification studies of biofilm model for bacterial substrate utilization." *Journal Water Pollution Control Federation*, 48(2), 281-296.

Williamson, K., and McCarty, P. L. (1976b). "Model of substrate utilization by bacterial films." *Journal Water Pollution Control Federation*, 48(1), 9-24.

Zhang, T. C., and Bishop, P. L. (1994a). "Density, porosity, and pore structure of biofilms." *Water Research*, 28(11), 2267-2277.

Zhang, T. C., and Bishop, P. L. (1994b). "Evaluation of tortuosity factors and effective diffusivities in biofilms." *Water Research*, 28(11), 2279-2287.

Zinn, M., Witholt, B., and Egli, T. (2004). "Dual nutrient limited growth: Models, experimental observations, and applications." *Journal of Biotechnology*, 113(1-3), 263-279.

APPENDIX A

ONE-DIMENSIONAL DOUBLE SUBSTRATE-LIMITING HOMOGENEOUS MICROBIAL DENSITY BIOFILM MODEL ON INERT MEDIA SUMMARY

Surfactant Material Balance within Biofilm

$$\frac{\partial S_{f,S}}{\partial t} = \frac{D_{f,S}}{L_f}\frac{\partial^2 S_{f,S}}{\partial z_f^2} - \frac{\mu_{\max}}{Y}\frac{S_{f,S}S_{f,N}}{\left(K_{S,S}+S_{f,S}\right)\left(K_{S,N}+S_{f,N}\right)}X_f \qquad \textbf{(57)}$$

with initial conditions,

$$S_{f,S} = 0 \qquad \text{at } t = 0 \qquad \textbf{(58)}$$

and boundary conditions,

$$\frac{\partial S_{f,S}}{\partial z_f} = 0 \qquad \text{at } z_f = L_f \text{ and } t \geq 0 \qquad \textbf{(59)}$$

$$\frac{\partial S_{f,S}}{\partial z_f} = \frac{k_{f,S}}{D_{f,S}}\left(S_{b,S} - S_{f,S}\right) \qquad \text{at } z_f = 0 \qquad \textbf{(60)}$$

Nitrate Material Balance within Biofilm

$$\frac{\partial S_{f,N}}{\partial t} = \frac{D_{f,N}}{L_f}\frac{\partial^2 S_{f,N}}{\partial z_f} - \gamma\frac{S_{b,S}^0}{S_{b,N}^0}\frac{\mu_{\max}}{Y}\frac{S_{f,S}S_{f,N}}{\left(K_{S,S}+S_{f,S}\right)\left(K_{S,N}+S_{f,N}\right)}X_f \qquad \textbf{(61)}$$

with initial conditions,

$$S_{f,N} = 0 \qquad \text{at } t = 0 \qquad \textbf{(62)}$$

and boundary conditions,

$$\frac{\partial S_{f,N}}{\partial z_f} = 0 \qquad \text{at } z_f = L_f \text{ and } t \geq 0 \qquad \textbf{(63)}$$

$$\frac{\partial S_{f,N}}{\partial z_f} = \frac{k_{f,N}}{D_{f,N}}\left(S_{b,N} - S_{f,N}\right) \quad \text{at } z_f = 0 \tag{64}$$

Dynamic Biofilm Boundary

$$\frac{d\left(X_f L_f\right)}{dt} = Y\int_0^{L_f}\left[q_{\max}\frac{S_{f,S}}{\left(K_{S,S} + S_{f,S}\right)}X_f\,dz\right] - b\left(X_f L_f\right) \tag{65}$$

with the initial condition,

$$L_f = L_{f,0} \text{ at } t = 0 \tag{66}$$

Bulk Surfactant Material Balance

$$\frac{dS_{b,S}}{dt} = \frac{Q}{V\varepsilon}\left(S^0_{b,S} - S_{b,S}\right) - k_{f,S}\left(S_{b,S} - S_{f,S}\right)\frac{A}{V\varepsilon} \tag{67}$$

with the initial condition,

$$S_{b,S} = 0 \qquad \text{at } t = 0 \tag{68}$$

Bulk Nitrate Material Balance

$$\frac{dS_{b,N}}{dt} = \frac{Q}{V\varepsilon}\left(S^0_{b,N} - S_{b,N}\right) - k_{f,S}\left(S_{b,N} - S_{f,N}\right)\frac{A}{V\varepsilon} \tag{69}$$

with the initial conditions,

$$S_{b,N} = 0 \qquad \text{at } t = 0 \tag{70}$$

APPENDIX B

ONE-DIMENSIONAL DOUBLE SUBSTRATE-LIMITING BIOFILM MODEL ON INERT MEDIA USING THE CONCEPT OF SPACE OCCUPANCY

Concept of space occupancy

$$\nu_i = \frac{\partial V_{fl}}{\partial m_i} \tag{71}$$

Time-variant Spatial Distribution of Soluble Components within the Biofilm

$$\frac{\partial S_{f,i}}{\partial t} = \frac{\partial}{\partial z}\left(D_{eff,S,i} \frac{\partial S_{f,i}}{\partial z} \right) - r_{ut,S,i} \qquad 0 \le z \le L_f \tag{72}$$

with initial and boundary conditions

$$S_{f,i} = 0 \qquad \text{at } t = 0 \text{ and } 0 \le z \le L_f \tag{73}$$

$$\frac{\partial S_{f,i}}{\partial z} = 0 \qquad \text{at } z = L_f \text{ and } t \ge 0 \tag{74}$$

$$\frac{\partial S_{f,i}}{\partial z} = \left(\frac{D_{B,S,i}}{D_{eff,S,i} L_{BL}} + u_L \right)\left(S_{B,i} - S_{f,i} \right) \text{at } z = 0 \tag{75}$$

<u>*Rate of Surfactant Utilization*</u>

$$r_{ut,S} = -\frac{1}{Y_H}\left(\mu_{H,max} \frac{S_{f,S} S_{f,N}}{(K_S + S_{f,S})(K_N + S_{f,N})} X_{f,H} \right) + (1 - Y_I)\left(b_H X_{f,H} \right) + \left(b_H X_{f,H} \right) \tag{76}$$

<u>*Rate of Nitrate Utilization*</u>

$$\boldsymbol{r_{ut,N} = -\frac{(1 - Y_H - Y_E)}{Y_H}\left(\mu_{H,max} \frac{S_{f,S} S_{f,N}}{(K_S + S_{f,S})(K_N + S_{f,N})} X_{f,H} \right)} \tag{77}$$

Time-variant Spatial Distribution of Particulates within the Biofilm

$$\frac{\partial X_{f,i}}{\partial t} = \frac{\partial}{\partial z}\left(D_{eff,X,i} \frac{\partial X_{f,i}}{\partial z} \right) - u_f \frac{\partial X_{f,i}}{\partial z} - \frac{\partial u_f}{\partial z} X_{f,i} + r_{gr,X,i} \quad \textbf{(78)}$$

where

$$\frac{\partial u_f}{\partial z} = \sum_{k=1}^{n_x} \upsilon_k r_{gr,X,k} \quad \textbf{(79)}$$

with initial and boundary

$$X_{f,i} = 0 \qquad \text{at } t = 0 \text{ and } 0 \le z \le L_f \quad \textbf{(80)}$$

$$\frac{\partial X_{f,i}}{\partial z} = 0 \qquad \text{at } z = L_f \text{ and } t \ge 0 \quad \textbf{(81)}$$

$$\frac{\partial X_{f,i}}{\partial z} = D_{eff,X,i}\left((u_{de} - u_{at}) X_{f,i} - \left(k_{de,i} X_{f,i} - k_{at,i} X_{B,i} \right) \right) \qquad \text{at } z = 0 \quad \textbf{(82)}$$

where

$$u_{at} = \sum_{k=1}^{n_x} \upsilon_k k_{at,k} X_{B,k} \quad \textbf{(83)}$$

$$u_{de} = \sum_{k=1}^{n_x} \upsilon_k k_{de,k} X_{f,k} \quad \textbf{(84)}$$

$$k_{de,i} = c_{de,i} L_f^2 \quad \textbf{(85)}$$

Heterotrophs Growth rate

$$\boldsymbol{r_{gr,H} = \left(\mu_{H,max} \frac{S_{f,S} S_{f,N}}{(K_S + S_{f,S})(K_N + S_{f,N})} X_{f,H} \right) - \left(b_H X_{f,H} \right)} \quad \textbf{(86)}$$

Inert Growth Rate

$$\boldsymbol{r_{gr,I} = Y_I \left(b_H X_{f,H} \right)} \quad \textbf{(87)}$$

EPS Growth rate

$$r_{gr,E} = \frac{Y_E}{Y_H}\left(\mu_{H,max}\frac{S_{f,S}S_{f,N}}{(K_S+S_{f,S})(K_N+S_{f,N})}X_{f,H}\right) + \frac{Y_E}{Y_H}\left(b_H X_{f,H}\right) - \left(b_H X_{f,H}\right) \quad \textbf{(88)}$$

Time-variant Distribution of Biofilm Depth

$$\frac{dL_f}{dt} = u_L = u_f\left(L_f\right) - u_{de} + u_{at} \quad \textbf{(89)}$$

Time-variant Soluble and Particulate Components in the Bulk Phase

$$\frac{dS_{b,i}}{dt} = \frac{Q\left(S^0_{B,i} - S_{B,i}\right) + \frac{D_{B,S,i}}{L_{BL}}A\left(S_{f,i} - S_{B,i}\right)}{\left(V_r - AL_f\right)} \quad \textbf{(90)}$$

$$\frac{dX_{b,i}}{dt} = \frac{A\left(k_{de}X_{f,i} - k_{at}X_{B,i}\right) + \left(Au_L - Q\right)X_{B,i}}{\left(V_r - AL_f\right)} \quad \textbf{(91)}$$

VITA

Name: Julianna Gisel Camacho

Addresses: Department of Civil Engineering
Texas A&M University
3136 TAMU
College Station, Texas 77843-3136
c/o Robin Autenrieth

E-mail: julianna_camacho@neo.tamu.edu

Education: B.S., Chemical Engineering, 2001
Universidad de Puerto Rico, Recinto de Mayagüez

M.S., Environmental Engineering, 2004
Texas A&M University

Ph.D., Environmental Engineering, 2010
Texas A&M University